

**Development of Geobiophysical Models for
Cartographic Representation of Wetlands in Yellow
Creek Basin, West Virginia.**

**Thesis Submitted to
The Graduate College of
Marshall University**

**In partial fulfillment of the
Requirements for the Degree of
Master of Science in the
Physical Science of
Geobiophysical Modeling**

by

Ian Farrar

Marshall University

Huntington, West Virginia

04/01/2001

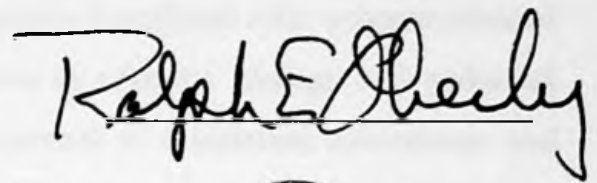


This thesis was accepted on April 1 2001
Month Day Year

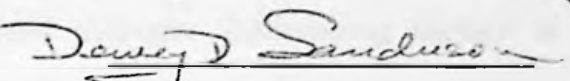
As meeting the research requirements for the master's degree

Thesis committee members:

Prof. Ralph Oberly PhD



Prof. Dewey Sanderson PhD



Prof. James O. Brumfield PhD



Advisor, Head of Graduate Program in
Physical Science, Graduate College.

Leonard J. Deutsch Dean of the Graduate College

Prof. Leonard Deutsch, PhD.

Abstract

In the Appalachian Mountains of Canaan Valley, the warmer temperatures and fading native species are conducive for invading foreign species. Localized relic communities of red spruce, sphagnum and polytrichum are sensitive to climatic change and potential indicators of global warming. Therefore, the development of a baseline assessment and further research are necessary to observe and model changes. Influencing factors in wetland ecology include slope, aspect, biologically rich and diverse vegetation associations, micro-topography, hydrology, underlying soils, and geology. Three uniquely independent study sites have been established along a single transect of the Yellow Creek stream terraces, in Tucker County, West Virginia. Vegetation physiognomic association, micro-topography, hydrology, and soils data were collected using a variety of technologies. A plane table polar coordinate paper, with K&E® alidade, and Sonin® sonic ranging device for vegetation physiognomic association mappings was originally employed. This was replaced by Magellan® ProMarkX-CP-GPS providing more efficient vegetation association delineation and registration to UTM mapping coordinates. A detailed micro-topographic survey was performed using Nikon® Theodolite Total Station to accurately determine the micro-topography. Collected field data were imported into ER Mapper®5.5 software, the geobiophysical modeling system, via an iterative registration process. Digitized 1995 color infrared one-meter resolution aerial imagery supplied by the United States Forest Service formed the base map for all registration. A combination of image processing techniques including principal component analysis and cluster analysis was applied to extract features for pattern recognition. The processed spectral, spatial, and multi-temporal components were geobiophysically modeled to characterize vegetation physiognomic associations and other identified features. The three-dimensional cartographic representations illustrate the subtle relationships between sphagnum, eriophorum and polytrichum physiognomic associations and surface hydrology.

Table of Contents

Chapter 1 Introduction	1
Background.....	1
Canaan Valley Region	3
Field Mapping.....	5
Image Processing	6
Geobiophysical Models	8
Study Objectives.....	10
Chapter 2 Methodology.....	11
Study Area Overview	11
Geography.....	11
Geology	11
Climate.....	14
Wetland Vegetation and Soil Associations	15
Wetland Surface Hydrology.....	15
Field Methods and Data Collection.....	18
Field Mapping	18
Field Preparation	20
Field Technologies	20
Lab Data Processing Model.....	21
Data Parameters & Processing.....	21
Data Standards and Integration	21
Data Registration and Rectification	22
Data Modeling Tools	22
Remote Sensing Methods	23
Imagery.....	23
Modeling Parameters & Processing	24
Statistics	24
Image Processing Methods.....	25
Image Classification	25
Supervised Classification	27
Unsupervised Classification	27
Principal Component Analysis	27
Enhancement	28
Geobiophysical Models for Cartographic Representation	28
Chapter 3. Techniques.....	30
Field Mapping.....	30
Yellow Creek 1	30
Yellow Creek 2	32
Yellow Creek 3	34
Alidade and Plane Table Mapping	36
Global Positioning System Mapping	36

Theodolite Mapping	38
Surface Hydrology and Soils.....	39
Lab Analysis and Modeling.....	39
Development Environment.....	39
Data Entry	40
Vegetation Digitizing.....	40
GPS Import.....	42
Image Conversion	42
Base Map Rectification	42
Micro-topographic Survey Data Import.....	43
Micro-topographic Gridding and Contouring.....	43
Data Preparation.....	43
Image Registration Procedure.....	43
Vegetation Rectification Procedure	47
Image Processing.....	48
Supervised Classification	48
Statistics	48
Unsupervised Classification	49
Principal Component Analysis.....	49
Enhancement.....	50
Three-dimensional Geobiophysical Modeling Procedure.....	51
Chapter 4 Results and Discussion	52
Introduction.....	52
Micro-topographic Digital Elevation Models.....	52
Vegetation Physiognomic Association Models.....	56
Vegetation Soil Sampling.....	60
Registration Modifications.....	65
Digital Aerial Imagery	65
Statistics	65
Geobiophysical Models	69
Yellow Creek 1	69
Yellow Creek 2	75
Yellow Creek 3	81
Chapter 5 Conclusions and Future Research Trends.....	89
Bibliography.....	93
Software Inventory.....	98
Hardware Inventory	98
Field Equipment	98
Laboratory Equipment	98
Appendix A – Description of the UTM Coordinate System	99
Appendix B – An Example of the Gridding Algorithm Report.....	100
Appendix C – Glossary of All Image Processing.....	103

List of Figures

Figure	Title	Page
1	Site Location Map	12
2	A Three-dimensional Multi-layered Representation of Canaan Valley and Surrounding Region, West Virginia, USA.	13
3	Secondary plant succession on wet organic soil in Canaan Valley.	16
4	Secondary Plant Succession on Moderately Drained to Somewhat Poorly Drained Abandoned Pastureland in Canaan Valley.	17
5	95 Color Infrared Aerial Imagery taken by the United States Geological Survey in June of 1995	26
6	97 Color Infrared Aerial Imagery taken by the US Forestry Commission in June of 1997	26
7	Site: Yellow 1, Description: Surface water source originates from groundwater seepage.	31
8	Site: Yellow 1, Description: Surface water passing through main channel in wetlands. Sphagnum association.	31
9	Site: Yellow 1, Description: Image of the entire site. Note the low-level cloud.	31
10	Site: Yellow 2, Description: Note the subtle Natural vegetation associations, fields and tree line in the distance	33
11	Site: Yellow 2, Description: Image covering the majority of the site. Note the subtle depression through the center of the site	33
12	Site: Yellow 2 Description: Note the misty weather conditions and the elevated bank toward the Yellow Creek	33
13	Site: Yellow 3, Description: Drainage channel flowing into Yellow Creek.	35
14	Site: Yellow 3, Description: Note the surface water in the former channel in the foreground. Undulating micro-topography.	35
15	Site: Yellow 3, Description: Following a drainage pattern to Yellow Creek.	35
16	Site: Yellow 2, Description: Plane table with alidade mapping procedures.	37
17	Site: Yellow 1, Description: GPS Survey of vegetation associations.	37
18	Site: Yellow 2, Description: Image of Yellow Creek between the sites. Note the low level cloud.	37
19	Two-dimensional Contour Map of Yellow Creek 1	53
20	Two-dimensional Contour Map of Yellow Creek 2	54
21	Two-dimensional Contour Map of Yellow Creek 3	55
22	Vegetation Association Map of Yellow Creek 1	57
23	Vegetation Association Map of Yellow Creek 2	58
24	Vegetation Association Map of Yellow Creek 3	59
25	Three-dimensional Structural Cell of Vegetation Associations and Micro-topography, Yellow Creek 1	61

26	Three-dimensional Structural Cell of Vegetation Associations and Micro-topography, Yellow Creek 2	62
27	Three-dimensional Structural Cell of Vegetation Associations and Micro-topography, Yellow Creek 3	63
28	Linear Enhanced Three Band Color Infrared 1995 Imagery, Yellow 1, Davis, West Virginia.	70
29	Histogram Equalization Enhancement of Three Band Color Infrared 1995 Imagery, Yellow 1, Davis, West Virginia.	70
30	Color Composite of the three bands with applied ISOCLASS Unsupervised Classification producing fifteen classes., Yellow 1, Davis, West Virginia.	71
31	Applied PCA to three bands, creating a composite band output, ISOCLASS Unsupervised classification with 15 Classes, Level-sliced Transform Enhanced. Yellow 1, Davis, West Virginia.	71
32	Three bands Linear Enhanced Color Infrared 1997 Imagery, Yellow 1, Davis, West Virginia.	73
33	Three bands of CIR 1997 with PC1,2,3 imagery producing single pseudocolor composite with Level-sliced enhancement., Yellow 1, Davis, West Virginia.	73
34	Applied PCA 1,2,3 to three bands with Pseudocolor Composite output, Level-Sliced Enhanced Color Infrared 1997 Imagery, Yellow 1, Davis, West Virginia.	74
35	Applied PCA 1,2,3 to three bands with pseudocolor composite output. Unsupervised 15 classes Level-Sliced enhanced CIR 1997 Imagery, Yellow 1, Davis, West Virginia.	74
36	Three CIR bands applied with linear enhancement, Yellow 2, Davis, West Virginia.	77
37	Vegetation Overlay with Color PseudoComposite Level-sliced Transform Enhanced Color Infrared 1995 Imagery, Yellow 2, Davis, West Virginia.	77
38	Pseudocolor CIR composite of ISOCLASS unsupervised 60 classes with 95% Clip transform enhancement, 1995 Imagery, Yellow 2, Davis, West Virginia.	78
39	Pseudocolor CIR composite of NDVI $(IR - R) / (IR + R)$ with level-sliced transform enhancement applied to 1995 Imagery, Yellow 2, Davis, West Virginia.	78
40	Three bands CIR linear enhanced CIR 1997 Imagery, Yellow 2, Davis, West Virginia.	79
41	Pseudocolor CIR composite with ISOCLASS unsupervised classification with 15 classes, and level-sliced enhanced 1997 Imagery, Yellow 2, Davis, West Virginia.	79
42	Pseudocolor CIR composite with unsupervised 80 classes Gaussian equalization enhancement 1997 imagery, Y2 WVa.	80
43	1997 Infrared and red bands with NDVI $(IR - R) / (IR + R)$ and histogram equalization enhancement, Yellow 2, Davis, West Virginia.	80
44	Three band CIR with histogram enhancement for the 1995 Imagery,	82

	Yellow 3, Davis, West Virginia.	
45	Two bands from 1995 imagery with NDVI $(IR - R) / (IR + R)$ and 95% Clip Enhanced in Red Band, Yellow 3, Davis, West Virginia.	82
46	Pseudocolor CIR composite with 95% Clip enhancement to the 1995 Imagery, Yellow 3, Davis, West Virginia	83
47	Three band 1995 CIR with PCA 1, 2, 3 and linear enhancement. Yellow 3, Davis, West Virginia.	83
48	PseudoColor 1997 CIR Composite with 95% clip enhancement, Yellow 3, Davis, West Virginia.	84
49	PCA1,2,3 applied to red and green bands from the CIR 1997 imagery with Gaussian transform enhancement, Yellow 3, Davis, West Virginia.	84
50	Three-dimensional representation composed of histogram equalized enhanced image processed CIR 1995 imagery draped over surveyed micro-topography. Yellow 1, Davis, WVa.	85
51	Three-dimensional representation composed of PCA1 pseudocolor composite with 15 unsupervised classes and level-sliced transform enhanced image processed CIR 1995 Imagery, Yellow 1, Davis, West Virginia.	85
52	Three-dimensional representation composed of PCA1,2,3 composite with 15 unsupervised classes and 95% clip transform enhanced image processed CIR 1997 Imagery, Yellow 2, Davis, West Virginia.	86
53	Three-dimensional representation composed of linear transform enhanced image processed CIR 1995 imagery draped over surveyed micro-topography, Yellow 2, Davis, West Virginia.	86
54	Three-Dimensional Perspective of a pseudocolor CIR 1997 composite image with 15 unsupervised classes and level-sliced enhancement. Y2, Davis, WVa.	87
55	Three-dimensional flythrough of the model shown above (Figure 54), Yellow 2, Davis, West Virginia.	87
56	Three-dimensional perspective of pseudocolor 1995 CIR composite with 15 unsupervised classes and level-sliced enhancement draped over micro-topography, Yellow 3, Davis, West Virginia.	88
57	Three-dimensional perspective of pseudocolor CIR 1997 composite enhanced with 95% clip draped over micro-topography, Yellow 3, Davis, West Virginia.	88

List of Tables

Table	Title	Page
1	TOSCA® Digitizing Module Procedures.	41
2	ERMapper Ground Control Point Registration Technique.	45
3	Applied Transformations for Image Enhancement	50
4	Vegetation Association Soil Sampling Results from August 1998	64
5	Statistical Results for Yellow Creek 1	66
6	Statistical Results for Yellow Creek 2	67
7	Statistical Results for Yellow Creek 3	68

Chapter 1 Introduction

Background

Wetland ecosystems support a broad spectrum of natural habitats and associative life forms of the natural world. Excessive carbon dioxide emissions occur with the potential for significant impact upon climate (Bloemer et al, 1997). Highly productive bio-diverse communities with unique habitats have developed a reputation as the "kidneys of the landscape" from a local, regional and global perspective. Their presence is represented on every continent except for Antarctica with total land coverage of approximately six percent (Mitsch & Gosselink, 1993).

Historically, wetlands have a global recognition. Many cultures developed in harmony providing economic wealth and lifestyles whilst others devalued the wetland, implementing land-use conversions. Over the past two hundred years the United States of America has seen a significant growth of population and industry accompanied by poor land management. This combination of factors and others have resulted in the lower forty-eight States losing more than fifty percent of the wetlands with West Virginia an estimated twenty-four percent of lost wetlands. A significant proportion of the remaining number have been converted into "anthropogenic oriented wetlands" (Mitsch and Gosselink, 1993).

In central West Virginia, scientific research discovered a significant change in red spruce populations reducing the total canopy by more than 25% (Adams et al., 1985). This is supported by an other abrupt reduction in red spruce growth rate in the late 1950's and early 1960's from studies performed on tree ring data. Sources of non-point pollution, such as fertilization, acidic rain, iron and aluminum concentrations from mining

activities, a 20% increase in precipitation over the past 50+ years, and stand aging and maturation, may have contributed to the decline, although current research indicates winter injury is an important contributor (Johnson et al., 1992; DeHayes, 1992).

Wetland bio-diversity and habitation are temporally and spatially dynamic systems. Physical landscape, geologic, hydrologic and vegetation physiognomic patterns are closely interconnected, establishing a healthy ecological community. Spatial patterns can influence ecological movements and resource utilization patterns. Landscape processes, such as disturbance-recovery, can predict patterned landscapes (Paine & Levin, 1981). The loss of wetlands can develop fragmented landscapes. Habitats disappear with the loss of terrestrial and aquatic species. The remaining habitats can become under-utilized as a result of dispersion, isolation and fragmentation (Paine and Levin, 1981).

Mountainous terrain possesses significant information on raw resources for the geosphere, biosphere and hydrosphere to understanding global ecology. The collection of data and methods of analysis provide many challenges for scientists, especially the remote sensing community. Biological and physiognomic diverse communities are sensitive to changes in aspect, slope, topography, hydrology, soils and geology. These factors can affect the extraction and manipulation of data, often in the form of imagery. Repetitive patterns throughout mountainous terrain may provide an insight to changes in ecology and the consequential effects. The spatial, spectral and temporal scale from which important information can be derived is therefore an important area of study.

Canaan Valley Region

Canaan Valley encompasses one of the largest inland freshwater wetland ecosystems in the eastern United States. A combination of bogs, marshes, wet meadows and swamps have developed within the bottomlands and surrounding of the breached anticline (Fortney and Sturm, 1998). Relic bio-diverse wetlands of red spruce, sphagnum and polytrichum bogs are present in localized areas providing the most southern examples of northern species from the last ice age in the West Virginia Appalachian mountain range (Brumfield et al, 1997; Fortney, 1975).

Historically, red spruce forests with rhododendron communities flourished under the favorable climatic and edaphic conditions dominating the Canaan Valley floor and surrounding lowland areas. The tolerant nature of both species to diverse environmental conditions resulted in extensive natural forests providing deep accumulations of organic materials. During the middle to late nineteenth century, extensive deforestation damaged the natural balance that maintained the forest for centuries. Logging companies exported vast quantities of red spruce and other associated hardwoods out of the valley via railroads. Fires damaged much of the remaining forest clearing the lands and exposing surface soils to the physical elements. Highly organic soils developed over thousands of years, and now exposed, offer new opportunities for new and varied habitats. Invasion of new species developed in the modified edaphic conditions around islands of regenerated forest. Imported mixed grass seeds from Europe and elsewhere were apparently sown over large areas for the grazing of cattle. These farms gradually were abandoned due to the short growing seasons and inherent transportation costs (Fortney, 1975)

The red spruce wetland communities in the bottomlands of the Canaan Valley region have already fallen below the lower elevation limit. Local conditions conducive for maintaining their existence are changing by a combination of potential influencing factors. Anthropogenic activities that impact the wetland communities have included acid precipitation, logging, fires and surface mining. The consequential effects of these activities resulted in a scarred landscape. Over time, natural reclamation processes of regeneration produced a change in ecology. Northern Hardwood cover types dominated by sugar maple, beech, black cherry, and yellow birch replaced the original coniferous forests. It is only on the mountain tops and former river terraces that there are sizable communities resembling the former forests (Fortney, 1975).

Regional temperature rise seen over the past decades impacts the local climate, increasing frequency of invasion by other species at lower elevations. Subtle successional changes within the relic wetland communities are potentially related current climate conditions. These changes are not easily to identify from static ground observation and therefore require monitoring through time series modeling (Brumfield et al, 1997).

The distribution pattern of vegetation physiognomic associations within relic wetlands is the product of successional changes though time. Vegetation patterns and successional changes reflect both interacting biotic factors and the impact of environmental patterns. To consider either successional trends or vegetation patterns independently would require significant additional effort in processing to extract the same information. It therefore appears logical and efficient to combine the two components of vegetation together and integrate the data into a centralized modeling

system that can extract this information using a series of specialized techniques in geobiophysical modeling (Brumfield, 1990).

Vegetation biomass provides absorption in the visible spectrum and scattering in the near Infrared (NIR) due to the presence of chlorophyll and the leaf structure. Density of vegetation, leaf structure, physiognomic traits and other functions differentiate vegetation associations. Therefore, to extract signatures from the collected imagery, the visible and near infrared portion of the electromagnetic spectrum should be fully utilized (Brumfield et al, 1997).

Field Mapping

To verify identity of extracted features from processed aerial imagery requires the implementation of field-checking procedures (Tiner, 1999). This is achieved through ground truth investigations that provide necessary quality control and detailed understanding of local environmental conditions. Factors that require attention include climate, topography geology and slope inclination and influence on the dynamics of the wetland is significant. However, it appears that surface and soil hydrologic conditions are the main point of control for determining successional trends together with past and current disturbances (Fortney, 1975). The mapping of the micro-topography at a high resolution will contribute to the understanding the surface hydrology (Lyon & MaCarthy, 1995). In addition, mapping of the vegetation physiognomic associations may indicate natural or anthropogenic changes that are currently occurring within the limits of the wetlands (Brumfield, 1997).

To overlay spatial data within the same model requires a common coordinate system. Registration of remote aerial imagery into a world geographic coordinate system

necessitates the mapping of ground control points requiring identification and survey from field investigations. Global Positioning System (GPS) technologies are widely available and are specifically employed for the purpose of locating positional information on field measurements (Sabins, 1997).

Image Processing

Image processing techniques have been widely accepted for identification and delineation of wetland vegetation patterns for more than thirty years. Federal regulatory agencies have utilized remote sensing and image processing techniques for management, inventory, and distribution of wetland information (Tiner, 1977). From 1979, the U.S. Fish and Wildlife Service (USFWS) published a nationwide classification scheme for use in the national wetland inventory (Cowardin et al., 1979). In 1981 to 1984, the United States Geological Survey under the National High Altitude Aerial Photography Program (NAAP) acquired nationwide Color Infrared aerial (CIR) imagery at a scale of 1:58000 (Carter, 1982) and again in 1996 and 97 with 1 meter instantaneous field of view (IFOV) for West Virginia. State regulatory agencies including New Jersey, Delaware, and Maryland have produced wetland maps based upon large scale imagery (1:12000) facilitating identification of discrete plant communities (Tiner, 1999).

Image scale establishes baseline limits on interpretation of the imagery. The minimum mapping unit (mmu) determines the degree of resolution between different wetland types and the detail of the vegetation associations within the wetland boundaries (Tiner, 1999). High-resolution aerial imagery possessing a small instantaneous field of view (IFOV) is recommended for small wetlands where precise boundaries and identification of vegetation associations are required (MacConnell et al, 1992).

Accurate interpretations of aerial imagery are dependent upon quality, scale of imagery, the experience of the image-analyst with specific wetland expertise and the amount of ground truth verification performed. Quality and timing of aerial imagery are prerequisites for accuracy, overexposed and underexposed film is of little value as are photographs with considerable cloud and snow. Hydrologic characteristics significantly impact feature extraction with the wettest wetlands usually the easiest to interpret, while the drier ones are more problematic. Maps produced by image processing will not be as accurate as a detailed ground truth except for where topographic differences are abrupt and hydrologic differences are obvious. However, detection of boundary, identification and change may provide significant efficiencies. Extreme conditions such as flooding and droughts create problems for accurate wetland photointerpretation (Tiner, 1999).

Spectral and spatial relationships between and within wetland boundaries have been manipulated and extracted for interpretation. Scrub-shrub wetlands are comprised of bogs and pocosins dominated by ericaceous shrubs, and other wet areas dominated by true shrubs or tree saplings. These wetlands have characteristic plant species that may be easily interpreted, for example leatherleaf st johns wort (*hypericum*) cranberry (*Vaccinium*) especially on color infrared imagery. (Tiner, 1999)

Pattern recognition algorithms are extensively utilized within this study for feature extraction of wetland vegetation physiognomic associations and low order surface hydrology. Principal component analysis (PCA) and unsupervised image processing methods facilitated the identification and delineation with the proximity of the wetlands. By using combinations of the two methods, each exchange the other, in maximizing

variance along the axis (PCA) and grouping probability density fluctuations in the data swarm (Bloemer et al, 1996).

Geobiophysical Models

According to Brumfield, 1990: “A geobiophysical Model System (GMS) is an integrated series of analytical modeling procedures. It provides spatial and statistical scientists, engineers, and multi-disciplinary resources planners with a framework for integrating many different types of information in a decision making process. Through these procedures, volumes of geobiophysical data for example, physical, biological, environmental, and socio-economic information pertaining to the geosphere, biosphere, hydrosphere, and atmosphere, can be stored, managed, manipulated, analyzed, modeled and displayed.”

Research performed by Mills et al, 1963, was based upon the concept of the minimal structural cell that incorporated physiognomic associations within and among vegetation assemblages in the Florida Everglade wetlands. Physiognomic classifications were based upon categorizing plant height and the field analysis of variance with spatial distribution for a minimum frequency and spacing with 10% error for a confidence level of 95%.

The basis of this thesis extends Mills' concept by including hydrologic, physiognomic and micro-topographic parameters in the development of geobiophysical models. Hydrologic low order patterns, surface moisture change, edaphic factors detection, using dominant species vegetation physiognomic associations of intensely studied sites, are referred to as structural cells. Vegetation physiognomic associations, micro-topographic and multi-temporal image processed data are incorporated into a

geobiophysical modeling system to develop three-dimensional models of structural cells for visualization and analysis (Brumfield, 1990).

A series of image processing techniques developed for feature extraction in pattern recognition may enhance subtle relationships not apparent from direct photointerpretation. For example, hydrologic low order patterns and ground moisture change detection may correlate to vegetation physiognomic assemblages via high spatial resolution multi-temporal, broad multispectral banded image processed color infrared aerial imagery. Geobiophysical modeling of the specified data may potentially illustrate land surface moisture patterns and energy flux components of regional mountainous vegetative, hydrologic cycles and global climate models (Bloemer et al, 1999).

Study Objectives

The development of cartographic representation of wetland geobiophysical models requires a multi-disciplined scientific approach. Dynamic biological, hydrological and geological processes within wetland ecosystems require a variety of parameters to be recorded, integrated and modeled. Therefore, a background in field methods, data management, geographical information systems, image processing and earth science is a necessity for the development of geobiophysical models (Lyon & McCarthy, 1995).

Thesis research objectives:

- Develop a baseline for predictive modeling of climate change in mountainous wetlands.
- Develop and assess techniques for geobiophysical modeling of wetland structure and relic association change.
- Cartographically represent in two and three dimensions various feature extractions using pattern recognition algorithms within a geobiophysical modeling system.

Chapter 2 Methodology

Study Area Overview

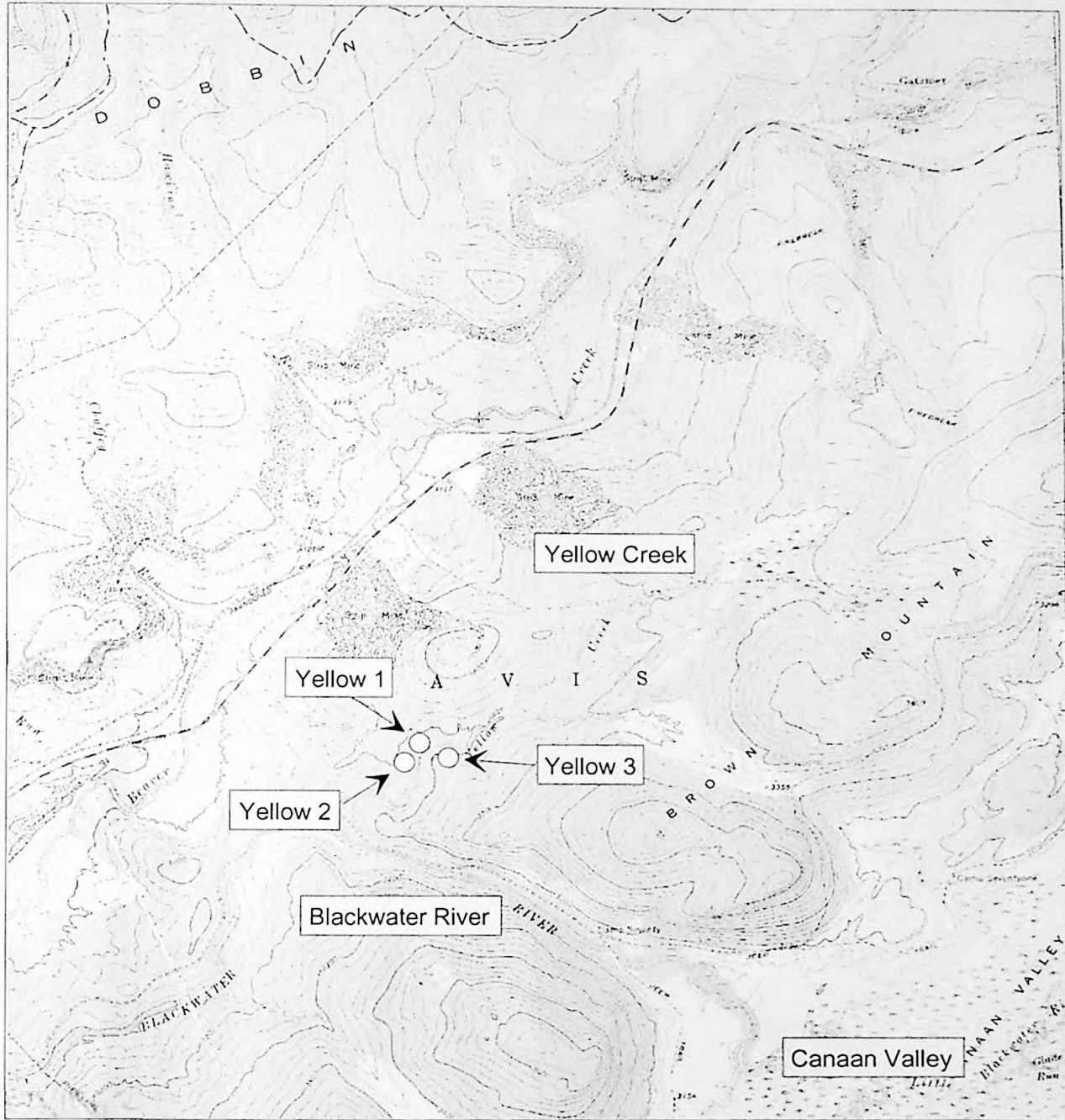
Geography

The Yellow Creek study area is located in the Blackwater River watershed of Tucker County, West Virginia. Precise ground truth sites are illustrated in Figure 1 on the USGS Davis 7.5 minute topographic quadrangle at geographic coordinates, N39.0, W79.5, at an elevation of approximately 3,200ft. Brown Mountain, Canaan Valley and the headwaters of the Blackwater River lie to the east with abandoned mines to the north and northeast (Figure 1). To the south is the water gap formed between Cabin and Middle Mountains providing the opening for the Blackwater River to leave Canaan Valley. To the southwest is the Yellow Creek / Blackwater River confluence flowing south toward the town of Davis (Fortney, 1975).

Geology

The Yellow Creek watershed is part of the Allegheny Mountains of the Appalachian province that are contained within the Allegheny Plateau. The region is predominantly underlain by the Pottsville group geological formations which is a member of the Pennsylvanian System shown in Figure 2 (Ludlum and Arke, 1971). The average thickness of the formation is sixty meters, composed primarily of sandstone, siltstone, shale and coal. The resistant sandstone units in the Pottsville group form the outer flanks of the breached anticline (Fortney, 1975).

Site Location Map of the Yellow Creek Watershed



Source:
 Mapped, edited and published by
 the Geological Survey in cooperation
 with the State of Maryland agencies.
 US Geological
 Survey
 Denver, Colorado,
 80225



Scale
 1:12000
 MN
 GN
 124MILS

Contour Interval 20 Feet
 National Geodetic Vertical
 Datum of 1929

Davis Quadrangle
 West Virginia - Maryland
 7.5 Minute Series (Topographic)
 SW section of the NW Quarter:
 Created 1967, Photo-revised 1981

02/16/1998

Figure 1

A Three-dimensional Multi-layered Representation of Canaan Valley and Surrounding Region, West Virginia, USA.

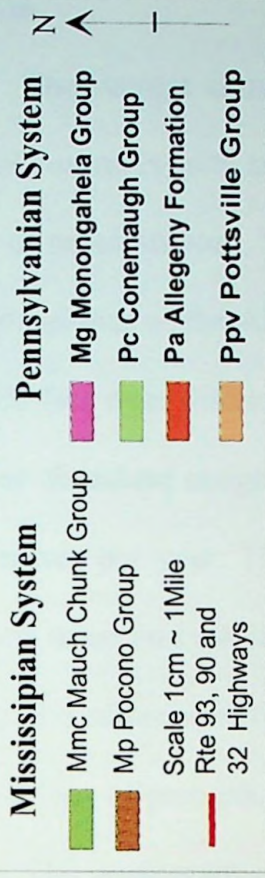


Figure 2

Climate

The current climatic conditions in the Yellow Creek watershed are characterized by cool summers with moderate to severe winters accompanied by cloudy skies and high levels of precipitation. These conditions are attributed to the topographic location on the westerly slopes of the Allegheny Mountains. Moisture laden air from the west is forced to rise 500 feet over distance of 15 miles up the slopes of the mountains. Adiabatic cooling induces abundant orographic precipitation on the leeward side of the valley averaging 53.3 inches per year. This equates to an average of four inches per month and ranging between three and six inches. Periodically, extreme conditions have occurred producing high levels of precipitation in relatively short periods of time. In the month of July 1958, 11.27 inches of precipitation fell (Fortney, 1975).

The temperature regime around Yellow Creek is currently colder than that of the surrounding areas. Summer conditions are relatively cool for the region with an average temperature falling around 75F or less. During winter months, average daily temperatures range between 38F to -20F fueled by Katabatic winds generated by the surrounding slopes. Freezing conditions occur on average 270 days of the year with frosts occurring on a monthly basis limiting the growth and development of new species and maintaining the existing northern species (Fortney, 1975).

Clouds prevail over the entire valley for the majority of the year. On average, 70 percent cloud cover occurs during daylight hours in the winter months and 45 percent during the summer months. The number of clear days approximates to 80 days (0 –30 percent cloud cover) and the cloudy days (80 –100 percent cloud cover) about 160 days.

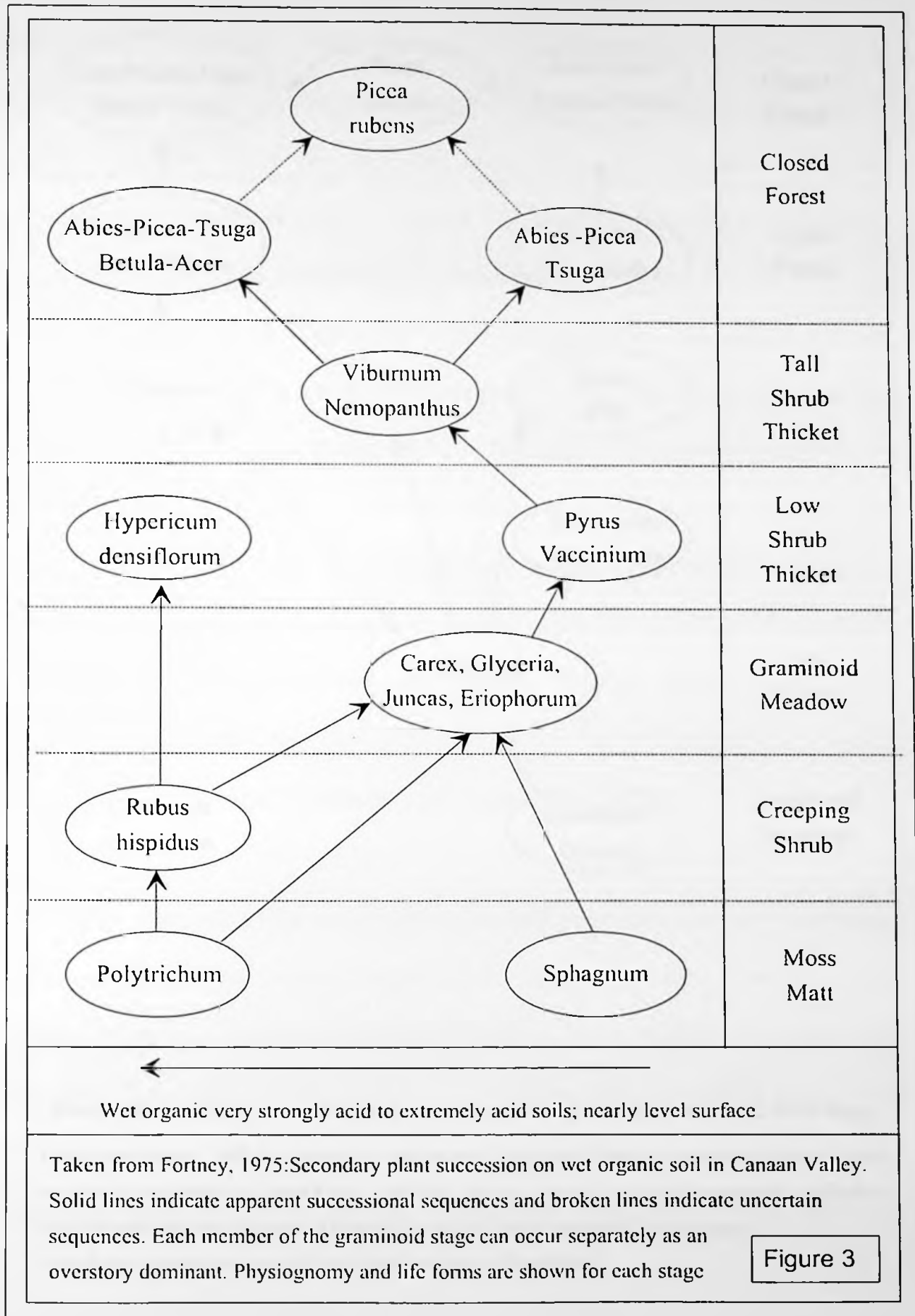
(Fortney, 1975). It is note worthy that imagery is difficult to obtain as a result of the extensive periods of cloud cover.

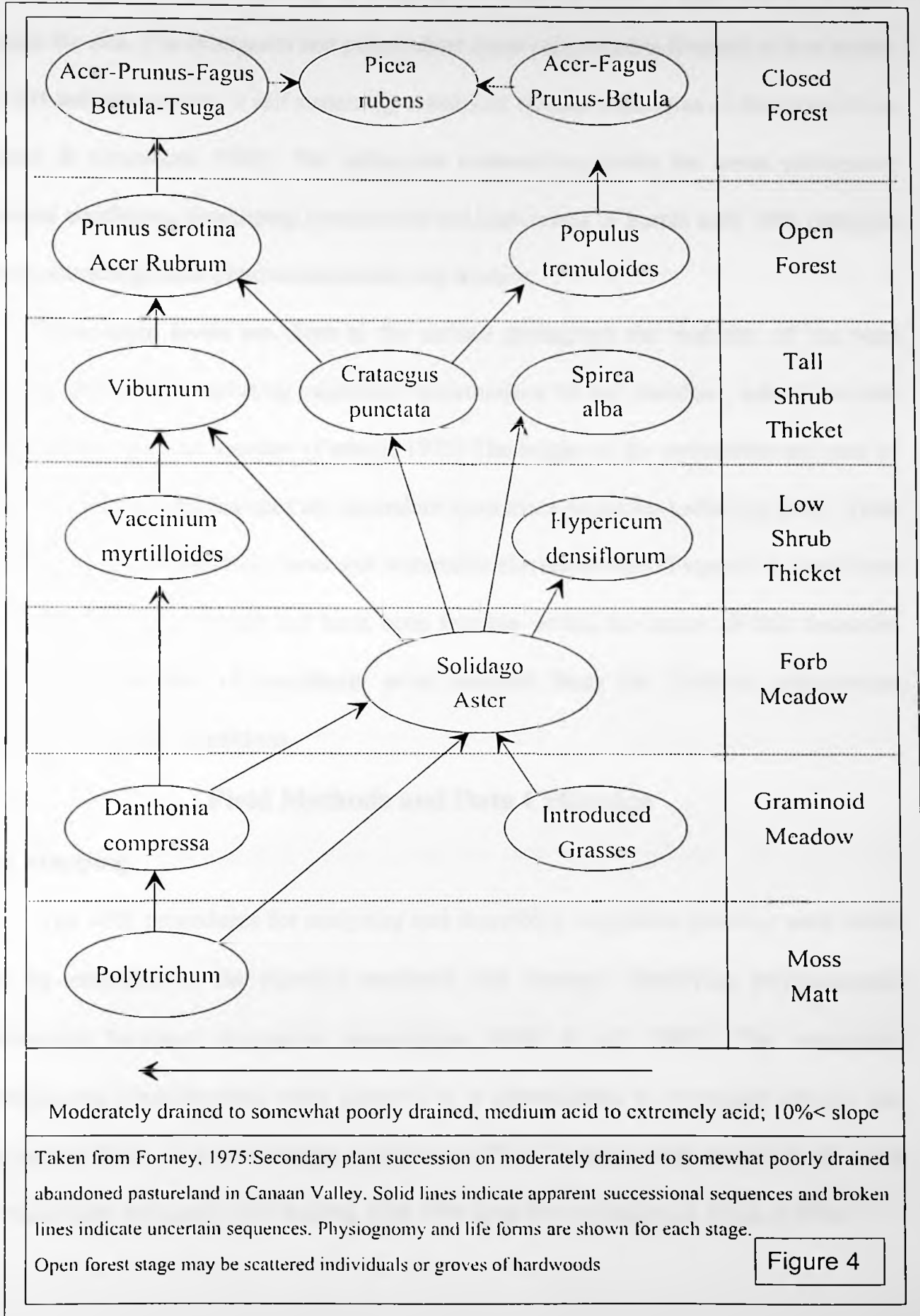
Wetland Vegetation and Soil Associations

Wetland soils and vegetation associations demonstrate a close correlation within the region of Canaan Valley. This relationship is exemplified by the Polytrichum sp and Sphagnum sp. associations that are confined to the extent of the hydric and highly acidic organic soils (Figure 3). These soils are characteristically two to four feet in depth underlain by impermeable clay layers and predominantly saturated. Toward the wetland boundaries, mineral soils become interlaced with organic material providing suitable edaphic conditions for invasion of successional species. Communities such as Solidago sp., Vaccinium sp., Rubus sp., Eriophorum sp., Hypericum sp., Juncas sp., Carex sp. and Glyceria sp. naturally occur in a wide range of edaphic conditions from moderately well drained soils to very poorly drained soils (Figures 3&4). However, the distribution of wetland communities seems closely correlated with the availability of non-forested areas rather than with a distribution of specific soil types (Fortney, 1975).

Wetland Surface Hydrology

The Yellow Creek basin is dominated by Polytrichum sp. and Sphagnum sp. moss associations. Their correlation with the amount of available nutrients is well documented throughout the scientific community (Fortney, 1975; Mitsch & Gosselink, 1993; Tiner, 1999). Research suggests that surface water sources for polytrichum bogs possess a high mineral content. Sediments and solutions rich in minerals are entrained and dissolved as the waters move across the surface (Gorham, 1967). Sphagnum bogs are associated with





fresh water sources from springs or seepage areas that possess a higher rate of flow through the site. The sphagnum and polytrichum moss communities flourish in low acidic <4.0 pH settings creating a self sustaining conditions through high rates of decomposition (Mitsch & Gosselink, 1993). The sphagnum communities prefer the more permanent saturated conditions developing hydric soils and high levels of humic acid with nitrogen content attracting other plant communities, e.g sundew.

Watertable levels are close to the surface throughout the majority of the year currently providing supporting vegetation communities of wet meadow, sphagnum and polytrichum bogs, and marshes (Fortney, 1975) The height of the watertable and rate of subsurface flow within the sites are dependent upon many variables including time. Time series analysis of subsurface flows and watertable elevations would require a significant level of effort which would not have been feasible within the scope of this research. Therefore a snapshot of conditions were recorded from the field to characterize subsurface moisture conditions.

Field Methods and Data Collection

Field Mapping

The field procedures for analyzing and describing vegetation patterns were based upon an extension of the minimal structural cell concept, identifying physiognomic associations between vegetation assemblages (Mills et al, 1963). The vegetation physiognomic classifications were grouped by a combination of dominant species and plant height from an aerial imagery perspective. Field variance with spatial distribution for a minimum frequency and spacing with 10% error for a confidence level of 95%.

A soil survey was required to ascertain an understanding of underlying soil conditions in relation to identified vegetation physiognomic associations and surface hydrology within the structural cell. The nature of the subsurface soils should indicate recent and historic conditions and the relative impact to surface vegetation. (MacBeth, 1992).

The enhancement of features for visual interpretation by the utilization of topography has been well understood within the geobiophysical modeling community (Brumfield, 1997; Bloemer et al, 1999). Historically, stereoscopic analysis has enabled multi-dimensional spatial relationships to be viewed, as they are not apparent through statistical analysis (Brumfield, 1990). Digitization software for stereoscopic imagery has not been widely available for low funded projects. A detailed topographic survey can provide the third dimension to develop high spatial resolution digital elevation models (DEM). These models can emphasize subtle vertical changes throughout wetlands not apparent to the field observer or from imagery providing an insight to surface hydrology and vegetation physiognomic associated patterns.

Wetlands are transient between uplands and aquatic ecosystems responding dynamic behavior of the hydrology (Mitsch & Gosselink, 1993). Monitoring moisture conditions within the surface or near subsurface provides an understanding of the hydroperiod and long-term changes and effects. Due to the physical nature and size of the wetlands, hydrological monitoring using temporary driven well points or permanent well fixtures is not practical. A snapshot of surface hydrology and moisture conditions can be identified through periodic field observations, soil sampling and aerial imagery.

Processed CIR aerial imagery provides the most practical long-term approach to identify surface moisture patterns over a remote area (Howland, 1980; Everitt & Escobar, 1989).

Field Preparation

To accomplish field objectives, a series of refinements to methods were necessary to overcome associated natural obstacles encountered when studying remote wetlands. Problems previously identified from literature have included inaccessible roads by motor vehicles, unstable terrain with near surface high watertable, stream crossings, dense vegetation with undefined paths and remote locations (Jehson, 1986). Field equipment required suitable properties for field application, these included rugged, lightweight, mobile, autonomous, and scaled for practical application whilst meeting accuracy and precision specifications. Digital technologies were employed where possible to support the field process for efficient data collection, transfer and processing.

Field Technologies

Developments in computer technology have transformed field methods to new levels of accuracy. Mobile Global Positioning Systems (GPS) with handheld devices provide real-time data recording, storage and high-speed data transfer. Digital theodolite surveying enabled the collection of real-time spatial data that can be downloaded, processed and mapped if necessary in the field. High spectral and spatial imagery is widely available for commercial and educational use through digital data sharing. Mobile computers have enabled the scientific community to process field data directly.

Lab Data Processing Model

Data Parameters & Processing

Spatial data sets for vegetation physiognomic associations, micro-topography and CIR imagery are recorded in vector, grid and raster format respectively. The vector data sets are composed of points, lines and polygons; the grid data sets are in ASCII format and the digitized imagery in binary format. Processing of the data sets requires algorithms and procedures to manipulate the spatial data. For example, image-processing techniques perform mathematical operations such as rotation, scaling of coordinates, translation, geometric correction, and radiometric correction (Brumfield et al, 1995; Sabins, 1997). Spatial data sets require registration to map projections or correction for geodetic points. File exchange protocols, software utilities and standards provide for data transfer and manipulation (Douglas, 1995).

Data Standards and Integration

The integration of the field data for the development of models requires a significant level of effort. The utilization of automated procedures have made the integration process more efficient but manual manipulation is still significant. Software vendors and research organizations have developed scripts for transforming multi-dimensional spatial and non-spatial data sets into required formats. A single standard for data storage is not currently available for modeling systems and not a single software vendor has interfaced with all data standards. Consequently, data encoding, preprocessing and preparation are still manual time-consuming tasks that increase the potential for error (Brumfield, 1990).

Data Registration and Rectification

Spatial data sets require geo-referencing under the same coordinate system for accurate representation and overlay. This method is accomplished by applying transformations from known ground control points identified within the base map. Map projection and datum are chosen for the base map meeting the mapping requirements. Universal Transverse Mercator (UTM) map projection provides equal area gridding and is the common standard for areas less than 10,000 square kilometers. Large mapping and modeling software vendors provide utilities for representing and transforming the UTM map projection (Terry, 1996).

Data Modeling Tools

Mapping and modeling software for geobiophysical modeling necessitates broad and flexible methods for loading data. The capacity to integrate combinations of data types, both spatial and non-spatial nature, from multiple devices must be considered when choosing the software vendor. Vendor technical staff or user groups may provide a second tier support to resolve integration and software issues. For this research, evaluation of software products include ERDAS Imagine®, IDRISI®, Earth Resource Mapping ERMMapper®, Golden Software Surfer®, Micrographix Designer®, AutoCAD®, FRAME®, ESRI Arcview®.

Aerial imagery provides support to the development of the multi-dimensional geobiophysical models within the context of a GIS (Gervin, 1996, Brumfield, 1997, Bloemer, 1994; 1997). The wide commercial availability of aerial imagery is driving new mapping standards throughout many organizations. For spatial modeling, the aerial

imagery component is a necessity, not only for feature extraction, but contributes significantly to developing new levels of accuracy (Brumfield, 1990).

Remote Sensing Methods

Mountainous wetland terrain is composed of a dynamic combination of biological, geological and hydrological processes. Gathering of field data for these variables requires extensive time and resources prompting the employment of efficient methodologies. Remote sensing of wetlands through processed aerial imagery has been widely used for the purpose of wetland inventory and identification of discrete plant communities in low-lying flat regions (Tiner, 1999). Mountainous terrain is subject to frequent topographic changes inhibiting small-scale imagery to identify wetland features. Aspect, perspective, shadow and image warping can alter spectral signatures and spatial scales. To overcome these inherent problems a higher spatial resolution must be used to extract features from wetlands (Brumfield et al, 1997).

Imagery

Remotely sensed multi-temporal color infrared aerial imagery contributes spectral and spatial database to the development of geobiophysical models (Bloemer et al, 1997). The application of image processing techniques provides feature extraction of vegetation physiognomic boundaries and identification of particular species. The distribution of species and vegetation types that are present today are more separable than those existing when the red spruce dominated and then a deep organic layer was on the forest floor (Fortney, 1975).

Low-order hydrologic patterns and surface water conditions should be visible within the processed imagery. All aerial imagery should possess a similar spectral

bandwidth and spatial resolution for comparable features extraction. The timing and atmospheric conditions of image acquisition must be consistent to achieve the desired results (Teillet et al, 1997).

Modeling Parameters & Processing

Registered CIR one-meter resolution aerial imagery, vegetation physiognomic associations and contoured micro-topography will be geobiophysical modeled for three independent Yellow Creek sites. Processing and analysis should provide insights into natural and anthropogenic processes, hydrologic low order patterns, surface moisture change, and edaphic factors using dominant species vegetation, and physiognomic associations that are geobiophysically modeled (Brumfield et al, 1997).

Statistics

Statistical analysis is employed for each site to determine which bands possess the greatest information for feature discrimination and data reduction. The degree of separability among bands within a site guide image-processing techniques for feature extraction. The statistical process involved computing the minimum and maximum values for each band of imagery, the mean, standard deviation, variance-covariance matrix, correlation matrix, and frequencies of brightness values (Jahne, 1991; Jensen, 1986).

Multi-temporal and multispectral CIR aerial imagery provide significant quantities of spectral and spatial information requiring image processing for feature extraction. Data reduction through statistical analysis would benefit long-term data processing and storage needs. Univariate statistics such as minimum, maximum, mean, median, and standard deviation would not indicate spectral dependency. However,

multivariate statistical measurements would provide relational information between bands, identifying bands with the greatest spectral and relevant information. Those bands that possessed redundant information or poor separability would be omitted (Jehnsen,1986).

Image Processing Methods

Image Classification

Image classification methods extract and enhance information from spatial data sets. Standard methods employed by the remote sensing community provide the foundation for image interpretation of vegetation, hydrologic and topographic features. Examples of these methods include, the supervised, unsupervised and PCA for image analysis and enhancement to extract features and patterns for recognition (Sabins, 1997; Brumfield et al, 1997).

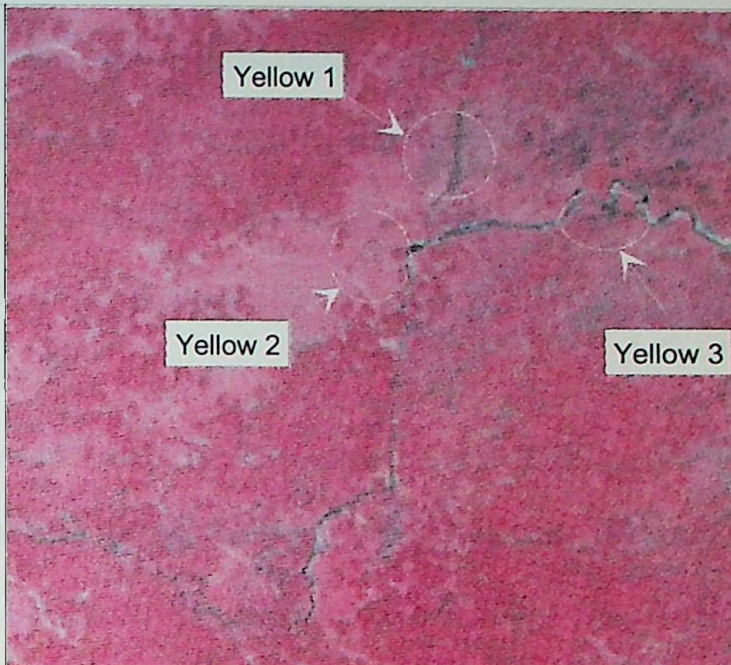
Modified image classification techniques are applied to the registered 1995 and 1997 aerial imagery (Figure 5&6) to extract features for pattern recognition to determine pattern associations. Combinations of supervised, unsupervised classification algorithms, PCA, and image enhancement methods are tested independently on each site to determine the best method of feature extraction. Regions of approximately two acres are defined around the wetland sites to provide adequate coverage of surrounding topography without significant interference from anthropogenic features.

Site Imagery

Color Infrared Aerial Imagery
taken by the United States
Geological Survey in
June of 1995

Resolution is one and a half
meters

Scale
1~12000
MN
GN
124MILS

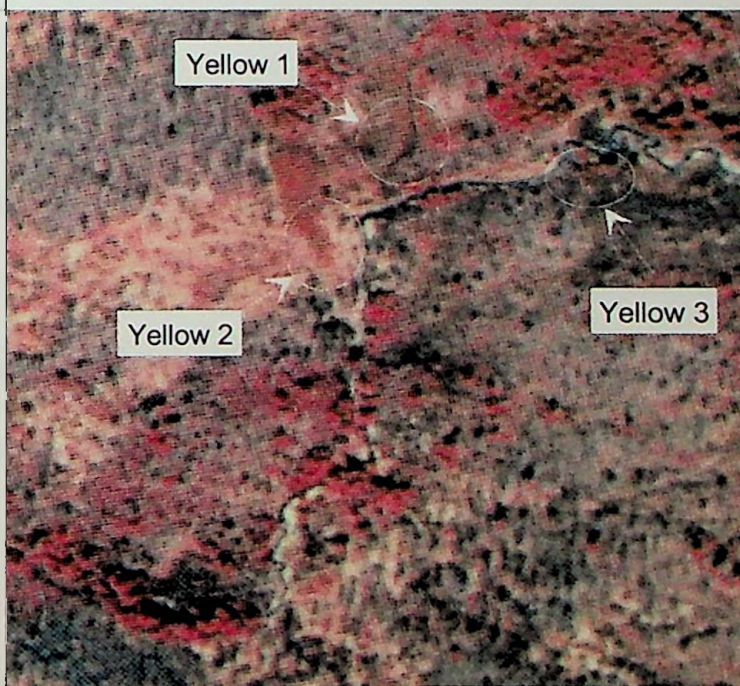


Date of Imagery 07/16/1995

Figure 5

Color Infrared Aerial Imagery
taken by the United States
Geological Survey
Resolution is one and a half
meters

Scale
1~12000
MN
GN
124MILS



Date of Imagery 06/16/1997

Figure 6

Supervised Classification

The supervised classification process utilizes homogenous land covers derived from ground truth sites. For this research, the land covers are dominant physiognomic vegetation associations that are identifiable from an aerial perspective within the wetland. The signature patterns within supervised groups are compared to vegetation physiognomic associations for separability, applying the concept of identified features in the spatial domain being classified in the spectral domain (Brumfield et al, 1997).

Unsupervised Classification

The unsupervised classification procedure performs calculations on the spectral component of CIR imagery data generating natural thematic groups (classes / clusters). Iterative processing of imagery form statistically derived vectors of the mean, correlation and covariance matrices and, generate a series of unclassified groups. These groups are generated in the spectral domain and compared with ground truth data in the spatial to determine the level of success (Sabins, 1997).

Principal Component Analysis

The principle component analysis (PCA) performs statistical functions on multispectral imagery to provide data, reduction and identification of the information. New components are ordered in the amount of image variation between bands on a pixel basis. The first component possesses the majority of the original variance, while later components hold only minor variations. The correlation between a particular spectral band and principal component determines how each band loads variability. A high loading indicates that the majority of the information is within the particular band

providing good separability. A high correlation between bands is indicative of data redundancy and could be ignored or removed from image processing (Sabins, 1997)

Enhancement

Enhancing portions of a particular spectral band or multiple bands highlights features of interest to the user. Visual interpretation of vegetation groupings is significantly improved once initial processing and classifications are performed. Enhancement techniques for vegetation studies include contrast enhancement, linear contrast stretch (autoclip), Gaussian contrast stretch, density slicing, histogram equalization, Logarithmic transform, exponential transforms, and smoothing (Table 2) (Sabins, 1997). The application of the appropriate enhancement function is dependent upon the individual scene and feature of interest. The enhancement process is performed before or after image processing (Sabins, 1997).

Geobiophysical Models for Cartographic Representation

The modeling of the processed aerial imagery with vector and raster grid data is not an effortless task in two or three dimensions. Two-dimensional cartographic representations may not illustrate features identified within the results set when more than two spatial data sets are presented. Three-dimensional modeling enables the presentation of multiple spatial data sets within a single scene (Douglas, 1995; Bloemer, 1997; Bloemer, 1998).

The three-dimensional model presented for visual interpretation provides a more simplistic and effective method of viewing relationships between data than abstract statistical analysis. Geobiophysical modeling for cartographic representation enhances visibility of patterns and associations between all data layers emphasizing subtle features.

Dynamic visualization of data from fly-through, perspective and animation support the visual understanding and interpretation of results to technical and non-technical personnel. (Brumfield, 1990; Douglas, 1995; Bloemer, 1997; Bloemer, 1998)

Chapter 3. Techniques

Field Mapping

Three characteristic wetland sites are selected along a single transect of the Yellow Creek stream, chosen from direct observation to represent the local wetland ecology (Figures 1, 2, 5, & 6). Each of the sites possesses a unique set of localized controlling parameters that affect the type and development of the wetland. These parameters include vegetation physiognomic associations, low order hydrology, soil and micro-topography among others. Modeling these parameters for change detection and simulation requires snap shot recording of current ecological conditions in sufficient detail and plot size to extract and verify pertinent information. Wetland coverage of approximately two acres is assessed to be sufficient for measurement of among group variance of dominant associations.

Yellow Creek 1

Yellow Creek 1 is located to the north of the Yellow Creek in between sites two and three on the alluvial slopes of Yellow Creek. To the north of the site is the upper slopes covered by the northern hardwood forests (Figure 7). To the east and west are the boundaries of the bottomland forests (Figure 8) and to the south is Yellow Creek, a low order stream. The site possesses a low relief (approximately one-meter), with minor changes in micro-topography that are not apparent from general observation. A gentle slope trending from north to south toward the Yellow Creek follows the natural form of the regional topography. A perched watertable to the north provides the main water source that feeds the wetlands throughout the year. Groundwater seeps through

Site Photographs

Site: Yellow 1

Description: Surface water source originates from groundwater seepage. Image of source

Direction: North



04/23/2000

Figure 7



Site: Yellow 1

Description: Image of the entire site. Note the low-level cloud

Direction :North-east



04/23/2000

Figure 8



Site: Yellow 1

Description: Surface water passing through main channel in wetlands. Sphagnum association.

Direction :North-east



04/23/2000

Figure 9



Jointing of relatively impermeable sandstone of Pottsville / Pennsylvanian age appearing at the base of the slope providing a continuous single slow-flow low order stream. The stream passes through the center of the wetland partially contained by its channel, but disperses into a disjunctive sphagnum mat community at the interface of the water table (Figure 9). The underlying saturated soils are very soft and highly organic. Vegetation associations of Polytrichum sp. mosses and disjunctive relic cotton grass form parallel to the stream channel where the water table falls beneath the surface. Other subordinate communities have developed on the higher elevations where the water table is consistently below the surface and the soil substrate is firm. Observed communities included the genera Rubus sp., Vaccinium sp., Pyrus sp., Carex sp., Prunus sp., Abies sp., Salix sp., Acer sp., Juncus sp. and Hypericum sp..

Yellow Creek 2

Yellow Creek 2 is located east of Yellow Creek and to the southwest of site one. Open fields dominated by shrub thicket communities form to the west and Northern Hardwood communities encroaching along the river's edge to the south (Figure 10&11). The site is elevated two meters higher than the streambed and protected by a high bank that formed on the outer bend of a meander (Figure 12). The surface topography possesses a low relief (approximately one-meter) over the majority of the site. The slopes are gentle, descending from north-west to south-east towards the raised bank, forming the shape of a bowl. Surface runoff from the east and spring seepage from the north collect in the bowl bringing the watertable close to the surface during the winter season. Hummocky polytrichum mosses have spread under the damp conditions forming a

Site Photographs

Site: Yellow 2

Description: Note the subtle
Natural vegetation
associations, fields and tree
line in the distance

Direction: West



08/23/1998

Figure 10



Site: Yellow 2

Description: Image covering
the majority of the site.
Note the subtle depression
through the center of the site

Direction :North



08/23/1998

Figure 11



Site: Yellow 2

Description: Note the misty
weather conditions and
the elevated bank toward
the Yellow Creek

Direction :North-east



04/23/2000

Figure 12



continuous mat with only mildly interspersed by associated communities, such as velvet-leaf blueberry and black chokeberry (Figure 11). A small community of Carex sp. and st. johns wort have formed at the tail of the polytrichum mat. Red spruce, yellow birch and cherry trees have developed on the elevated surfaces.

Yellow Creek 3

Yellow Creek 3 is located to the west of the Brown Mountains on the southern floodplain of Yellow Creek, (Figure 13) and to the east of the other Yellow Creek sites. The wetland has developed on a former cutoff stream channel bounded to the south by an old raised bank and to the north by Yellow Creek (Figure 14). The relief is low with subtle changes of less than a half a meter and no more than two meters over the entire site (Figure 15). The main slope descends from east to west following the former river channel through the southern portion of the site. Further south, steeper slopes rise beyond the raised bank, providing un-channeled overland flow during intense periods of precipitation. Additional identified water sources also located from the southern slopes include seepage from perched water tables. The surface waters collect in the former stream channel, elevating the watertable to the surface during periods prolonged with intense precipitation. Slowly the water moves down gradient toward the two confined channels that lead into Yellow Creek. During the summer months the water table drops below the surface, leaving the channels dry and the surface firm.

Hummocks of Eriophorum sp. and Polytrichum sp. communities follow the former stream channel. The Polytrichum sp. community forms in circular growth patterns, indicating colonial expansion. The hummocky Eriophorum sp. communities form the dominant upper story. Black chokeberry and velvet-leaf blueberry communities

Site Photographs

Site: Yellow 3

Description: Drainage channel flowing into Yellow Creek.

Direction: North-east



04/23/1998

Figure 13



Site: Yellow 3

Description: Note the surface water in the former channel in the foreground. Undulating micro-topography

Direction: North



04/23/2000

Figure 14



Site: Yellow 3

Description: Following a drainage pattern to Yellow Creek.

Direction :South-east



04/23/2000

Figure 15



have developed adjacent to the polytrichum communities where the water table is close to the surface. Stressed relic communities of red spruce are present on the higher drier areas.

Alidade and Plane Table Mapping

During the summer growing season of 1997, the vegetation physiognomic associations of the three Yellow Creek sites were mapped. Keuffel and Esser (K&E) siting Alidade with polar coordinate mapping paper and plane table was one of the initial technologies employed (Figure 16). The mapping process included the setting of the plane table in the center of the site, referencing its location with a wooden stake. The polar coordinate mapping paper was aligned to grid north by use of a Brunton® compass, magnetic declination was set to 124 milliradians (MILS) west in accordance to US Geological Survey recommendations. The magnitude was determined from site center and recorded with the appropriate scale. Plot sizes were restricted to a maximum radius of thirty-two meters, providing a significant representation of the vegetation associations. Sonin® sonic range finders were initially used in the field and provided imprecise performance over short distances (Sonin® inc.). As a consequence, the units were replaced with Leica® laser-ranging finders that provided better usability, accuracy and precision (Leica inc.). All data, annotations and variances were recorded on hardcopy in the field logbook.

Global Positioning System Mapping

In 1998, the sites were revisited throughout the growing season to develop more efficient and accurate field techniques for mapping the boundaries of vegetation associations (Figure 17). Two ProMARK X-CP Magellan® Global Positioning System handheld units were set to record data in the Universal Transverse Mercator (UTM)

Photographs

Site: Yellow 2

Description: Plane table with alidade mapping procedures.

Direction: North



04/23/1998

Figure 16



Site: Yellow 1

Description: GPS Survey of vegetation associations.

Direction: West



04/23/2000

Figure 17



Site: Yellow 2

Description: Image of Yellow Creek between the sites. Note the low level cloud.

Direction :North-east



04/23/2000

Figure 18



projection in Zone 17 North and a World Geographic Survey 1984 (WGS84) datum for the vertical geode were used (Magellan inc.). One unit was configured as a base station, recording satellite data continuously from a fixed location generating the carrier file. The other unit was set to roaming mode, recording discrete geographical data every second generating mobile files (-.MOB). The mobile unit was walked around the borders of the vegetation physiognomic associations creating a very time efficient process. The total time taken for data collection was approximately thirty minutes per site. The data were automatically stored into the random memory ready for download to computer software for analysis and modeling.

Theodolite Mapping

Surface elevation data were collected during fieldwork for development of the micro-topographic layer. Utilizing refined procedures with new technologies provided time efficient data collection techniques for the two-person field team. Such equipment included a Laser Range Theodolite Total Station, Nikon® DM510 with integrated data storage and microcomputer, providing sub-centimeter accurate three-dimensional data.

The theodolite was setup at the center of each site for geographic overlay and maximum visibility. Benchmarks were taken from natural objects such as trees and rock outcrops due to the lack of survey reference points. Data were collected in a grid pattern aligned to grid north at observed topographic or vegetation physiognomic boundaries. This equated to a range of 150 –250 data points per site, collected at a rate of 60 points per hour. The data were automatically stored directly into the random memory ready for download into the computer.

Surface Hydrology and Soils

Surface moisture patterns from direct field observation within the site boundaries are noted in the field logbook (Figure 18). Watertable elevations and soil samples are collected within vegetation physiognomic associations using a handheld Oakfield soil sampler. Soil physical characteristics such as homogeneity within horizons, depth of horizons, color, texture, composition, moisture content and depth to the top of the saturation zone are recorded.

The depth of soil horizons and moisture from the surface are recorded from soil probe cores using the direct push technique with metric tape measure. The physical characteristics of the soils were classified from direct field observation. The Wentworth scale classified particle sizes and moisture content were estimated (Mitsch & Gosselink, 1993).

Lab Analysis and Modeling

Development Environment

Recent technological advancements in personal computing have enabled the geobiophysical modeling community to perform data processing and analysis on mobile computers. For this research, all geobiophysical modeling and data processing were performed on a DELL Latitude® 366 Mhz Pentium® II mobile computer running the Microsoft Windows® 95 operating system with 128 megabytes of SDRAM and two megabytes of onboard Video RAM. Link to Ethernet Local Area Networks facilitated all data storage and recovery for digital data.

The rapid rate progress of desktop hardware has provided a vehicle for the software industry to follow suite. Spatial analysis software has progressed from the

workstation and mainframe environment to the development of new products for the personal computer with workstation capability. This study utilized software packages such as ERMapper® 5.5, IDRISIW® 2.0, Surfer®v7, Designer® v4.0 and Arcview® 3.1 to provide flexible raster and vector based data layers and develop geobiophysical models within a mobile environment.

Data Entry

Vegetation Digitizing

Plane table and alidade field data were copied onto Mylar® vinyl with the corresponding vegetation classes to provide a working hardcopy. The vegetation maps were then converted into digital format by a Calcomp® digitizer for the development of GIS database layers. This process consisted of digitizing the vegetation groups as arc and polygon vector files using the software TOSCA®, a module of the raster GIS software IDRISI®. TOSCA® is a digitizing platform capable of producing numerous different vector file types. A large CALCOMP® digitizing table was configured with TOSCA® on a Pentium® 90 MHz desktop computer.

The digitized data sets were converted from arcs to polygons using CYCLE, a module from IDRISI®. This process was not always accurate and resulted in unclosed polygons termed "Orphans". The autosnap settings or left-right numbering of the arcs produced the majority of errors resulting in an iterative digitizing time intensive process. Upon a successful generation of polygons, the vector data set was then converted as a boundary line file using the software program TOSCSURF®. The SURFER® mapping software then imported the vegetation polygons in the spreadsheet module. Additional

formatting and error checking of the data provided suitable data for overlay and representation.

TOSCA® Module Digitizing Procedure

1. Test Config: To Identify configuration problems.
2. Diagnostics: To check that the puck data stream is correctly reading.
3. Define File: To either open a previous file or create a new one.
Minimum and Maximum Coordinates of the Map:
Data type: Real or Integer, *Real*.
Control Points: From File or Keyboard: *N100,132 E132,100; S68,100; W68,100* coordinates on the perimeter of the circle. This gives a RMS value of how accurate the points are in relation to each other. This should be kept below 0.3.
Digitize to two opposite corners so that the screen display can be calculated. These should be outside of the control points or some of the data will be off of the screen.
4. Set AutoSnap: This displays the snap tolerance settings and allows changes to be made. This must be completed before digitizing. Defined as "The first and last point of a newly digitized line or node that falls within its tolerance radii after hitting the finish button". *The Autosnap was set at 0.23.*
5. Digitize
TOSCA® asks whether left and right polygons are to recorded. For arc files *Yes*, polygons *No*.
Enter Identification numbers, followed by ID (What value to be assigned to this line or polygon).
Note: Where islands are present will become part of the polygon file and where the three line join at a single node will become part of the arc file. The arcs had to be given new identifiers and with left and right values of the areas to either side
Polygon is by definition "A line with identical beginning and end nodes so that the line encloses a polygon".
Arc: Are features with two nodes, a beginning and an end node, as its end points.
6. Save File: The files were saved as real binary files. Other options include arcs for the arc data and polygons for the polygon data.
7. Point Tolerance: Refers to a distance that exists between a point just recorded and the next point to be recorded. *Set at 0.2*

Table 1. TOSCA® digitizing module procedures modified from the IDRISI® manual.

GPS Import

GPS data collected by the Magellan® ProMARK X CP units were downloaded onto the mobile computer and processed by the MSTAR® software package, developed by the Magellan® Systems Corporation. Mobile files collected by the roaming unit and the carrier files recorded by the fixed unit were then imported into the software and post-processed providing sub-meter accurate rectification through averaging. The GPS data were then exported as ASCII text for importing into the Surfer® spreadsheet for generation of the vegetation map layer.

Image Conversion

Image processing of aerial imagery utilized 1995 US Forestry 1:40,000 Color Infrared (CIR) and 1997 USGS 1:40,000 CIR. Both sets of imagery were digitized with an RGB Nikon® Flatbed scanner to a scale of one-meter resolution and filter separation into three colors. Each data set was then saved in Tagged Image File Format (TIFF) to minimize compression maintaining the spectral integrity. The files were then imported directly into ERMapper® 5.5® native file format for processing.

Base Map Rectification

The 1995 one-meter resolution aerial imagery was imported into ERMapper®5.5 native format. Twenty surface features were chosen from the aerial imagery as potential ground control points for geo-referencing that could be identified from the ground surface. All features were located near to the Yellow Creek sites reducing geometric error during the transformation process and for efficient data collection. The Magellan® GPS units were used to collect the field data and for post- processing the data.

Micro-topographic Survey Data Import

The micro-topographic data collected by the Nikon® DM310 Theodolite were downloaded directly to the mobile field computer via a serial port interface in ASCII format using the packaged Nikon® software. The theodolite data were then converted into the Cartesian coordinate system using the EDM conversion utility (Sanderson, 1997). The XYZ output data is a compatible format for gridding in Surfer®7.

Micro-topographic Gridding and Contouring

The coordinate data require processing into grid format for contouring and generation of the base map. A Kriging algorithm with linear variogram and 0.5 meter grid was applied to all micro-topographic data sets producing Surfer®7 ASCII grid files. A variation in relief between Yellow Creek sites was noted and adjustments to the contour interval were made accordingly. Yellow Creek 1 had a total change in relief of 1.92 meters requiring decimeter contours. Yellow Creek sites 2 and 3 possessed a greater change of relief with 2.74 meters and 3.39 meters respectively and required twenty-centimeter contours. All contouring required high smoothing algorithms to increase the roundness of the contours reducing the high sensitivity of closely spaced gridding.

Data Preparation

Image Registration Procedure

The unregistered 1995 imagery required registration to the Universal Transverse Mercator (UTM) projection, Zone 17N with WGS84 Datum. The process required selecting ground features close to the area of interest during field excursions that are identifiable from an aerial perspective. Eighteen ground control points were identified

close to the Yellow Creek sites utilizing both natural and anthropogenic spectral and spatial patterns.

ERMapper®5.5 was the application of choice for registration of the raw aerial imagery. The rectification process utilized the module "Define Ground Control Points" to identify the GCP features (Table 2). Adjusting the zooming from low to high resolution provides an accurate technique for identification of GCP's. Real-time calculation of Root Mean Square error (RMS) during GCP selection provides flexibility and efficiency. The GCP's with higher RMS error are individually selected and omitted reducing the overall error factor until acceptable standards are attained. The acceptable total RMS error for the registration of the 1995 imagery was 10.

Defining Ground Control Points

Select the following criteria

TO coordinate space: **UTM***

TO Geodetic Datum. **WGS84***.

TO Map Projection: Select the Map Projection. The first Map Projection is **RAW/RAW*** to allow you to change back to a raw coordinate space.

TO coordinates. Choose **RAW/RAW*** when the dataset is not referenced to any known map projection. The Datum and Map Projection should also be RAW. The other options are Easting/Northing and Latitude/Longitude.

TO Rotation Angle. Specify the rotation required for the OUTPUT dataset,.

Select the Rectification Parameters:

Type of rectification. **Polynomial*** or Triangulation

Rectification polynomial order. Specify the order of the polynomial to be used for the rectification.

Select **Linear***, Quadratic or Cubic.

Rectification Sampling. Select **Nearest Neighbor***, Bilinear, or Cubic. See "Resampling the dataset" on page 360 of the Reference manual for details.

* The settings and parameters highlighted in **bold** were used for this study.

Reference: ERMapper®5.5 software corporation technical manual.

Table 2. ERMapper Ground Control Point Technique for Registration.

The 1997 one-meter resolution CIR aerial imagery required registration to the 1995 one-meter resolution CIR aerial imagery. The registration procedure would need to meet the Minimum Mapping Unit (mmu) standard of one-meter for all three sites. Identifying the same features close to the mapping scene from different years and atmospheric conditions would prove difficult. Effects of rotation, "Rubber Sheeting" (Brumfield, 1994) and differing spatial resolutions would compound registration error.

The registration of CIR 1997 aerial imagery extended the current methods available through ERMMapper®. The map-to-map method requires identifying control points within the registered imagery. Twenty-eight control points identified within the region of the Yellow Creek sites to register against. The total RMS values of 10 was still not sufficient to register all three sites collectively using the same image.

An extended approach was employed to provide better vertical overlay between the image data sets. The solution involved cutting the inaccurately registered 1997 aerial imagery to three separate regions, each slightly larger in size than the wetland providing suitable coverage and maximizing edge distortions. The cut imagery provides ease of manipulation without effecting the other sites. To finely adjust the registration requires visual interpretation of the features within each scene. The displaying of micro-topography and modeling in a three-dimensional perspective view improves the visual interpretation. The Algorithm Geoposition Extents window provides the bounding coordinates for that view. Applying a transformation algorithm converts the coordinates to the new extents within the 1997 imagery. The ERMMapper®5.5 GCP module proved to be an inefficient tool for fine tuning the registration. A newly devised technique of directly editing the header file proved more efficient. Changing the bounding coordinates

and refreshing the screen resulted in a fast iterative process, increasing accuracy through trial and error. As a result, the minimum mapping unit (MMU) for the 1997 CIR aerial imagery is attained and the registered imagery is useful for spatial resolution modeling.

Vegetation Rectification Procedure

The vegetation data derived from the plane table/alidade required registration to the UTM coordinate system and import into the geobiophysical modeling software ERMapper®5.5. This was accomplished using three staged conversion processes consisting of Surfer®7 ASCII files exporting to a registered AutoCAD®14 DXF file format followed by a direct import into ERV ERMapper®5.5 vector format. The identification of features present in both the registered imagery and vegetation data sets provided approximate corresponding coordinates. The results were then used to calculate the coordinates of the bounding box surrounding the vegetation data set. This provided an iterative process of visual adjustment and manual correction of coordinates to meet the required one-meter registration accuracy to the 1995 imagery.

The post-processed GPS vegetation data sets did not meet the one-meter registration accuracy required for the geobiophysical models. As a result, the same techniques were applied to the GPS data as were used for the plane table/alidade data sets to achieve the registration one-meter accuracy.

Survey Rectification Procedure

The registration of the micro-topographic data sets utilized a variation of the vegetation data registration technique. The surveyed three-dimensional data sets are copied through the Windows®95 clipboard from Surfer®7 spreadsheet into Microsoft Excel®97 to apply translation formulae, currently available in Surfer®7. Data is then

translated by predetermined factor into UTM coordinates and copied back into the Surfer®7 application. Gridding, contouring, conversion and exporting procedures are performed on the data within the Surfer®7 application and imported into ERMapper®5.5. The contour data is then applied to the three-dimensional perspective models with the registered vegetation and imagery data sets for visual verification.

Image Processing

Supervised Classification

The supervised classification procedure was performed using ERMapper®5.5. Imported vegetation vector data and aerial imagery were displayed in the image window showing the entire site. Using the vector annotation tools, each classified polygon was copied to a separate file and assigned the appropriate vegetation association attribute and color for identification. In addition, a regional polygon was created to form the extent of the classification algorithms thereby limiting the interference from other features within the entire data set. The polygons were then converted into raster regions within the image data sets for statistical calculations and defining training regions. This procedure was repeated for all polygons and each site.

Statistics

Univariate and multivariate statistical analyses were performed within the STATISTICS module of the ERMapper®5.5 software. Regions previously defined by vector overlays within both years of imagery defined the outer limits of the statistical analyses. A sub-sampling interval of one was chosen due to the small acreage of the sites providing greater accuracy. The results were written into the header file of the processed

image and displayed within ERMapper® statistics dialog box. The results could then be imported into Microsoft Excel® for further processing and storage.

Unsupervised Classification

The unsupervised classification process was performed using the modules STATISTICS and ISOCLASS. The STATISTICS module calculated the statistical information from the three spectral bands required by the ISOCLASS module. The ISOCLASS module performed searches for natural clusters in the spectral domain, assigning each pixel to a classified group based upon specified input parameters. These parameters were dependent upon the number of vegetation groupings seen at each site from ground truth investigations.

Principal Component Analysis

The Principal Component Analysis was performed on the aerial imagery using the FORMULA module, within ERMapper® 5.5. Minor adjustments to the default settings produced the first component image from all three bands. The PC1 data set was then saved as a virtual data set minimizing the file size. The ISOCLASS unsupervised classification was then applied using the same settings as previously specified. The second and third principal components were generated for each data set by repeating the procedure.

Enhancement

This process improves the contrast of the imagery and aids in the feature extraction process. In addition, turning on 'Smoothing' algorithm from the algorithm dialogue box enhanced the aerial imagery by removing the 'blocky' effect of individual pixels.

Transform Types

- Linear transform allows creation of a piecewise linear transform, including a step function, sawtooth, or any other transformation which can be expressed by a piecewise linear relationship between the input and output values.
- Autoclip transform clips at 99%, excluding the first and last 0.5% of the data. Double-click on the button to change the percentage clip.
- Level-slice transform clips in 'steps', which can be used to create contour lines. Double-click on the button to change the number of steps.
- Histogram match is used when there is more than one layer of the same type - for example, two Red layers - and you wish them both to have similar contrast and brightness.

Note: Histogram match transforms the final output histograms of the other layers of the same type to match the final output histogram of the current layer.

- Histogram equalize creates a piecewise linear transform modifying the values so that all values occur with equal probability.
- Gaussian equalization creates a piecewise linear transform modifying the values to match a Gaussian probability distribution. Double-click on the button to change the half-width of the Gaussian envelope.
- Logarithmic transforms are useful for processing geophysical data with a large dynamic range, in order to compress the dynamic range.

A Logarithmic transform can also be applied to the intensity layer of a color draped algorithm, to reduce the darkness of the image while retaining the variation of the intensity.

- Exponential transforms can be used to stretch the dynamic range in an image using geophysical data with a small dynamic range.
- Display Histogram only enables viewing an output histogram of the data at a specific point of the processing.
- Smoothing reduces the blocky "pixelated" look of raster images and makes general features easier to interpret.

Reference: definitions are derived from the ERMapper 5.5 Help System.

Table 3. Applied Transformations for Image Enhancement

Three-dimensional Geobiophysical Modeling Procedure

Vegetation layers, aerial imagery and micro-topographic data were selected for three-dimensional geobiophysical processing. Pre-processed aerial imagery was imported as three separate data layers in RGB mode and assigned the appropriate colors. Post-processed imagery was imported as a single data set and applied in Pseudocolor mode utilizing the most appropriate color table for enhancing feature extraction. Micro-topographic data was incorporated as the height layer providing a surface for draping the other data sets.

The three-dimensional perspective viewer provided a fixed viewing point of the model appearing as an object in space. This functionality enables the entire site to be viewed from any angle providing an excellent overview of associations. The three-dimensional flythrough viewer simulates moving through space with the views constantly changing. This functionality of the flythrough provides a close view of the site enabling a detailed study of areas of interest.

Upon a satisfactory navigation through the site, the view is saved as an algorithm and the screen captured by the Fullshot®V6 software for export. The captured image is then available through the Microsoft Windows® 95 clipboard for direct import into the Micrographix® Designer V4.1 software for cartographic representation.

Chapter 4 Results and Discussion

Introduction

The study of mountainous wetlands has contributed significantly to understanding trends that have impacted the landscape on local and regional scales. For example, wetland sphagnum bog relics from the last ice age are used extensively as sensitivity indicators of anthropogenic and natural variation. Subtle changes to the equilibrium may be due to a shift in local, regional or even global climatic patterns. However, present methods embraced by the scientific community for determining such changes are being refined for an accurate assessment.

Vegetation physiognomic associations, surface hydrology and micro-topographic patterns provide the necessary information for modeling the relationships between climate trends and their expression in natural and anthropogenic surface vegetation and moisture conditions. The processing of both aerial imagery (Figures 5,6) and field mapped data (Figures 22,23,24) are required to derive micro-topographic, surface hydrologic patterns and vegetation physiognomic associations layers which provide the foundation to extract natural and anthropogenic features.

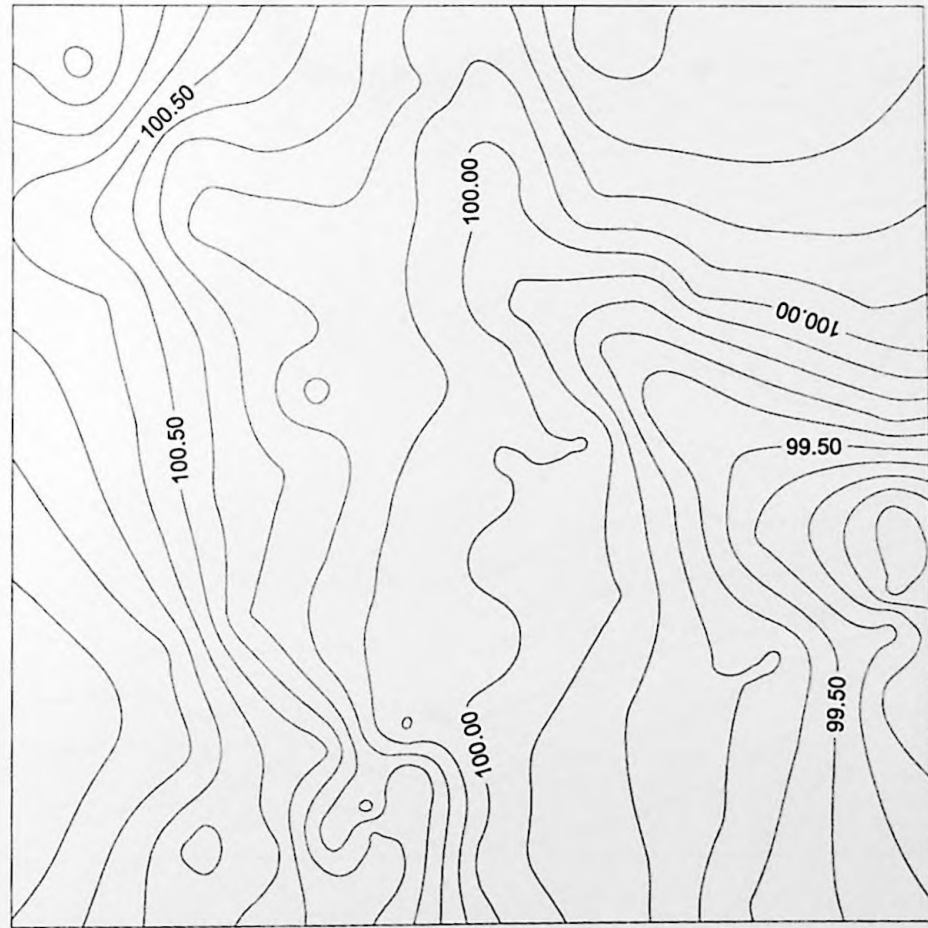
Micro-topographic Digital Elevation Models

Micro-topographic digital elevation models (DEM's) (Figures 19,20,21) are generated, providing the base map for three-dimensional modeling. Yellow Creek 1 DEM with decimeter contours and grid spacing (Figure 19) illustrates the low relief across the entire site with a surface channel that dips from the Northeast to the South. At the center of the site is a gentle slope that is paralleled by two ridges, providing a second channel during high flow conditions. The Yellow Creek 2 DEM (Figure 20) is decimeter grided

Two-dimensional Contour Map Of Yellow Creek 1

Theodolite Survey with Kriging Grid

Scale
X axis = 1cm:8M
Y axis = 1cm:8M



Yellow 1

Contours = 0.1 Meters

Gridding = 0.1 Meters

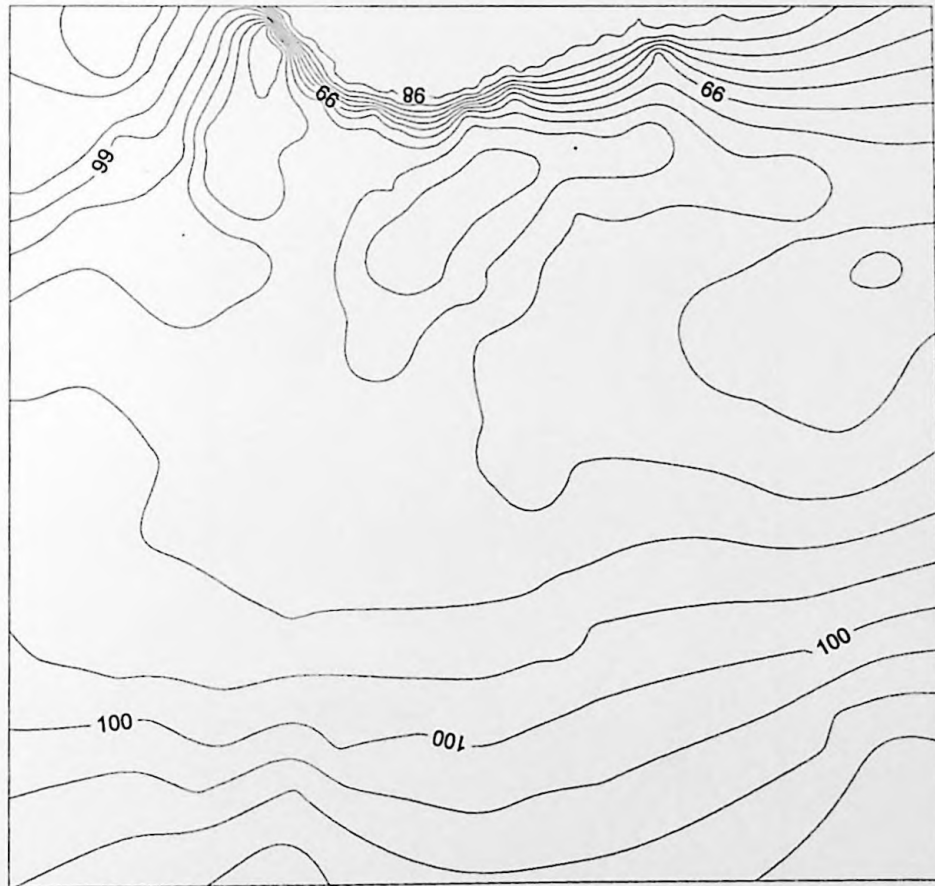
02/16/1998

Figure 19

Two-dimensional Contour Map Of Yellow Creek 2

Theodolite Survey with Kriging Grid

Scale
X axis = 1cm:8M
Y axis = 1cm:8M



Yellow 2

Contours = 0.2 Meters

Gridding = 0.1 Meters

02/16/1998 Figure 20

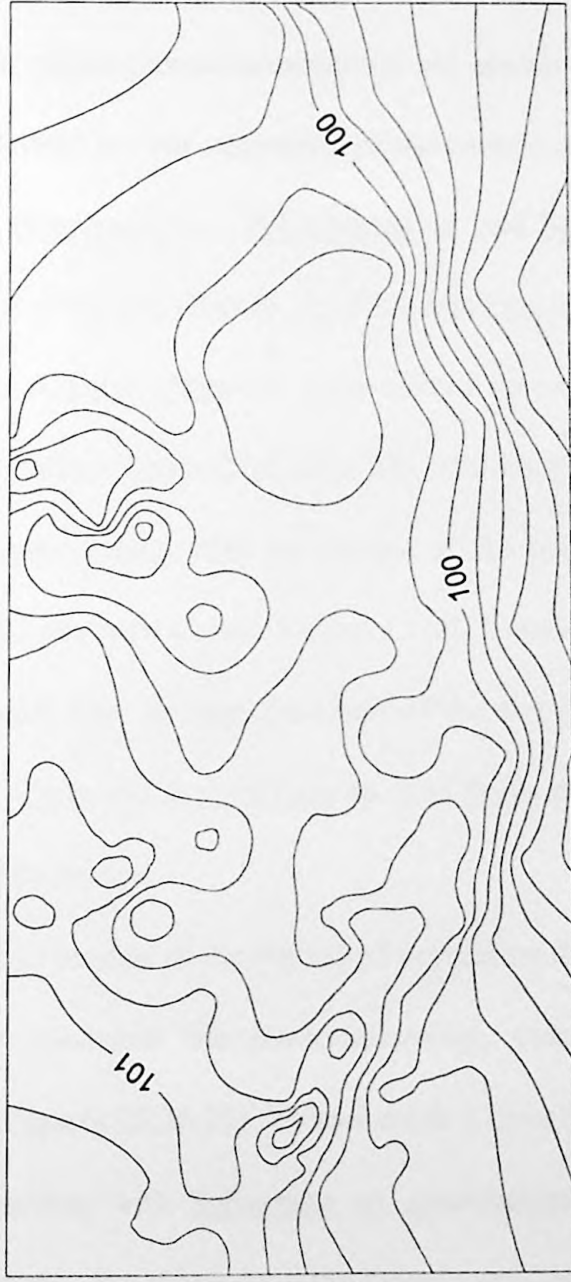
Two-dimensional Contour Map Of Yellow Creek 3

Theodolite Survey and Kriging Grid Method

Scale
X axis = 1cm:8M
Y axis = 1cm:8M



Yellow 3
Contours = 0.2 Meters
Gridding = 0.1 Meters



02/16/1998 Figure 21

with twenty-centimeter contours to adjust for the increased gradient at the riverbank on the east. Surface waters flowing from the surrounding meadows would flow from the west and north toward the south and east and collect in the bowl in the center of the site. Yellow Creek 3 DEM (Figure 21) are also grided and contoured with the same parameters as Yellow Creek 2. Central and northern sections show minor undulation with the steeper gradients to the south forming a curved bank.

Vegetation Physiognomic Association Models

Representations of vegetation physiognomic associations are shown in Figures 10,11 and 12. Yellow Creek 1 is dominated by four vegetation physiognomic associations consisting of genera Sphagnum sp., Eriophorum sp., Polytrichum sp. and Solidago sp., covering approximately eighty percent of the site (Figure 22). Nine other groups make up the other twenty percent of the site. A Polytrichum sp. monoculture running north to south through the center dominates Yellow Creek 2 (Figure 23). Mature Picea ruben, Betula alleghaneinsis and Prunus pennsylvanica trees are present at the perimeter. An ATV trail is visible cutting through the southern corner. Yellow Creek 3 possesses a thin band of Eriophorum sp. that trends east west through the south of the site (Figure 24). Red spruce, Vaccinium myrtilloides, Carex sp., Polytrichum sp. and Pyrus melanocarpa associations form the remaining wetland groups.

Three-dimensional structural cell models of the registered vegetation data sets and draped over the micro-topography illustrates the interrelationship, enhancing any potential surface hydrology patterns (Figures 25,26,27). Yellow creek 1 clearly displays a low order drainage channel corresponding with Sphagnum sp. associations indicating saturated conditions (Figure 25). Parallel to the channel are the Eriophorum sp.

Vegetation Map Of Yellow Creek 1, Davis, West Virginia.

Plane Table and Alidade Mapping Technique



Scale

X axis ~ 1cm:6m

Y axis ~ 1cm:6m



Yellow 1

Picea ruben

Vaccinium myrtilloides

Carex sp.

Polytrichumsp.

Sphagnumsp.

Solidago uiginosa

Juncas sp.

Abies balsamea

Eriophorum sp.

Pyrus melanocarpa

grasses

, 08/12/1998

Figure 22




Vegetation Association Map Of Yellow Creek 2

Global Positioning System Technique

Scale
 X axis = 1cm:8M
 Y axis = 1cm:8M



Yellow 2

-  Picea ruben
-  Vaccinium myrtilloides
-  Pyrus melanocarpa
-  Carex sp.
-  Polytrichum sp.
-  Hypericum densiflorum
-  Crataegus punctata
-  Rubus hispidus
-  Betula alleghaniensis
-  Prunus pennsylvanica
-  ATV Channel
-  Yellow Creek

02/16/1998

Figure 23

Vegetation Association Map Of Yellow Creek 3

Global Positioning System Technique

Scale

X axis = 1cm:8M

Y axis = 1cm:8M



Yellow 3

- Picea ruben
- Vaccinium myrtilloides
- Pyrus melanocarpa
- Eriophorum sp.
- Carex sp.
- Polytrichum sp.
- Bypass
- Wetland Boundary
- Depressed Channel
- Yellow Creek

02/16/1998

Figure 24

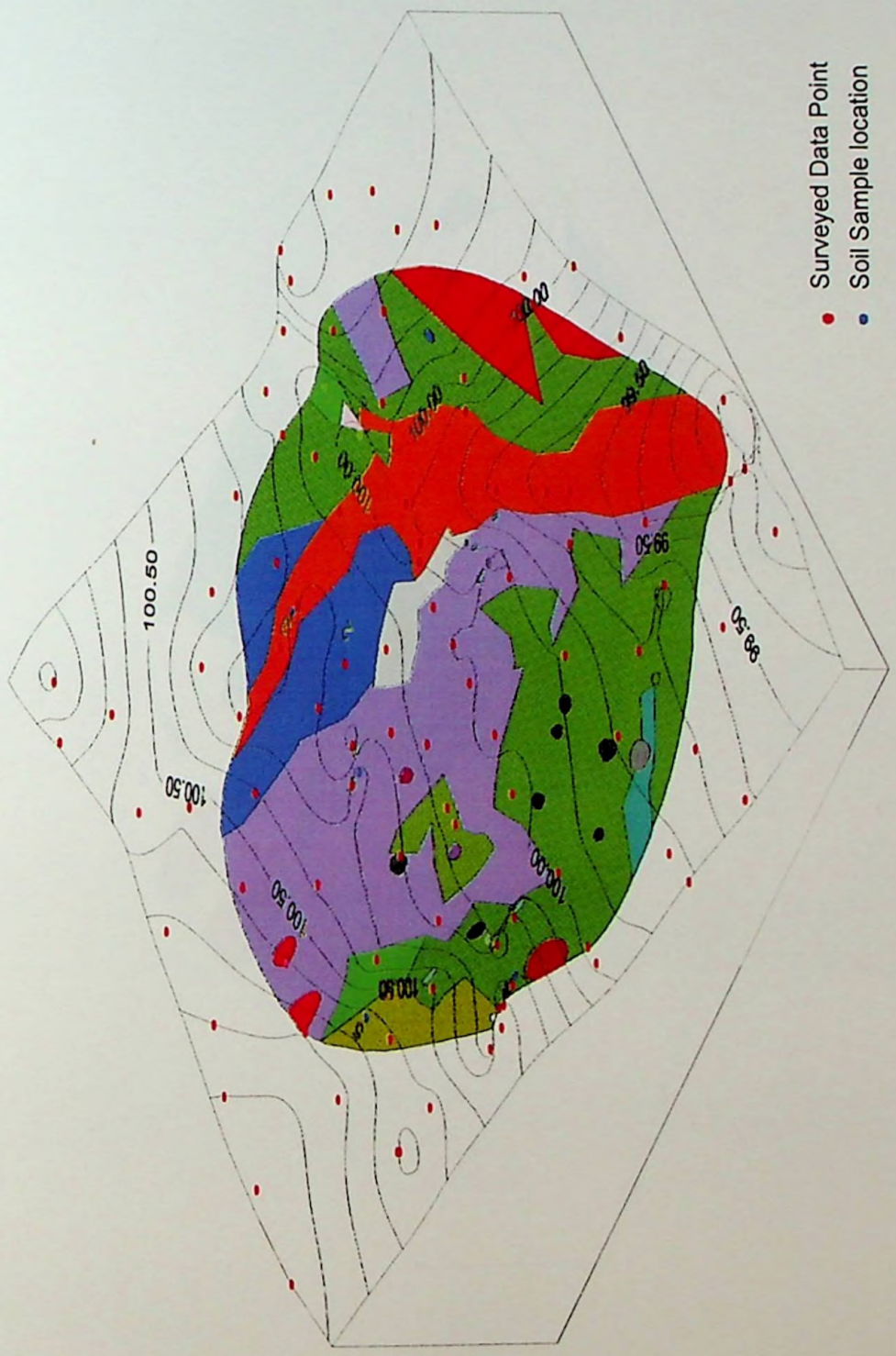
associations. The Solidago uliginosa associations prevail on the steeper drier slopes whilst the Polytrichum sp. associations form in the moist soils regions. Yellow Creek 2 illustrates the close relationship between the Polytrichum sp. association and the topographical bowl and the trees on the higher ground (Figure 26). Yellow Creek 3 has a similar relationship between the Eriophorum sp. association and the micro-topographic depression of the former stream channel (Figure 27).

Vegetation Soil Sampling

The vegetation soil sampling results (Table 4) illustrate a potential relationship between the depth of water table, vegetation physiognomic association and soil composition. The Polytrichum sp. association soils in Yellow Creek 1 & 2 demonstrate similar organic layers that are underlain by oxidized clays and saturated conditions around twenty centimeters. Carex sp. associations soil samples from Yellow Creek 3 developed on sandy soils substrates providing good surface drainage. Sphagnum sp. associations possess a ten-centimeter surface organic layer in saturated conditions illustrating the excessive growth rate of sphagnum moss, approximately one to ten centimeters per year (Mitsch & Gosselink, 1993). The Eriophorum sp. in the Yellow Creek 1 site possesses drier conditions than the often-associated Sphagnum sp..

Three-Dimensional Structural cell of Vegetation Categories and Micro-topography with Soil, Hydrology and Survey.

Scale
 X axis ~ 1 cm:6m
 Y axis ~ 1 cm:6m
 Z axis ~ 1 cm:0.5m
 CI = 10 cm



Yellow 1

- Picea ruben
- Vaccinium myrtilloides
- Carex sp.
- Polytrichum sp.
- Sphagnum sp.
- Solidago uliginosa
- Juncas sp.
- Abies balsamea
- Eriophorum sp.
- Pyrus melanocarpa
- Grasses

- Surveyed Data Point
- Soil Sample location

02/16/1998 Figure 25

Three-dimensional Structural Cell of Vegetation Associations and Micro-topography, Yellow Creek 2

Global Position System derived Vectors.

Scale
 X axis = 1cm ~ 8M
 Y axis = 1cm ~ 8M
 CI = 20cm



Yellow 2

- Picea ruben
- Vaccinium myrtilloides
- Pyrus melanocarpa
- Carex sp.
- Polytrichum sp.
- Hypericum densiflorum
- Crataegus punctata
- Rubus hispidus
- Betula alleghaniensis
- Prunus pennsylvanica
- ATV Channel
- Yellow Creek

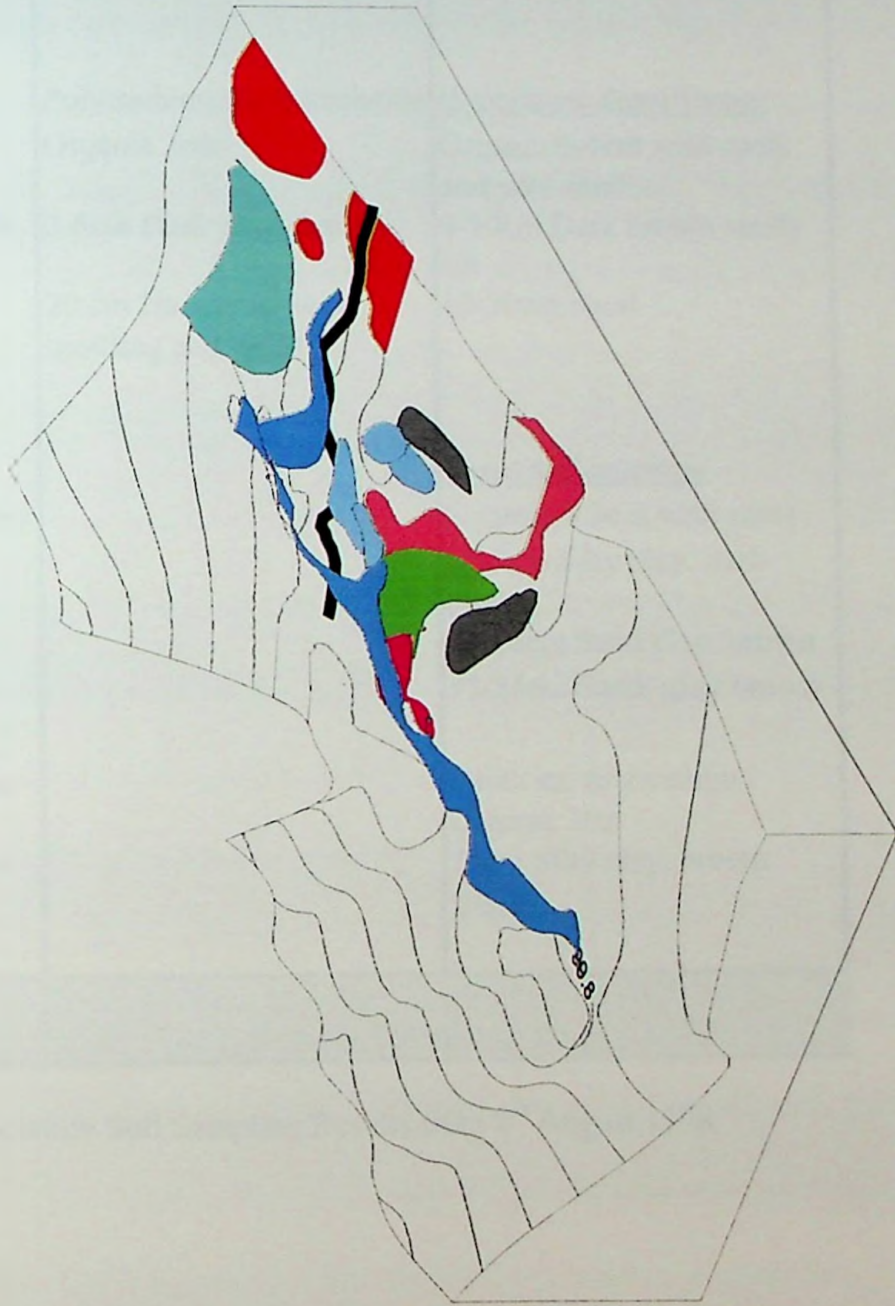
02/16/1998

Figure 26











Three-Dimensional Structural Cell of Vegetation Categories and Micro-topography, Yellow Creek 3

Global Positioning Derived Vectors

Scale
 X axis = 1cm:8M
 Y axis = 1cm:8M
 CI = 20cms



Yellow 3

-  Picea ruben
-  Vaccinium myrtilloides
-  Pyrus melanocarpa
-  Eriophorum sp.
-  Carex sp.
-  Polytrichum sp.
-  Bypass
-  Wetland Boundary
-  Depressed Channel
-  Yellow Creek

02/16/1998 Figure 27

Yellow Creek Site 1	Yellow Creek Site 2	Yellow Creek Site 3
<p>Polytrichum sp. Association Organic 2cm 2-6cm Organic clay 6-26cm Oxidized clay organic 26~ very moist</p>	<p>Polytrichum sp. Association Organic 2cm 2-6cm Dark gray clay 20 cm Dark gray and moist</p>	<p><u>Eriophorum virginicum</u> Organic 1 cm 1cm to 1 meter Silty clay Very moist at 1 meter</p>
<p><u>Vaccinium myrtilloides</u> 6cm dry organic 6-18 cm Green orange soils and slightly moist Refusal at 20 cms</p>	<p>Polytrichum sp. Association Organic 2cm 2-8cm Dark gray clay 20 cm Dark gray with mottling and moist</p>	<p><u>Hypericum densiflorum</u> Organic 0-4cm with roots and silty sand 4-10cm Dark brown sandy silt 10-30cm Sand</p>
<p><u>Solidago uliginosau</u> 0-5cm black humus and dry 5-25 cm grey brown silty clay and dry</p>		<p><u>Pyrus melanocarpa</u> Organic 0-3cm with roots 3-11cm Silty clay. dark brown 11-15cm Sand clay, brown 15-24cm Sand, gray brown</p>
<p>Sphagnum sp. association Highly organic 0-10cms Saturation at surface</p>		<p>Carex sp. association Organic 2cm 25cm Silty clay, brown Black</p>
<p>Average depth to water table: Surface</p>	<p>Average depth to water table: 1 meter below surface</p>	<p>Average depth to water table: 60cm</p>

Table 4. Vegetation Association Soil Sampling Results from 8th August 1998

Registration Modifications

A combination of control points from GPS and USGS topographic maps were initially tested but proved to be unsuccessful, causing distortion to aerial imagery as a result. The USGS data were employed for georeferencing the data sets. As a consequence, poor alignment between aerial imagery and ground truth occurred. This further illustrates the inaccuracies of using USGS 7 ½ minute topographic maps (NAD27) as a geo-reference data source. Visual adjustment to the data layers was necessary to achieve the required accuracy of less than two meters. Using the same specific classification of the mapped vegetation in the structural cell, overlaid and registered to the rectified imagery demonstrates a similar matching of patterns. Rectified 1995 aerial imagery is used as the base map for registering all other data sets.

Digital Aerial Imagery

Digitized 1:40,000 resolution of one-meter CIR three-banded imagery from 1995 and 1997 provided the source for observations, trends and modeling (Figures 2 & 3). Both years of data possess the potential for extraction of features within the Yellow Creek sites. Three broad spectral bands are used to capture change and patterns in vegetation associations and surface moisture conditions.

Statistics

Statistical results were performed for each site and year of imagery. All sites from the 1995 imagery (Table 5,6,7) possess a high correlation between the red and green bands ($Y1=0.915, Y2=0.952, Y3=0.917$) and high loading of the infrared and green bands for the PC1 ($Y1=0.601, Y2=0.631, Y3=0.601$). This opens the potential to remove the

Statistics for Yellow Creek 1, Region 1

Statistics for the 1995 CIR Imagery

DATASET: ERMapper2000/Y1_95_Imagery
REGION: 1

Spatial Data	Band1	Band2	Band3
Non-Null Cells	5226	5226	5226
Area In Hectares	0.523	0.523	0.523
Area In Acres	1.291	1.291	1.291

Spectral Data	Band1	Band2	Band3
Minimum	125	106	127
Maximum	219	186	215
Mean	187.606	147.481	177.695
Median	190	149	180
Std Dev	15.417	12.695	14.656
Std Dev (n-1)	15.418	12.696	14.658
Corr Eigenval	2.693	0.271	0.036
Cov Eigenval	552.876	53.675	7.223

Correlation Matrix	Band1	Band2	Band3
Band1	1	<u>0.73</u>	0.891
Band2	0.73	1	0.915
Band3	0.891	<u>0.915</u>	1
Determinant	0.026		

Covariance Matrix	Band1	Band2	Band3
Band1	<u>237.722</u>	142.841	201.377
Band2	142.841	161.199	170.343
Band3	201.377	<u>170.343</u>	214.853
Determinant	214357.7		

Cov. Eigenvectors	PC1	PC2	PC3
Band1	<u>0.616</u>	<u>0.71</u>	0.341
Band2	0.492	-0.685	0.537
Band3	0.615	-0.163	-0.772

Statistics for the 1997 CIR Imagery

DATASET: ERMapper2000/Y1_97_Imagery
REGION: 1

Spatial Data	Band1	Band2	Band3
Non-Null Cells	5226	5226	5226
Area In Hectares	0.523	0.523	0.523
Area In Acres	1.291	1.291	1.291

Spectral Data	Band1	Band2	Band3
Minimum	34	29	21
Maximum	226	201	193
Mean	134.977	101.93	102.379
Median	136	100	99
Std Dev	32.878	26.717	27.157
Std Dev (n-1)	32.881	26.72	27.159
Corr Eigenval	2.89	0.095	0.015
Cov Eigenval	2433.77	87.814	11.158

Correlation Matrix	Band1	Band2	Band3
Band1	1	0.944	0.91
Band2	0.944	1	0.979
Band3	<u>0.91</u>	<u>0.979</u>	1
Determinant	0.004		

Covariance	Band1	Band2	Band3
Band1	<u>1081.17</u>	829.798	812.712
Band2	829.798	713.939	710.709
Band3	812.712	<u>710.709</u>	737.636
Determinant	2384653		

Cov. Eigenvectors	PC1	PC2	PC3
Band1	<u>0.651</u>	-0.739	-0.171
Band2	0.536	0.289	0.793
Band3	0.537	<u>0.609</u>	-0.584

Table 5. Statistical Results for Yellow Creek 1

Statistics for Yellow Creek 2, Region 2

Statistics for the 1995 CIR Imagery

DATASET: ERMMapper2000/Y2_95_Imagery
REGION: 2

Spatial Data	Band1	Band2	Band3
Non-Null Cells	8096	8096	8096
Area In Hectares	0.81	0.81	0.81
Area In Acres	2.001	2.001	2.001

Spectral Data	Band1	Band2	Band3
Minimum	68	73	80
Maximum	222	202	218
Mean	199.341	150.563	183.819
Median	204	154	188
Std Dev	17.411	15.489	17.959
Std Dev (n-1)	17.412	15.49	17.96
Corr Eigenval	2.731	0.241	0.028
Cov Eigenval	790.098	67.493	8.107

Correlation Matrix	Band1	Band2	Band3
Band1	1	<u>0.769</u>	0.872
Band2	0.769	1	0.952
Band3	0.872	<u>0.952</u>	1
Determinant	0.018		

Covariance Matrix	Band1	Band2	Band3
Band1	<u>303.18</u>	<u>207.435</u>	272.846
Band2	207.435	239.949	264.936
Band3	272.846	264.936	322.569
Determinant	432317.4		

Cov. Eigenvectors	PC1	PC2	PC3
Band1	0.575	<u>0.781</u>	0.242
Band2	0.521	-0.578	0.629
Band3	<u>0.631</u>	-0.236	-0.739

Statistics for the 1997 CIR Imagery

DATASET: ERMMapper2000/Y2_97_Imagery
REGION: 2

Spatial Data	Band1	Band2	Band3
Non-Null Cells	8096	8096	8096
Area In Hectares	0.81	0.81	0.81
Area In Acres	2.001	2.001	2.001

Spectral Data	Band1	Band2	Band3
Minimum	27	13	2
Maximum	236	216	211
Mean	169.917	130.499	128.345
Median	172	130	129
Std Dev	35.331	33.818	34.524
Std Dev (n-1)	35.333	33.82	34.527
Corr Eigenval	2.875	0.115	0.01
Cov Eigenval	3431.6	140.829	11.904

Correlation Matrix	Band1	Band2	Band3
Band1	1	0.926	0.898
Band2	0.926	1	0.987
Band3	<u>0.898</u>	<u>0.987</u>	1
Determinant	0.003		

Covariance	Band1	Band2	Band3
Band1	<u>1248.43</u>	1106.13	<u>1096.063</u>
Band2	1106.13	1143.82	1152.86
Band3	1096.06	1152.86	1192.086
Determinant	5752829		

Cov. Eigenvectors	PC1	PC2	PC3
Band1	<u>0.581</u>	-0.805	0.124
Band2	0.572	0.295	-0.765
Band3	0.579	<u>0.515</u>	0.632

Table 6. Statistical Results for Yellow Creek 2

Statistics for Yellow Creek3, Region 3

Statistics for the 1995 CIR Imagery

DATASET: ERMMapper2000/Y3_95_Imagery
REGION: 3

Spatial Data	Band1	Band2	Band3
Non-Null Cells	8346	8346	8346
Area In Hectares	0.835	0.835	0.835
Area In Acres	2.062	2.062	2.062

Spectral Data	Band1	Band2	Band3
Minimum	68	68	76
Maximum	224	215	223
Mean	176.543	135.034	164.026
Median	183	136	168
Std. Dev.	21.311	17.434	19.321
Std. Dev (n-1)	21.313	17.435	19.322
Corr Eigenval.	2.617	0.335	0.048
Cov Eigenval.	985.083	129.607	16.859

Correlation Matrix	Band1	Band2	Band3
Band1	1	0.673	0.829
Band2	0.673	1	0.917
Band3	0.829	0.917	1
Determinant	0.042		

Covariance Matrix	Band1	Band2	Band3
Band1	454.229	250.05	341.551
Band2	250.05	303.965	309.026
Band3	341.551	309.026	373.355
Determinant	2152459		

Cov. Eigenvectors	PC1	PC2	PC3
Band1	0.623	0.741	0.251
Band2	0.501	-0.624	0.6
Band3	0.601	-0.248	-0.76

Statistics for the 1997 CIR Imagery

DATASET: ERMMapper2000/Y3_97_Imagery
REGION: 3

Spatial Data	Band1	Band2	Band3
Non-Null Cells	8360	8430	8449
Area In Hectares	0.836	0.843	0.845
Area In Acres	2.066	2.083	2.088

Spectral Data	Band1	Band2	Band3
Minimum	1	1	1
Maximum	230	226	218
Mean	101.507	88.43	91.738
Median	97	83	87
Std. Dev.	43.176	33.616	34.348
Std. Dev (n-1)	43.179	33.618	34.35
Corr Eigenval.	2.808	0.175	0.017
Cov Eigenval.	3883.37	271.17	19.925

Correlation Matrix	Band1	Band2	Band3
Band1	1	0.889	0.843
Band2	0.889	1	0.978
Band3	0.843	0.978	1
Determinant	0.008		

Covariance	Band1	Band2	Band3
Band1	1864.42	1290.87	1250.223
Band2	1290.87	1130.15	1129.212
Band3	1250.22	1129.21	1179.899
Determinant	2.1E+07		

Cov. Eigenvectors	PC1	PC2	PC3
Band1	0.665	-0.738	0.114
Band2	0.528	0.356	-0.771
Band3	0.528	0.573	0.627

Table 7 Statistical Results for Yellow Creek 3

green band from further image processing reducing both time and storage. However, high loading of the green band in the PC3 ($Y1=0.537, Y2=0.629, Y3=0.6$) warrants further investigation. The 1995 imagery demonstrates a high correlation among all three bands, a potential sign of scene saturation. All bands demonstrate a high loading in at least one of the principal components suitable for feature extraction.

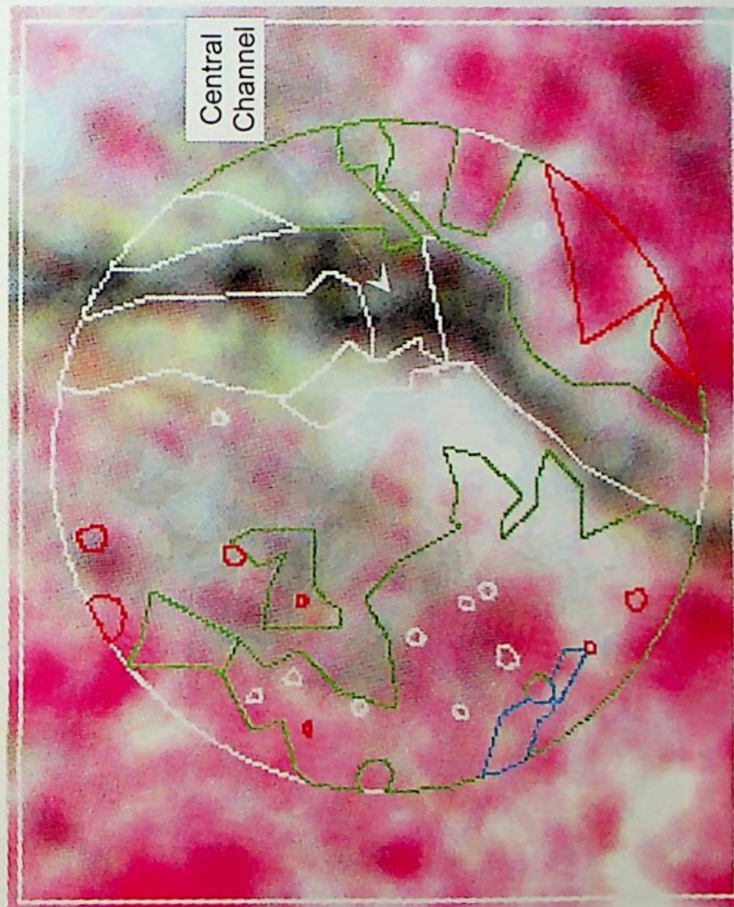
The 1997 imagery from all three sites (Table 5,6,7) possesses a high correlation among all bands, a potential indicator for poor data reduction in feature extraction. Yellow Creek 1 illustrates high loading in the first three principal components, PC1 in the infrared band (0.651), PC2 in the green band (0.609) and PC3 in the red band (0.793). Yellow Creek 2 shows a high loading of all three bands in the PC1 ($IR=0.581, R=0.572, G=0.579$), and significant results in the green band in the PC2,3 (0.515),0.632). In Yellow Creek 3, the red band illustrates a relatively low loading, a potential candidate for omission from image processing.

Geobiophysical Models

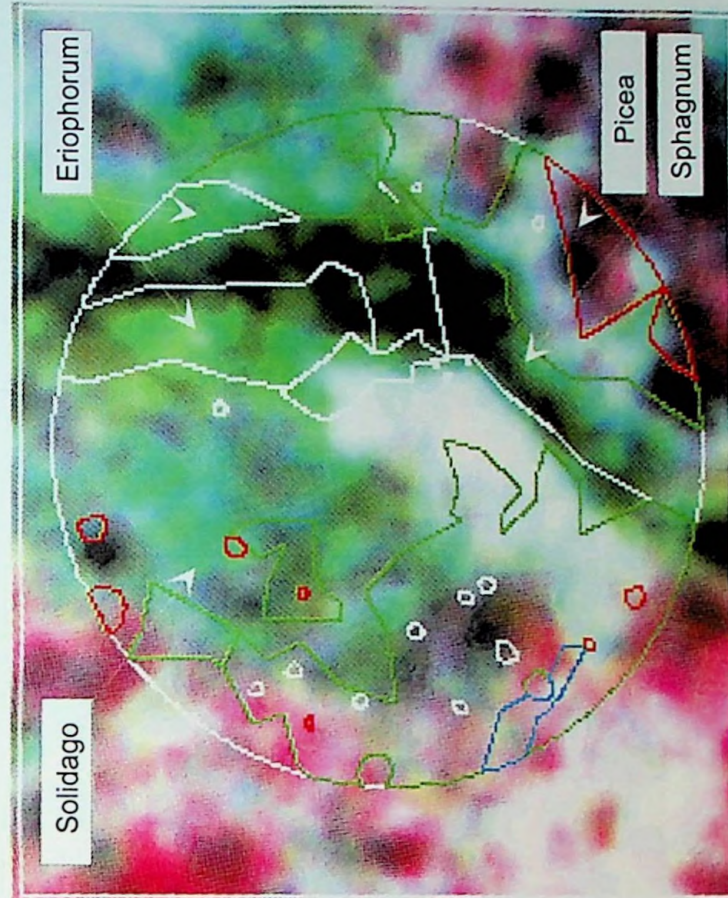
Yellow Creek 1

The Yellow Creek 1 site mapped with vegetation physiognomic associations vector data overlaid with processed 1995 imagery demonstrate similar matching of patterns (Figure 28). Figure 29 illustrates this point with the Sphagnum sp. association acting as a precision indicator for the surface ground water flow through the site. Eriophorum sp. associations run parallel to the Sphagnum sp. association, which further demonstrate a high correlation to the mapped vegetation patterns. Solidago uliginosau and Picea ruben associations possess higher structural characteristics that are not as well defined but demonstrate a potential for feature extraction. Figure 30 utilizes the

Feature Extraction for Pattern Recognition in Two-Dimensional Geobiophysical Models for Cartographic Representation

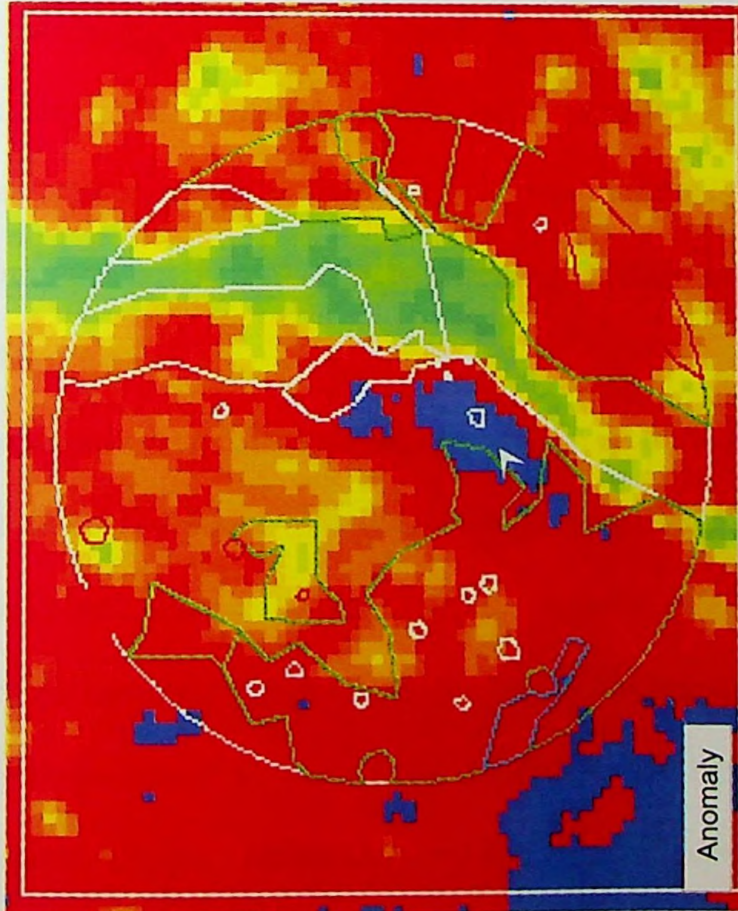


Linear Enhanced Three Band Color Infrared 1995 Imagery. Color coded vegetation vector overlay. Note the surface channel running North / South through the center of the site and the *Sphagnum* sp. moss association. Yellow 1, Davis, West Virginia. Figure 28



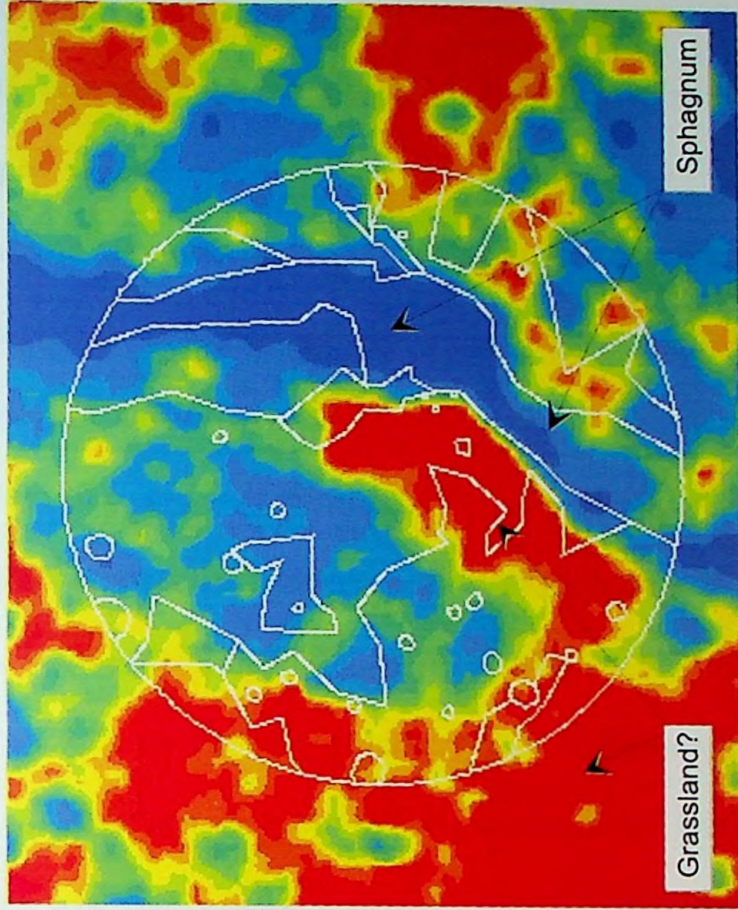
Histogram Equalization Enhancement of Three Band Color Infrared 1995 Imagery. *Eriophorum* sp. associations are identified parallel to the central channel. *Picea ruben*, *Prunus melanocarpa* and *Solidago uliginosa* associations can be distinguished. Yellow 1, Davis, West Virginia. Figure 29

Feature Extraction for Pattern Recognition in Two-Dimensional Geobiophysical Models for Cartographic Representation



Color Composite of the three bands with applied ISOCCLASS Unsupervised Classification producing fifteen classes. Level-sliced Transform Enhancement. Anomaly at center of site. Merging of detail. Color Infrared 1995 Imagery , Yellow 1, Davis, WV.a.

Figure 30



Applied PCA to three bands, creating composite band output, ISOCCLASS Unsupervised classification with 15 Classes, Level-sliced Transform Enhanced. Clearly defined Sphagnum sp. moss channel, potential grassland succession. Color Infrared 1995 Imagery, Yellow 1, WV.a

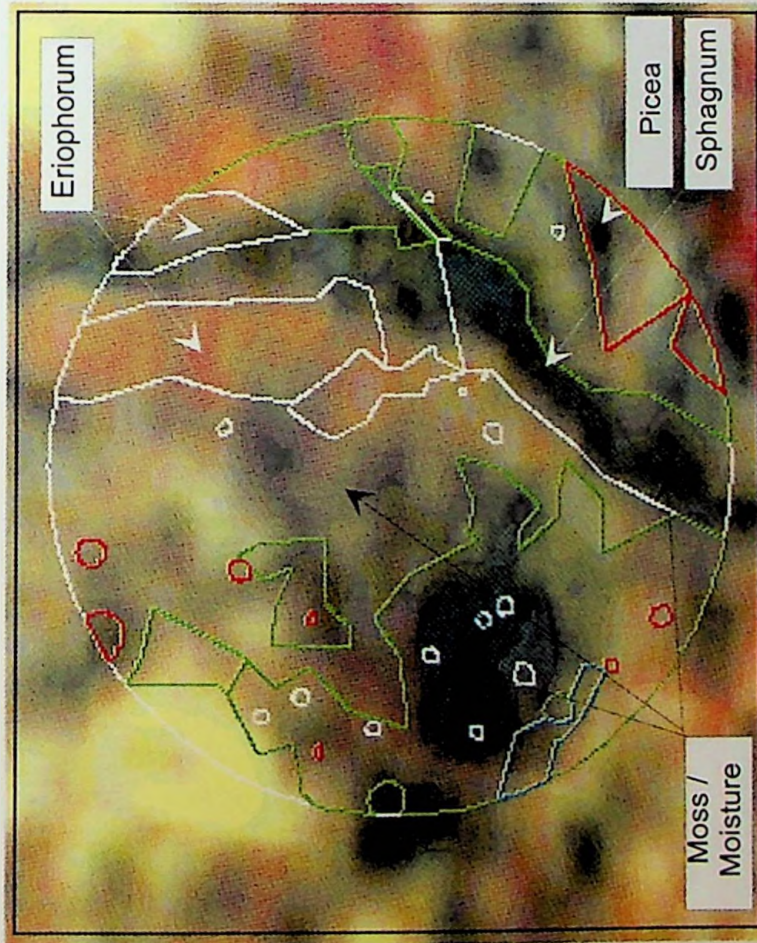
Figure 31

the ISOCLASS unsupervised classification producing 15 classes within the Yellow Creek 1 region. Results demonstrate a smoothing of spectral patterns inconsistent with the majority of mapped vegetation associations except for the Sphagnum sp. and succession grassland community. Figure 31 portrays the Principal Components with 1,2,3 weighting of all three bands with unsupervised classification resulting in enhancement of the Solidago uliginosau association pattern.

Two-dimensional geobiophysical models with the processed 1997 CIR imagery for Yellow Creek1 illustrate the Sphagnum sp. and Eriophorum sp. associations (Figure 32). In addition, a moisture pattern and/or dense population of Polytrichum sp. moss appears to be present to the left of the model. Figure 33 illustrates the similarity to the sphagnum sp. association and the identified area using the first Principal Component and merging the data sets into a pseudocolor composite image. Figure 34 extends this investigation by utilizing Principal Components 1,2,3 as indicated from the statistical analysis. The resulting GBPM demonstrates a larger impacted area indicating a more likely relationship with moisture. In addition, unsupervised classification with 15 classes was applied to the PCA 1,2,3 1997 imagery producing a closer match to the Sphagnum sp. association (Figure 35).

The three-dimensional geobiophysical models accentuate findings presented by two-dimensional models by draping the vegetation physiognomic association vector data sets and the processed imagery of the Digital Elevation Models DEM's (Figures 19,20,21). Figure 50 confirms the close associations of the Sphagnum sp. to low-order hydrology by correspondence to the central channel in the 1995 processed imagery (Figure 28). The drier raised area at the center of the site shows a potential area for

Feature Extraction for Pattern Recognition in Two-Dimensional Geobiophysical Models for Cartographic Representation



Three bands Linear Enhanced Color Infrared 1997 Imagery. Notable central channel, Observed smoothing of the spatial boundaries. Potential accumulation of moisture or development of *Sphagnum* sp. / *Polytrichum* sp. communities. Yellow 1, Davis, West Virginia.

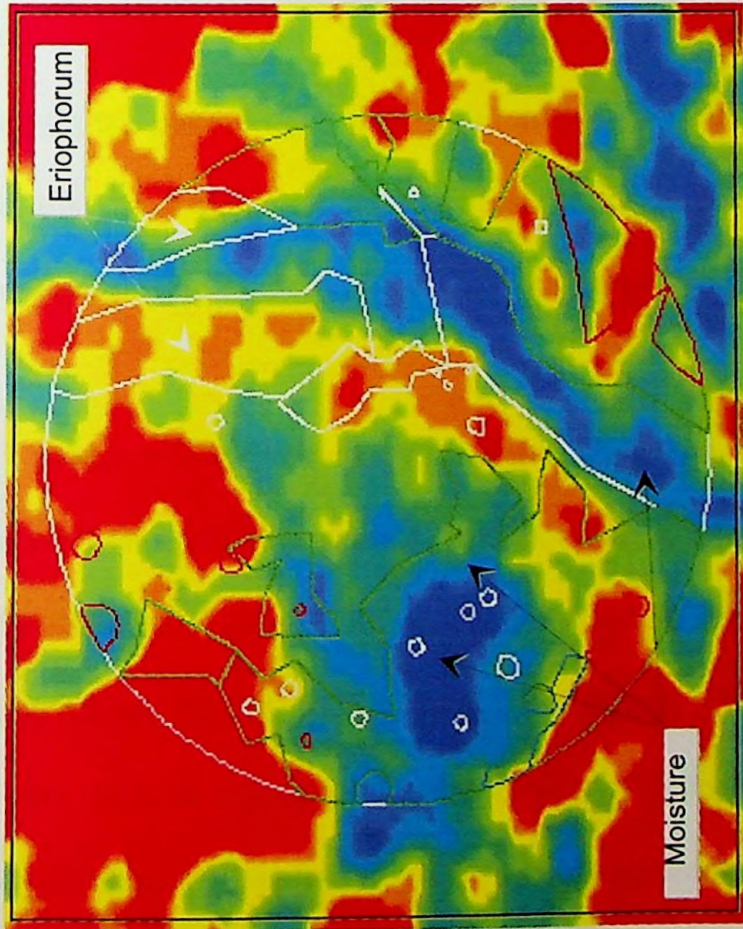
Figure 32



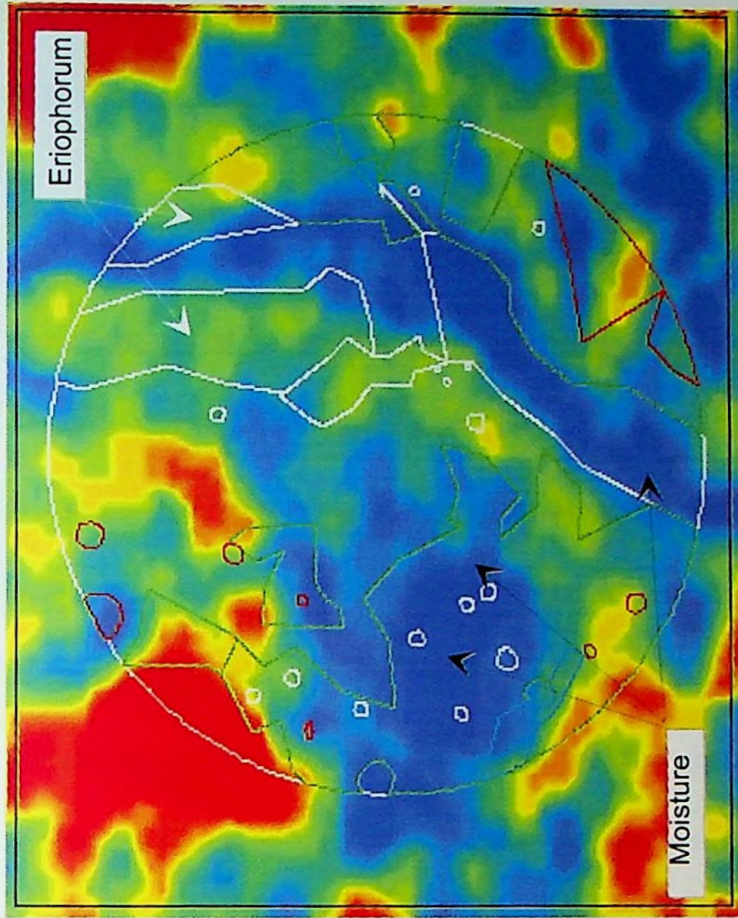
Three bands of CIR 1997 with PC1,2,3 imagery producing single pseudocolor composite. Level-sliced enhancement. Region 1 demonstrating similar characteristics to the central channel. Single band composite smoothes spectral detail in spatial domain. Y1, W Va.

Figure 33

Feature Extraction for Pattern Recognition in Two-Dimensional Geobiophysical Models for Cartographic Representation



Applied PCA 1,2,3 to three bands with Pseudocolor Composite output, Level-Sliced Enhanced Color Infrared 1997 Imagery. Potential signature within Eriophorum sp. association. Blue color indicative of moisture, extensive spatial distribution. Yellow1. WVa. Figure 34



Applied PCA 1,2,3 to three bands with pseudocolor composite output. Unsupervised 15 classes Level-Sliced enhanced CIR 1997 Imagery. Eriophorum sp. association spectral pattern not as visible. Yellow 1, Davis, West Virginia. Figure 35

succession by non-wetland communities (Figure 51). To the west is a small basin capable of collecting moisture from surface runoff from the north and west (Figure 52).

Yellow Creek 2

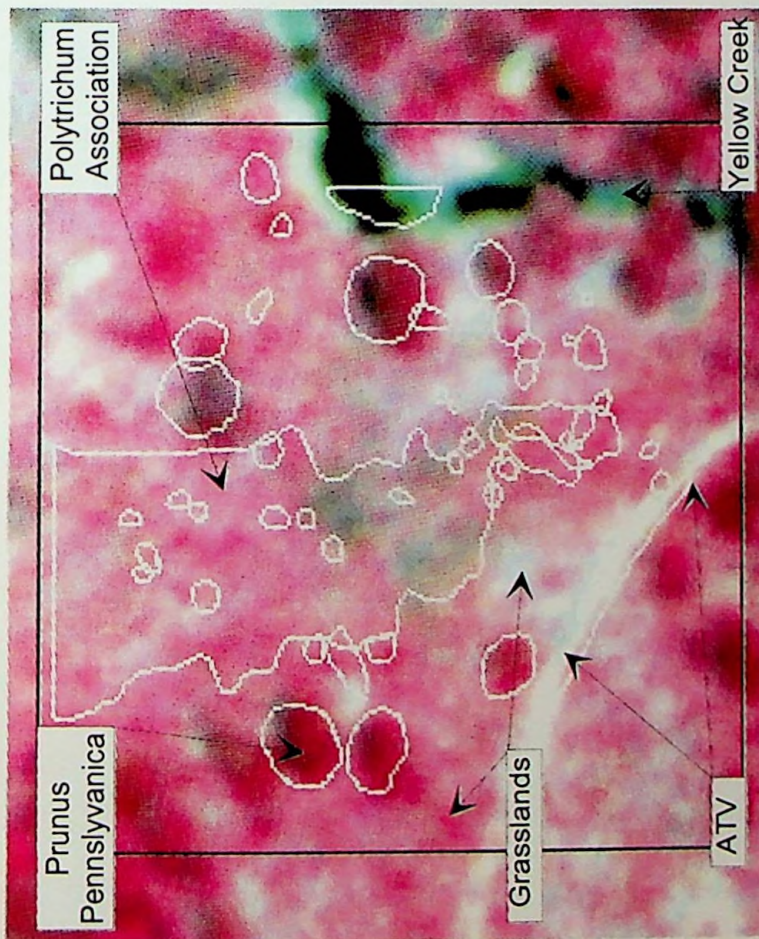
Yellow Creek 2 followed a similar procedure as Yellow Creek 1 for the development of geobiophysical models. The 1995 imagery with linear enhancement differentiates the Yellow Creek, ATV trail and tall trees within the boundaries of the site (Figure 36). The dominant Polytrichum sp. feature identified from ground truth investigations is not apparent within the imagery. However, a darker pattern is present within the center of the Polytrichum sp. association that could potentially point to moisture being present at the surface. This feature is better defined with a level-sliced enhanced pseudocolor composite image (Figure 37). However, a consequence of applying the level-sliced transform is the loss of information by merging spectral information into evenly spaced classes. Figure 38 shows the potential moisture/Polytrichum sp. pattern by applying an unsupervised classification to all three bands similar to that of Yellow Creek 1 (Figure 28). Additional experiments with different input parameters and class sizes did not extract any new features from the 1995 imagery (Figure 39).

The 1997 linear enhanced imagery illustrates the same features as identified previously in the 1995 imagery except for a clearly defined Polytrichum sp. association matching the ground truth data (Figure 40). In addition, the trees greater than three meters in diameter Picea ruben, Prunus pennsylvanica and Betula alleghaniensis could be differentiated by the spectral signatures for this imagery (Figure 41). In Figure 42, an unsupervised classification was applied to the data to categorize the spectral patterns for

feature extraction. Using a total of 80 classes, the Polytrichum sp. association became distinguishable from the majority of the vegetation present in the scene providing separability. Figure 43 demonstrates the results of a Normalized Difference Vegetation Index (NDVI) ratio $(IR-R / IR+R)$ demonstrating the separability between Yellow Creek and Polytrichum sp. association.

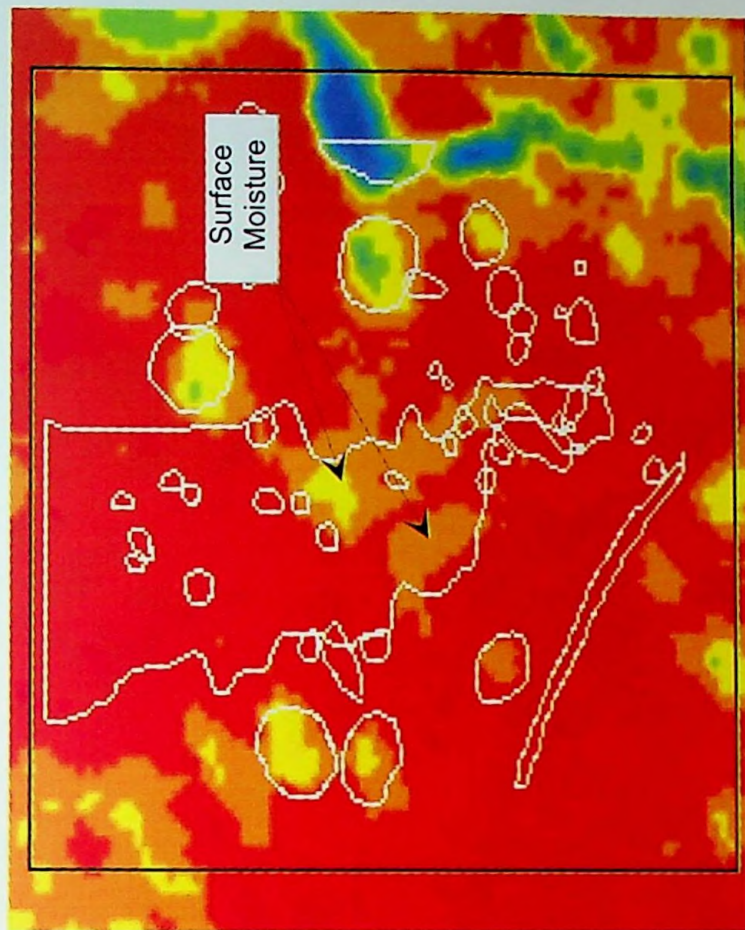
The three-dimensional geobiophysical models representing Yellow Creek 2 illustrate the relationships between trees, Polytrichum sp. association and the surface hydrology (Figure 53). The trees are located on higher ground on either Polytrichum sp. association that follows the main drainage pattern. Figures 54 & 55 show this relationship clearly with the unsupervised 1997 imagery (Figure 41) draped over the DEM for that site (Figure 20).

Feature Extraction for Pattern Recognition in Two-Dimensional Geobiophysical Models for Cartographic Representation



Three CIR bands applied with linear enhancement. Note that the moss associations are not apparent and merge readily with the grasslands. 1995 Imagery, Yellow 2, Davis, West Virginia.

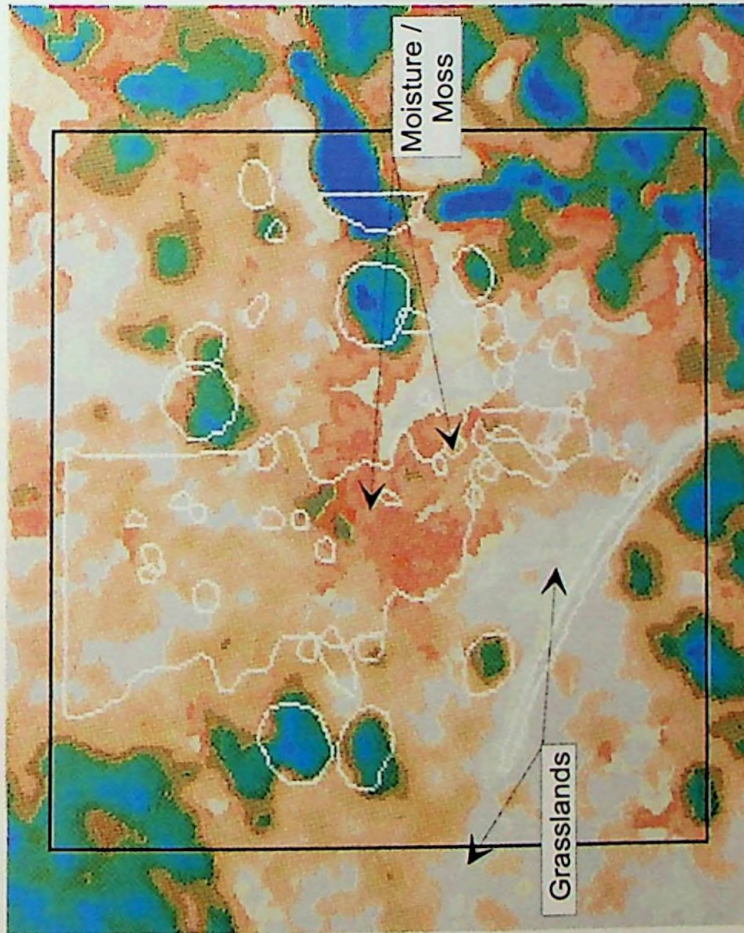
Figure 36



Vegetation Overlay with Color Composite Level-sliced Transform Enhanced Color Infrared Merging of spectral data by level-sliced enhancement can remove too much detail from the imagery.. 1995 Imagery, Yellow 2, Davis, West Virginia.

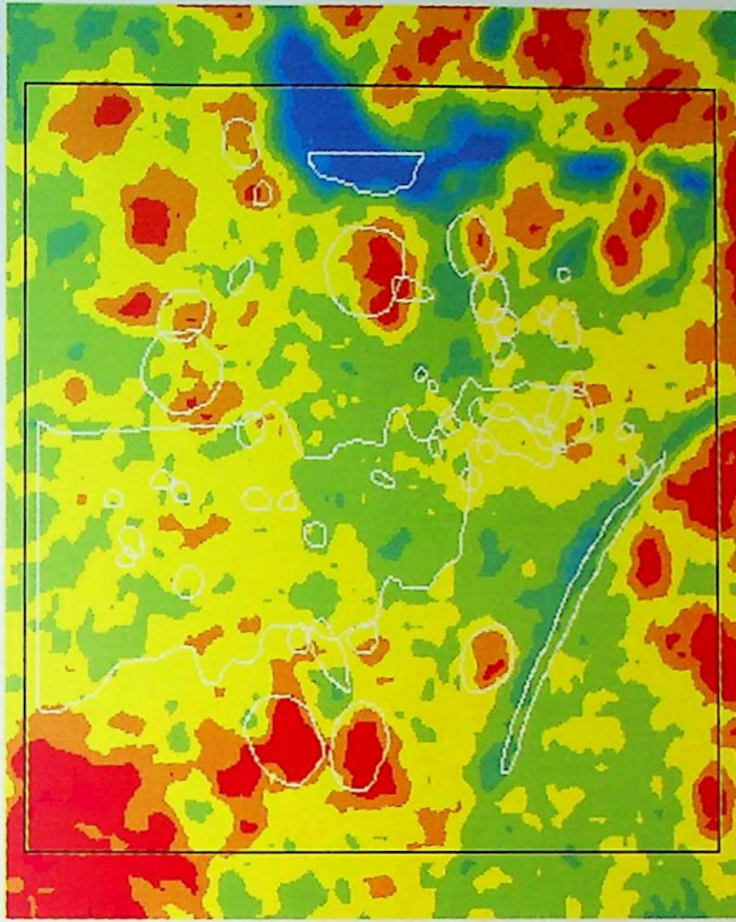
Figure 37

Feature Extraction for Pattern Recognition in Two-Dimensional Geobiophysical Models for Cartographic Representation



Pseudocolor CIR composite of ISOCCLASS unsupervised 60 classes with 95% Clip transform enhancement, 1995 Imagery. The center of the site showing the spatial characteristics of the moisture association. Yellow 2, Davis, West Virginia.

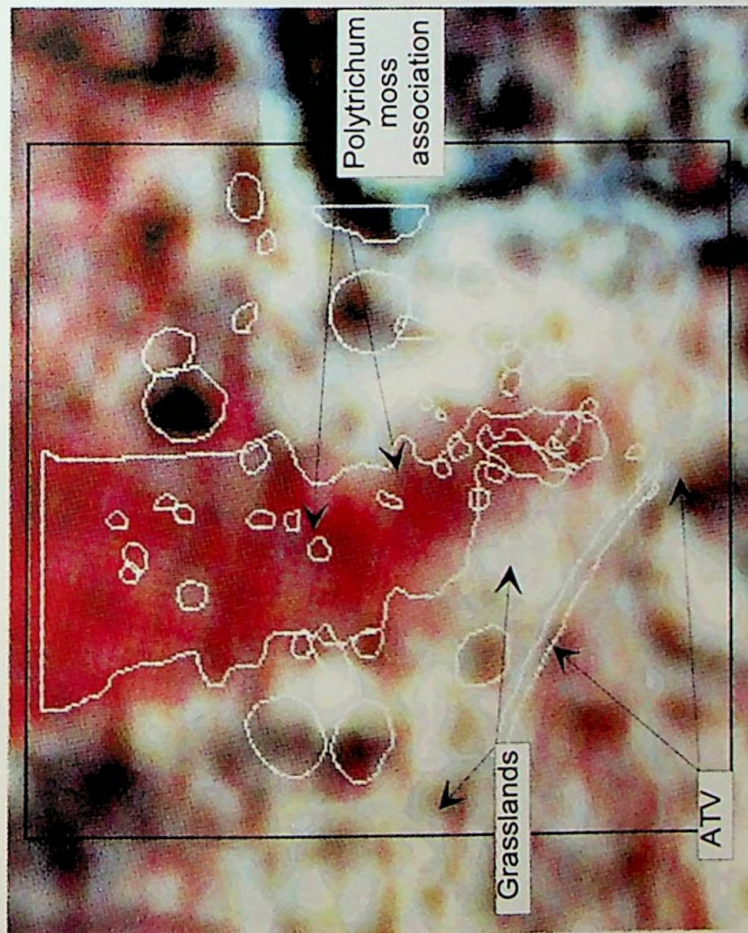
Figure 38



Pseudocolor CIR composite of NDVI $(IR - R) / (IR + R)$ with level-sliced transform enhancement applied to 1995 Imagery. Note that the smaller physiognomic vegetation associations and the *Polytrichum* sp. are indistinguishable. Yellow 2, Davis, WVa.

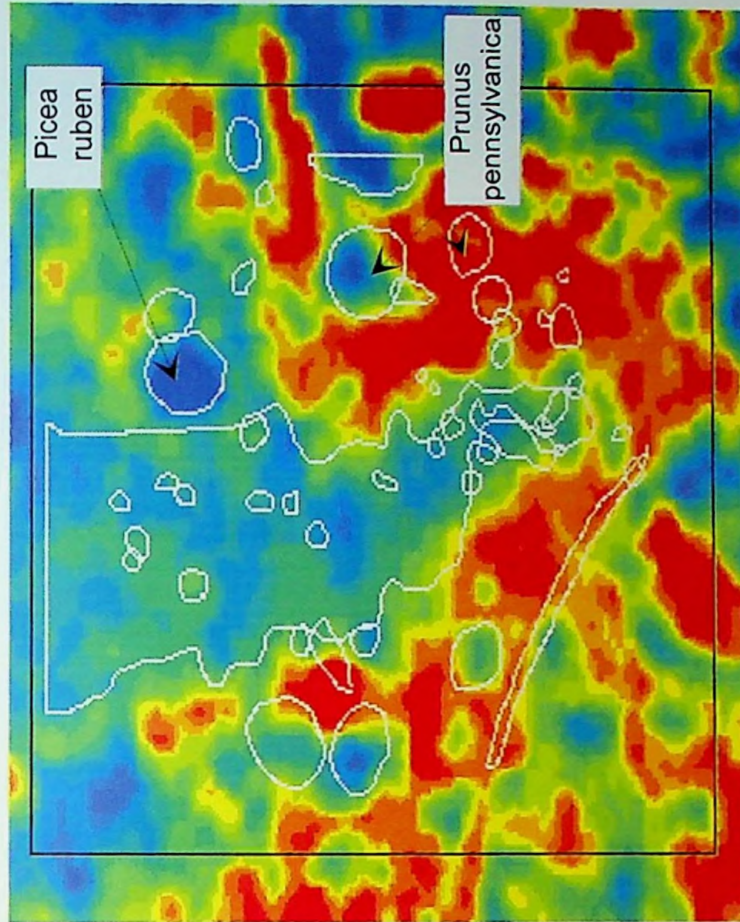
Figure 39

Feature Extraction for Pattern Recognition in Two-Dimensional Geobiophysical Models for Cartographic Representation



Three bands CIR linear enhanced CIR1997 Imagery. The Polytrichum sp. moss association feature provides a unique spectral signature. Physiognomic height classifications can be determined from imagery. Yellow 2, Davis, West Virginia.

Figure 40



Pseudocolor CIR composite with ISOCLASS unsupervised classification with 15 classes, and level-sliced enhanced 1997 Imagery. Note the Picea ruben is distinct from the Prunus pennsylvanica.

Yellow 2, Davis, West Virginia.

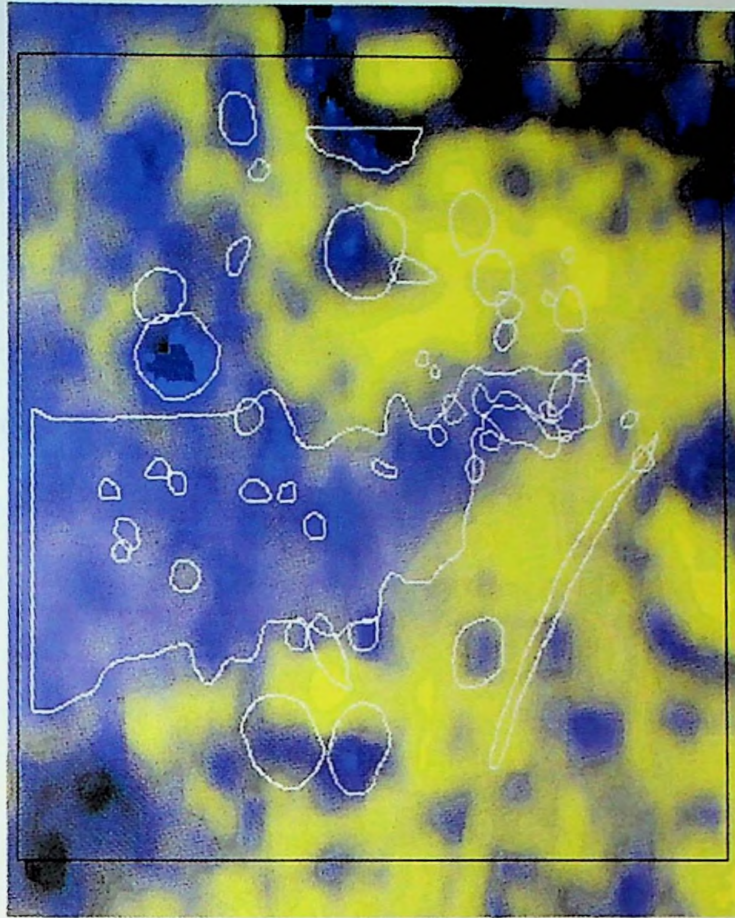
Figure 41

Feature Extraction for Pattern Recognition in Two-Dimensional Geobiophysical Models for Cartographic Representation



Pseudocolor CIR composite with unsupervised 80 classes Gaussian equalization enhancement 1997 imagery. Note the spatial correlation between the mapped *Polytrichum* sp. association and the image processed imagery. Y2 WVva.

Figure 42



1997 Infrared and red bands with NDVI $(IR - R) / (IR + R)$ and histogram equalization enhancement. Greater color contrast between the creek and the vegetation associations Yellow 2, Davis, West Virginia.

Figure 43

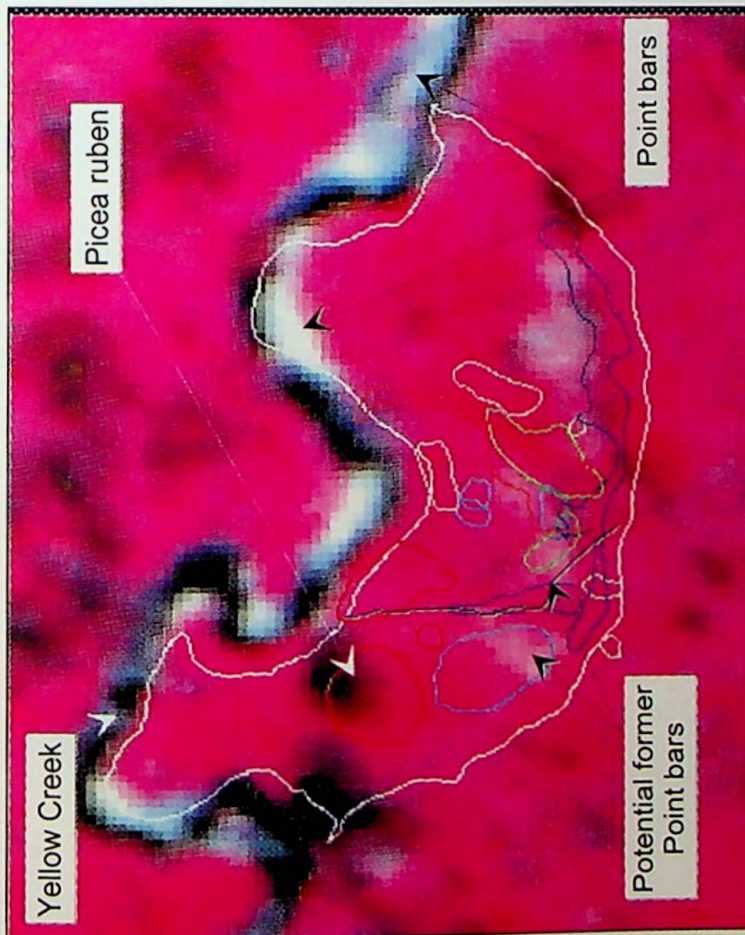
Yellow Creek 3

Two-dimensional geobiophysical models composed of enhanced 1995 imagery and mapped vegetation physiognomic associations can be viewed in Figure 44. Alluvial features visible within the former creek channel, are located toward the south of the site. A diffuse series of patterns with bright spectral signatures appear in six discrete groups. These patterns are similar in spectral composition to the point bars interleaved with the meandering Yellow Creek to the north. Figure 45 illustrates this feature by using the NDVI ratio with the infrared and red bands resulting in a bright yellow signature pattern. Figure 46 shows a mapped Eriophorum sp. association with a partial overlap to a darker extracted feature with lower spectral values. However, these patterns could be representative of moisture conditions developed within the former stream channel. Figure 47 further illustrates the relationship using the first three Principal Components.

The 1997 processed imagery shows similar spectral patterns to the 1995 imagery (Figure 48). The Eriophorum sp. association / moisture pattern is visually apparent within the pseudocolor composite image demonstrating a different spectral pattern to the Yellow Creek. PCA 1,2,3 with red and green bands did not provide additional extraction of surface features from the scene (Figure 49).

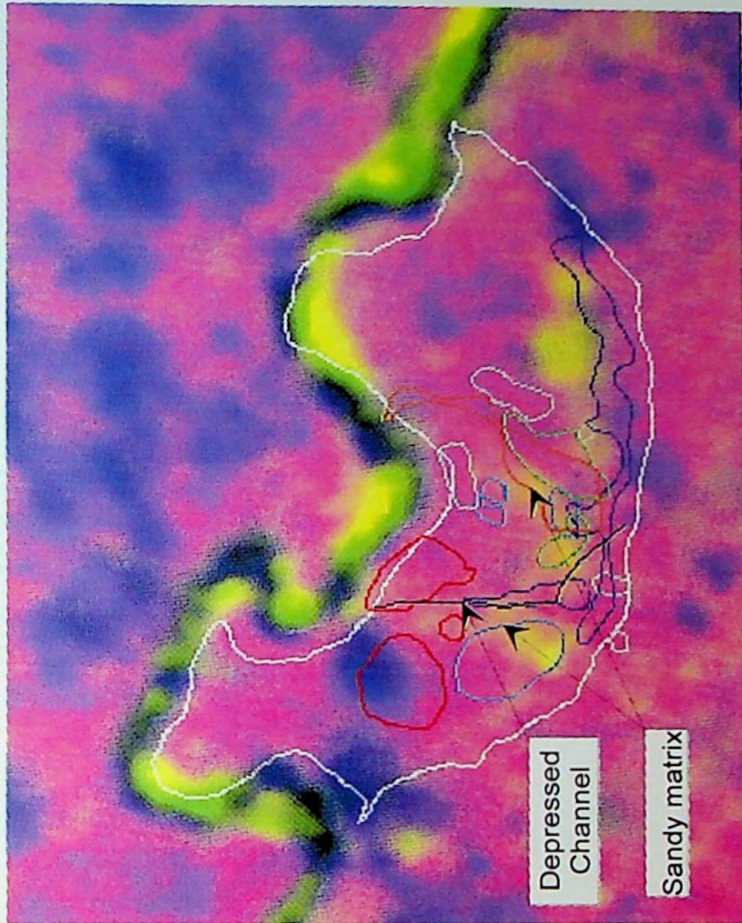
Three-dimensional models of Yellow Creek 3 further illustrate the relationship between the Eriophorum sp. association and moisture conditions with the micro-topographic depression of the former channels (Figures 56 & 57). Two identified surface runoff channels extend the Eriophorum sp. association toward Yellow Creek (Figure 56).

Feature Extraction for Pattern Recognition in Two-Dimensional Geobiophysical Models for Cartographic Representation



Three band CIR with histogram enhancement for the 1995 Imagery. Note the Red Spruce spatial and spectral characteristics, and sand banks of Yellow Creek.
Yellow 3, Davis, West Virginia.

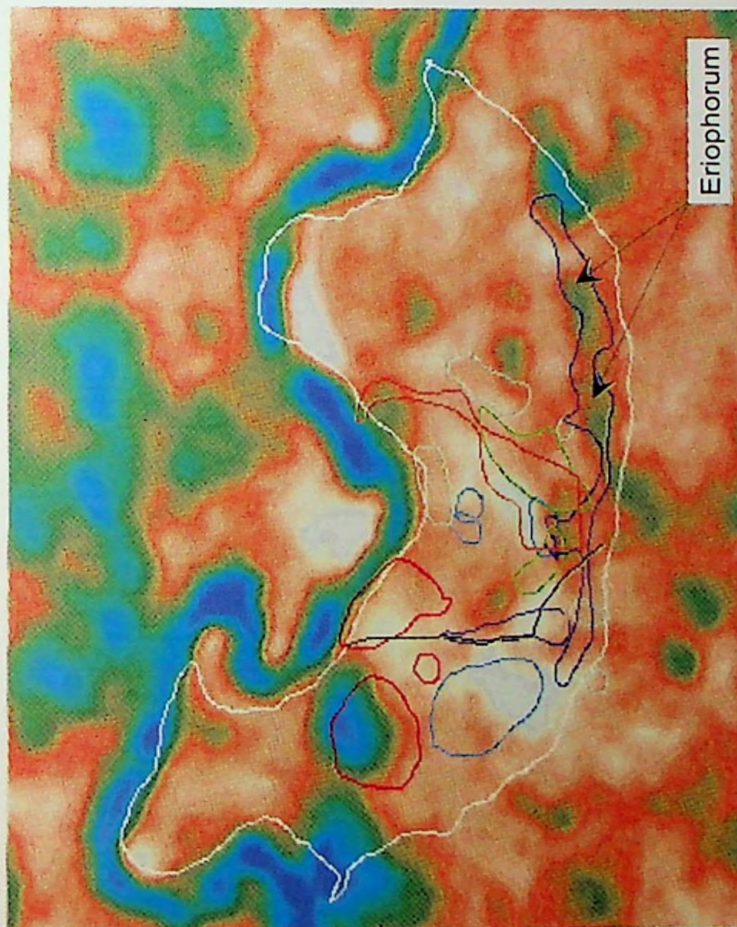
Figure 44



Two bands from 1995 imagery with NDVI $(IR - R) / (IR + R)$ and 95% Clip Enhanced in Red Band. The mapped depressed channel and bypass both are proximal to the yellow classes (sandy matrix)
Yellow 3, Davis, West Virginia.

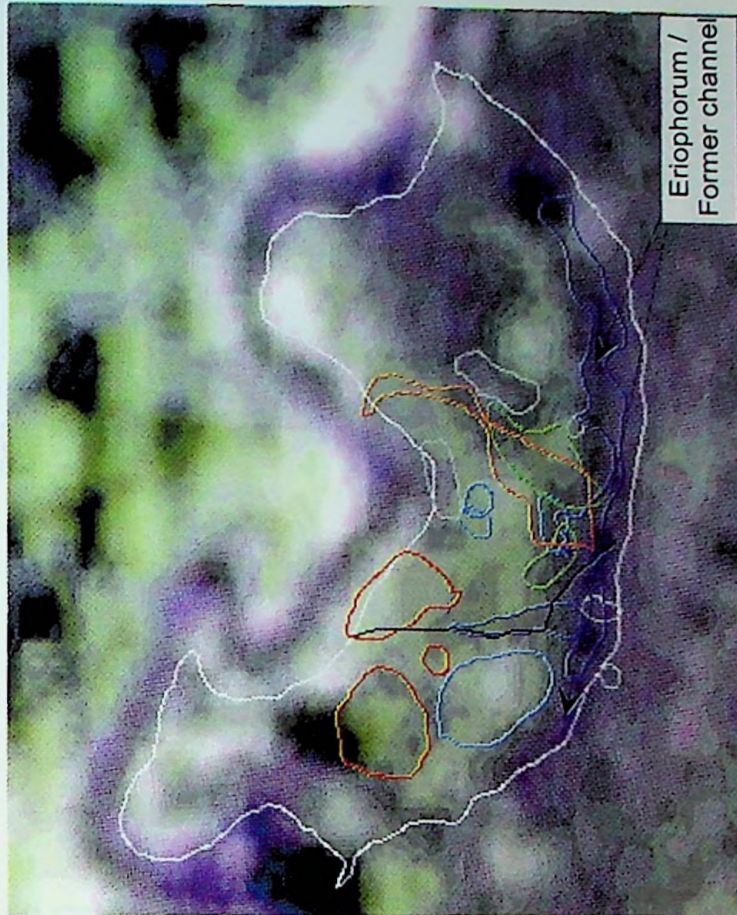
Figure 45

Feature Extraction for Pattern Recognition in Two-Dimensional Geobiophysical Models for Cartographic Representation



Pseudocolor CIR composite with 95% Clip enhancement to the 1995 Imagery. Merging of high values (brighter) due to clip. Eriophorum sp. association correlates spatially to dark spectral pattern within imagery. Yellow 3, Davis, West Virginia.

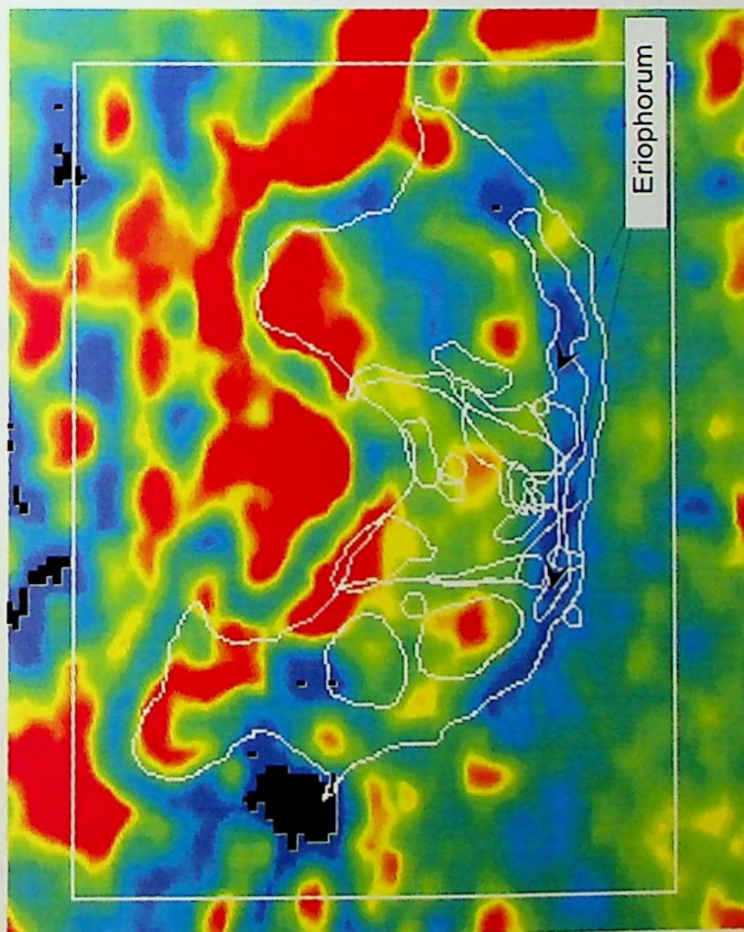
Figure 46



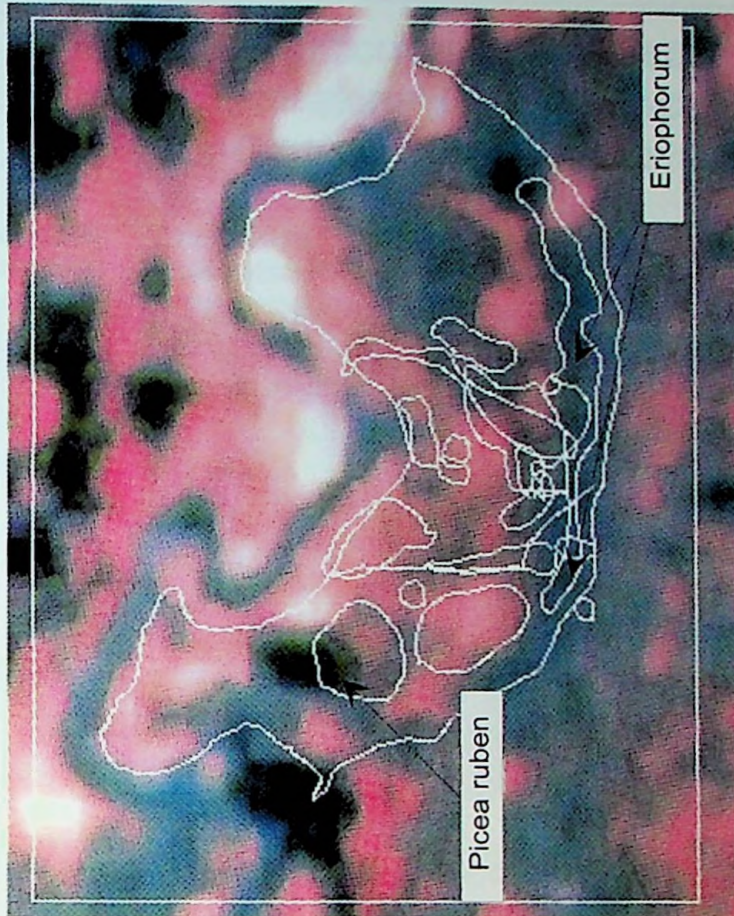
Three band 1995 CIR with PCA 1, 2, 3 and linear enhancement. The former channel / Eriophorum sp. vegetation association correlates with the spatial pattern seen in the imagery. Yellow 3, Davis, West Virginia.

Figure 47

Feature Extraction for Pattern Recognition in Two-Dimensional Geobiophysical Models for Cartographic Representation

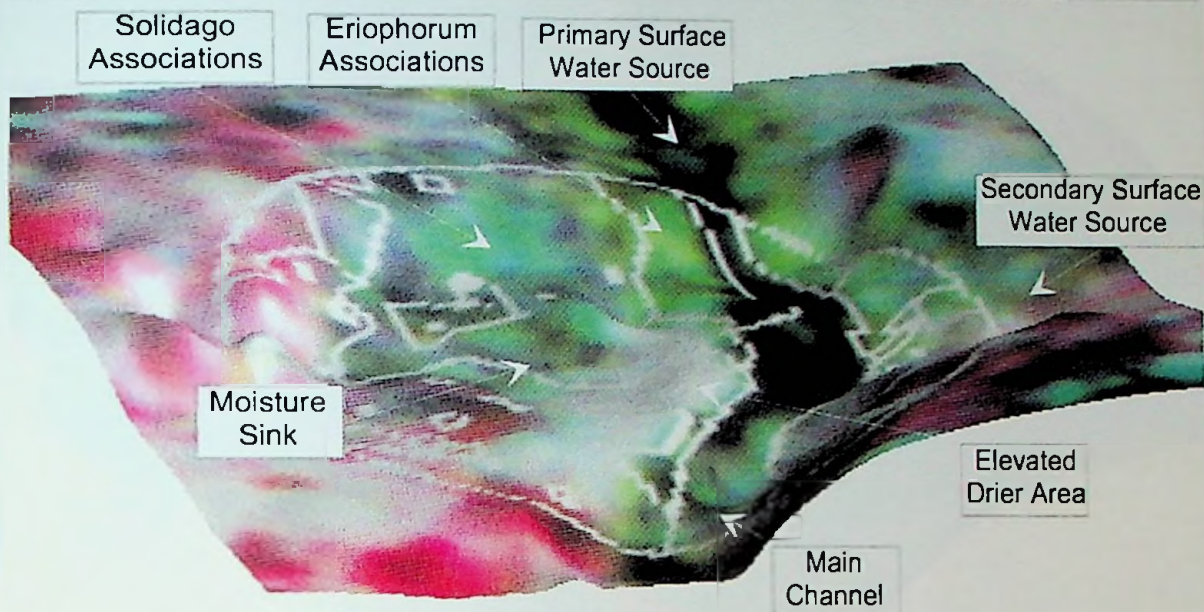


PseudoColor 1997 CIR Composite with 95% clip enhancement. The *Eriophorum*/former channel is providing a different spectral signature to creek and the banks. This indicates that the *Eriophorum* sp. association is more likely to be producing this feature. Yellow 3, Davis, West Virginia. Figure 48

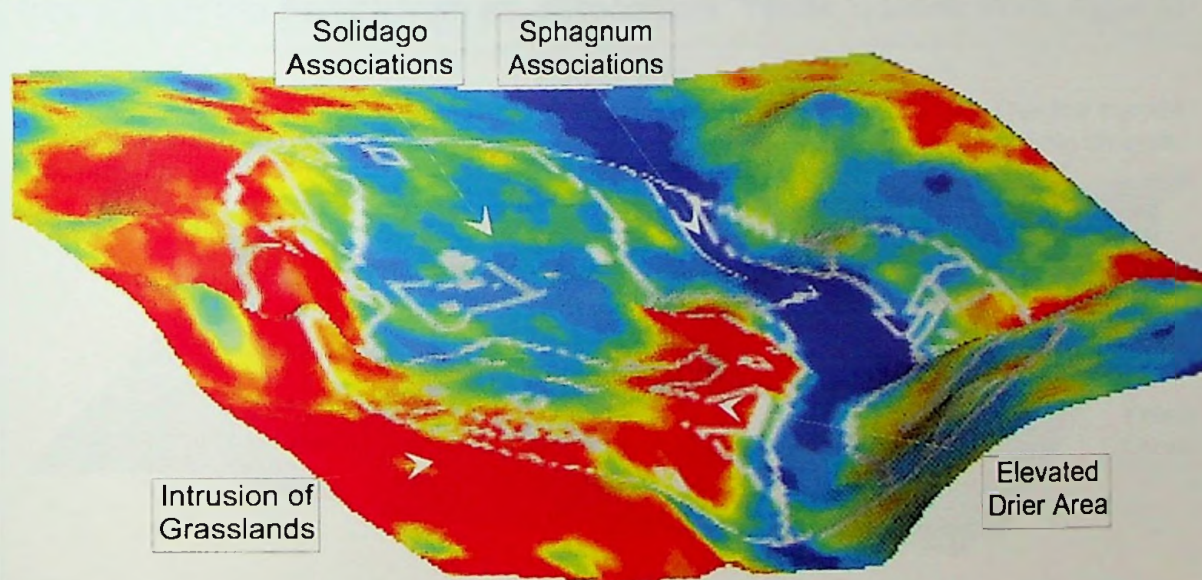


PCA1,2,3 applied to red and green bands from the CIR 1997 imagery with Gaussian transform enhancement. Utilized feature extraction techniques did not improve classification. Yellow 3, Davis, West Virginia. Figure 49

Feature Extraction for Pattern Recognition in Three-Dimensional Geobiophysical Models for Cartographic Representation

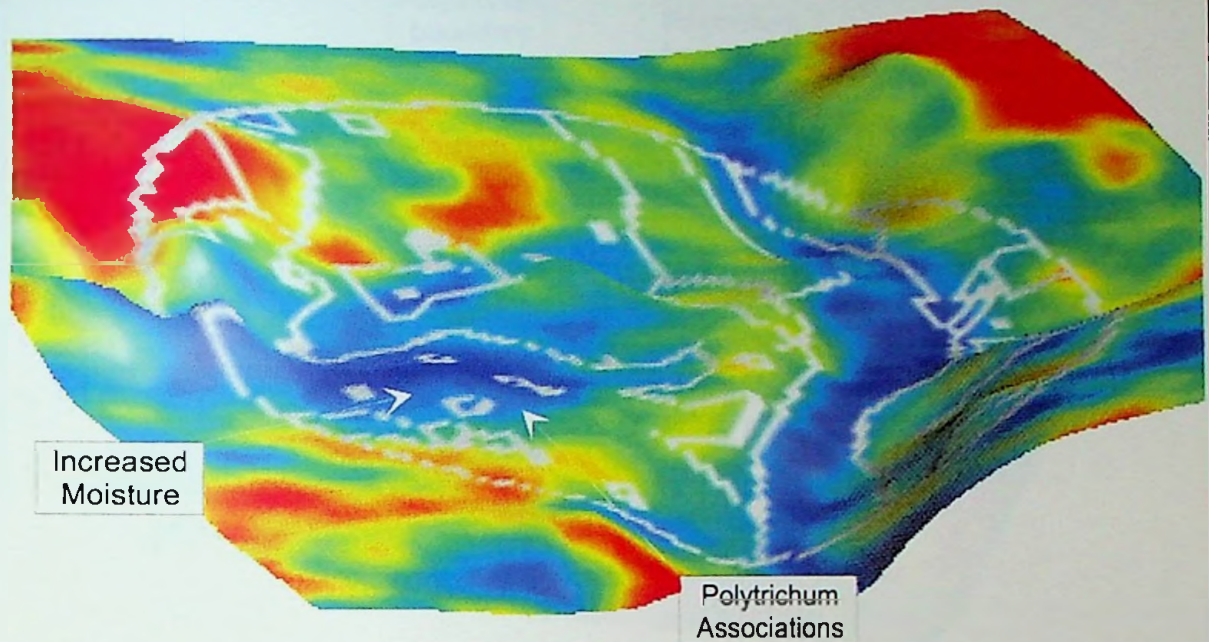


Three-dimensional representation composed of histogram equalized image processed CIR 1995 imagery draped over surveyed microtopography. Image spatial patterns are visible within the Eriophorum sp., Sphagnum sp., and Solidago sp. associations. Yellow 1, Davis, WV. Figure 50

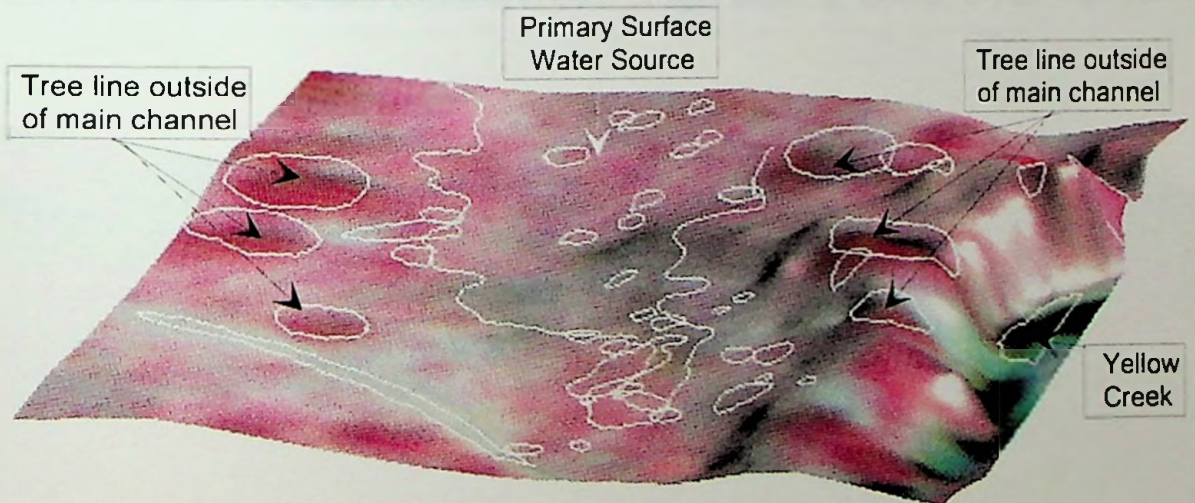


Three-dimensional representation composed of PCA1 pseudocolor composite with 15 unsupervised classes and level-sliced transform enhanced image processed CIR 1995 Imagery. Note the intrusion of grasses from the south-west along the elevated drier area. Yellow 1, Davis, WV. Figure 51

Feature Extraction for Pattern Recognition in Three-Dimensional Geobiophysical Models for Cartographic Representation

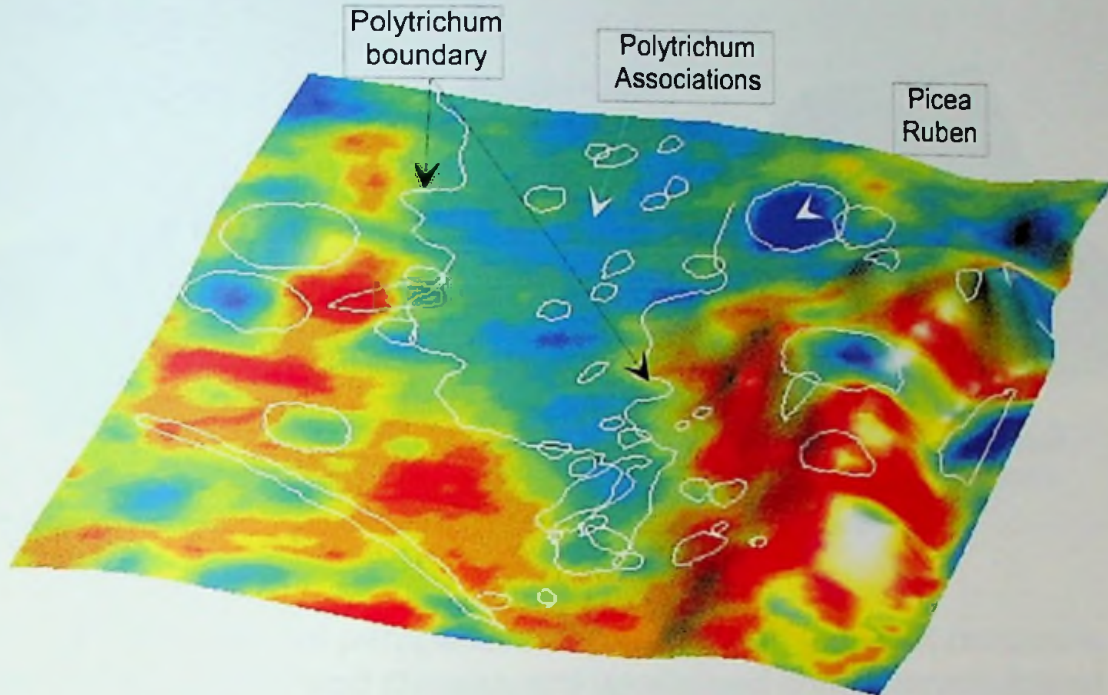


Three-dimensional representation composed of PCA1,2,3 composite with 15 unsupervised classes and 95% clip transform enhanced image processed CIR 1997 Imagery. Increased moisture levels and consistency throughout the Polytrichum sp. associations. Yellow 1, Davis, WV. Figure 52

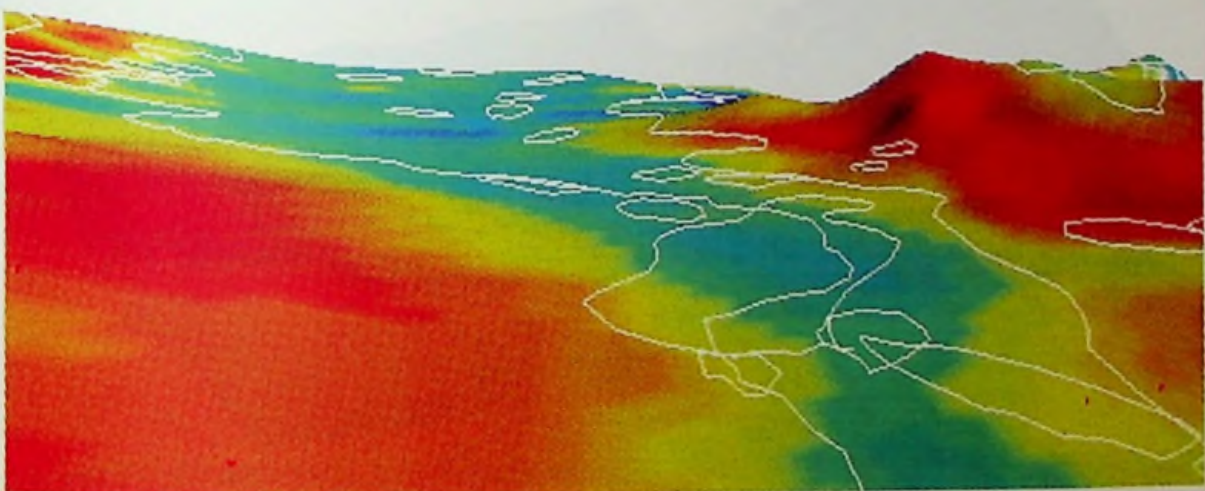


Three-dimensional representation composed of linear transform enhanced image processed CIR 1995 imagery draped over surveyed micro-topography. Trees greater than 2 meters in height and diameter are visible as features in the imagery. Note the geographical context in relation to the micro-topography. Yellow 2, Davis, WV. Figure 53

Feature Extraction for Pattern Recognition in Three-Dimensional Geobiophysical Models for Cartographic Representation

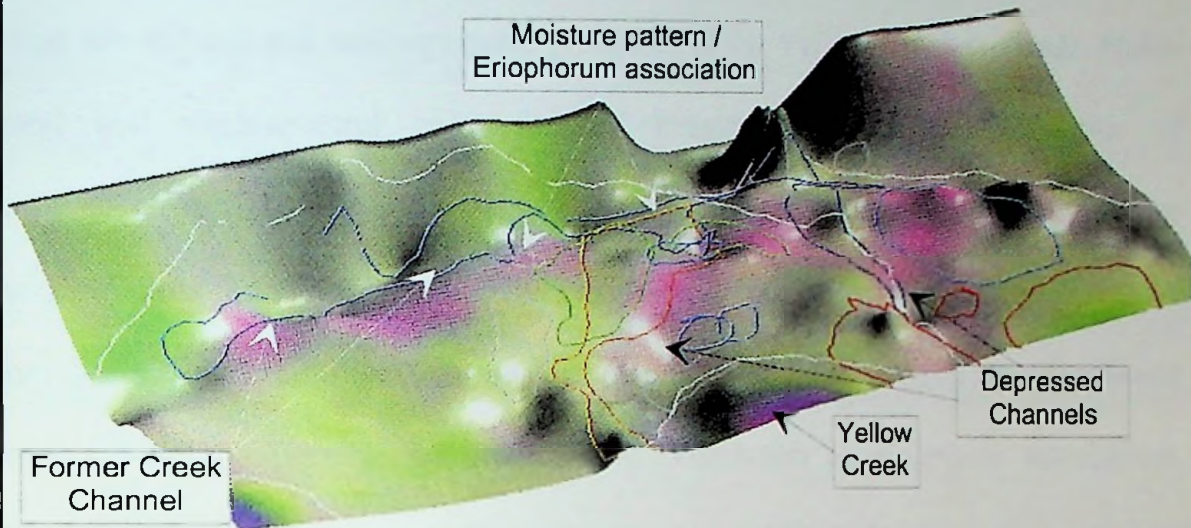


Three-Dimensional Perspective of a pseudocolor CIR 1997 composite image with 15 unsupervised classes and level-sliced enhancement. Note the separation of tree spectral patterns. Polytrichum sp. associations mapped very closely to the two classes shown in light blue. Y2, Davis, WV. Figure 54

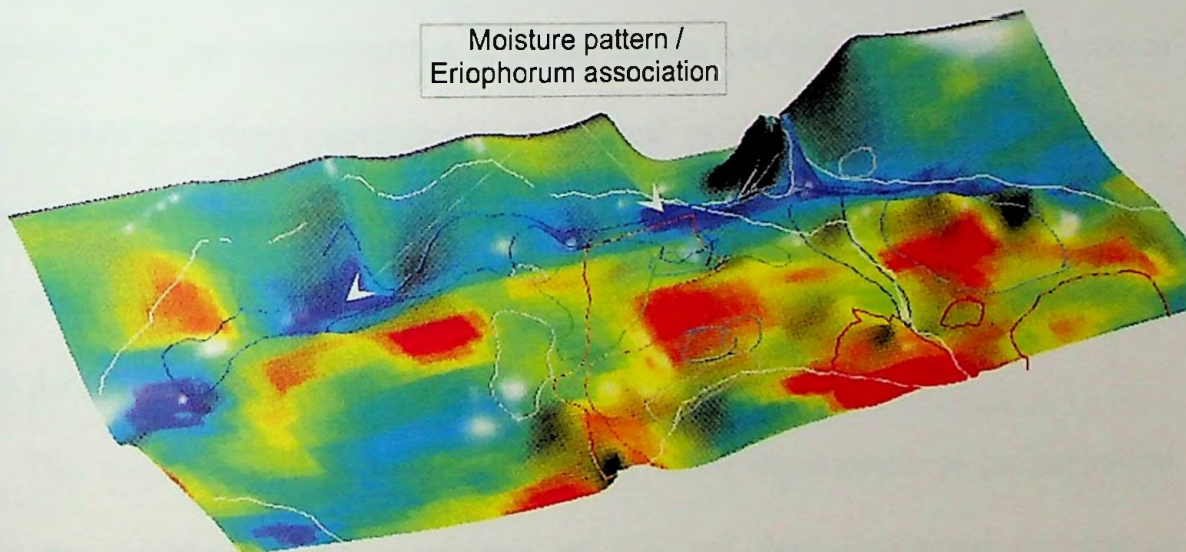


Three-dimensional flythrough of the model shown above (Figure 38). Note the subtle depression in the terrain and the mapped vegetation vector pattern. The relief is less than two meters and less than half a meter through the main channel. Yellow 2, Davis, West Virginia. Figure 55

Feature Extraction for Pattern Recognition in Three-Dimensional Geobiophysical Models for Cartographic Representation



Three-dimensional perspective of pseudocolor 1995 CIR composite with 15 unsupervised classes and level-sliced enhancement draped over micro-topography. Note the moisture pattern / *Eriophorum* sp. association with the micro-topography. Yellow 3, WVa. Figure 56



Three-dimensional perspective of pseudocolor CIR 1997 composite enhanced with 95% clip draped over micro-topography. *Eriophorum* sp. / moisture association visually apparent. Yellow 3, Davis, West Virginia. Figure 57

Chapter 5 Conclusions and Future Research Trends

Overall, this study demonstrated the utility of combining remotely sensed aerial imagery with ground truth data within the geobiophysical modeling environment for assessing the natural and anthropogenic processes of the Yellow Creek wetlands. Multi-temporal and multispectral color infrared imagery provided the foundation of geobiophysical models. The processing of imagery utilized feature extraction techniques to identify vegetation physiognomic associations and surface hydrological conditions by pattern recognition. Field investigations that employ digital technologies provide efficient and accurate data collection for ground truth. Vegetation physiognomic associations, micro-topography and surface hydrologic patterns contribute to the understanding of historical and recent trends in mountainous terrain wetlands. In particular, the emphasis is on red spruce, cotton grass and sphagnum moss as wetland relics of the last ice age as a sensitivity indicator of precipitation in surface runoff and throughflow as part of the hydroperiod to trend determination in global climate warming. The interaction between climate trends and their expression in the natural moisture conditions are reflected by changes in vegetation physiognomic associations with micro-topographic and subsequent effects on hydrology. Micro-topography highlights the usefulness of mountain terrain models for revealing patterns of global change.

The methods and techniques employed in the development of geobiophysical models are viable for the generation of two and three-dimensional cartographic representations in mountainous wetlands. However, development of these models requires a broad knowledge base of field parameters and the associated collection and processing. The mapping of the vegetation physiognomic associations with field based

GPS technologies increases efficiency, relative accuracy and transfer of data. Laser ranging theodolite surveys of micro-topography provide a level of accuracy above the required minimum mapping unit. Newer GPS technologies may provide greater efficiency for field collection of micro-topographic data, reducing the list of required field equipment whilst maintaining desired mapping standards.

Current automated registration processing techniques for vertical alignment of data layers are problematic due to inadequate integration and standardization of digital formats within the geospatial software community. Manual registration processes are subjective and inefficient requiring visual identification of features for control points. Each of the data layers requires iterative coordinate adjustment for greater registration accuracy, to improve the final quality of the geobiophysical models.

The development of two and three-dimensional cartographic representations of Yellow Creek wetlands from geobiophysical models is achieved using various combinations of standard image processing and visualization methods within ERMapper®5.5 software. Two-dimensional image processed models illustrate dominant vegetation physiognomic patterns of Sphagnum sp., red spruce, cotton grass relic communities in the dry 1995 and wet 1997 imagery. These communities are identifiable through combinations of image processing in the spectral and spatial domains demonstrating potential for time series monitoring in evaluating wetland change. Polytrichum sp. physiognomic associations possessing similar coverage appear to be more affected by changes in ground moisture and season. Three-dimensional geobiophysical models illustrate the correlation between relic vegetative physiognomic associations and surface hydrology patterns. Three-dimensional perspective and

flythrough modeling enhanced the cartographic representation of this relationship within the same model.

Applied feature extraction included combinations of unsupervised classification and principal component analyses did not produce vegetation physiognomic association boundaries that correlated to mapped ground truth vegetation boundaries. This observable fact may be due to zones of transition between associations and variations in density of dominant species that naturally occur within wetlands. However, this has the potential to increase the spectral variance within the vegetation physiognomic associations by merging spectral signatures, as a consequence, the within group variance can become the greater than the among group variance causing the misidentification of vegetation patterns. Smaller vegetation physiognomic associations, less than two meters are not identifiable for that same reason.

To achieve the long-term objective of monitoring changes in global climate, it will be necessary to extend current research methods. Advances in remote sensing systems and field mapping design are essential to accurately define vegetation physiognomic association for the relic species to identify changes within the wetlands. To achieve better discrimination between physiognomic groups and surface hydrology requires digital imagery of higher spatial and spectral resolution. Newer GPS technologies may improve upon current accuracy limitations providing a broader application in field mapping. Further evaluation of the soil and water chemistry with surface and subsurface hydrology may better indicate natural and anthropogenic causal relationships using geobiophysical models.

The limitations of client server technologies employed by the current system will be eradicated by the implementation of image processing web server technologies such as those provided by ER Mapper®. This will enable customization, efficient and secure data distribution and analysis by multiple user groups via standard web based browser technologies eg, Internet Explorer, Netscape Navigator.

Bibliography

- ADAMS, H.S., et al, 1985, *Growth-trend Declines of Spruce and Fir in the Mid-Appalachian Subalpine Forests*, Environmental and Experimental Botany, Vol. 25, pp. 315-325.
- ARNOLD, R.H., 1997, *Interpretation of Airphotos and Remotely Sensed Imagery*, Prentice Hall, Upper Saddle River, NJ.
- BARBOUR, M.G., J.H.BURK, and W.K.PITTS, 1980, *Terrestrial Plant Ecology*. Benjamin/Cummings Publishing Co., Menlo Park, CA.
- BLOEMER, H.H.L., et al, 1994, *A Laboratory With Out Walls for Advanced Resources Planning Systems in Mountainous Terrains*, Proceedings of the 3rd International Symposium on Remote Sensing in Cartography, Mendoza, Argentina.
- BLOEMER, H.H.L., et al, 1997, *A Comparative Analysis of Very High Resolution Multispectral Multistage Sensor Data in Feature Extraction for the Appalachian Mountains*, Presented Aug., 1996 and Published in the Proceedings of the 4th International Symposium on Remote Sensing in Cartography, in Karlstad, Sweden and Tromso, Norway sponsored by the space agencies of the Royal Academy of Sciences for Norway and Sweden.
- BLOEMER, H.H.L., J.O. BRUMFIELD, I.P. FARRAR, and D. SANDERSON, 1998, *Remote Sensing and Three Dimensional Cartographic Technologies in Modeling Mountainous Wetland Environments*. International Symposium on High Mountain Remote Sensing in Cartography, Hong Kong, China, sponsored by the Hong Kong University and the Chinese Academy of Sciences
- BLOEMER, H.H.L., J.O. BRUMFIELD, D. SANDERSON, I.P. FARRAR, J. LANGDON, and R. OBERLY, 1999, *Cartographic Representation Using a 3D Geographic Information System for the Assessment of Wetlands in Mountainous Areas*. International Symposium on Remote Sensing in Cartography, Humboldt State University, Humboldt. California.
- BOLSTAD, P.V., and J.L.SMITH, 1990, *Errors in GIS: Assessing Spatial Data Accuracy*, Journal of Forestry, Vol. 11.

- BRIDGHAM, S.D., et al, 1996, *Multiple Limiting Gradients in Peatlands: A Call For A New Paradigm*, WETLANDS, Vol.16, No.1, pp45-65.
- BRUMFIELD, J.O., et al, 1997, *Digital Evaluation of Optical Fourier Transforms of the Physiognomy for Vegetation Associations in Mountainous Terrain*. Presented in Aug., 1996 and Published in the Proceedings of the 4th International Symposium on High Mountain Remote Sensing in Cartography, in Karlstad, Sweden and Tromso, Norway, sponsored by the Space Agencies of the Royal Academy of Sciences for Norway and Sweden.
- BRUMFIELD, J., 1990, *Geobiophysical Modeling Systems*, Dissertation, Union Institute Graduate School, Cincinnati, OH.
- BURROUGH, P.A., 1986, *Principles of Geographic Information Systems for Land resource assessment*, Oxford University Press, New York, 193pp.
- CARTER, V., P.A., 1982, *Application of Remote Sensing Of Wetlands*, in *Remote Sensing and Resource Management*, Johannsen, C.J., and Sanders, J.L.,Eds., Soil Conservation Society of America, Akeny, IA.
- COWARDIN, L.M., et al, 1979, *Classification of Wetlands and Deepwater Habitats of the United States*. U.S. Fish & Wildlife Service, Report No. FWS/OBS70/31, Washington, D.C., p.103.
- DEHAYES, D.H., 1992, *Winter Injury and Developmental Cold Tolerance of Red Spruce*, Eagar and Adams (eds.), *Ecology and Decline of Red Spruce in the Eastern United States*, Springer-Verlag, New York Inc., pp. 295-333.
- DOUGLASS, W.J., 1995, *Environmental GIS Applications for Industrial Facilities*, Mapping Science Series, Lewis Publishers, CRC Press Florida.
- EVERITT, J.H., and D.E.ESCOBAR, 1989, *The Status of Video System for Remote Sensing Applications*, Proceedings of 12th Biennial Workshop on Color Aerial Photography and Videography, American Society of Photogrammetry and Remote Sensing, Falls Church, VA. P6-29.
- FARRAR, I.P., H.H.L. BLOEMER, D. SANDERSON, and J.O. BRUMFIELD, 1998, *Developing a Three-dimensional GIS for the Assessment of Wetlands and Related Environmental Concerns*. The Proceedings of the International Conference

InterCARTO4, Bernaul, Russia, Sponsored by the Ukraine Division of the Russian Academy of Science.

FEDERAL INTERAGENCY COMMITTEE FOR WETLAND DELINEATION, 1989, *Federal Manual for Identifying and Delineating Jurisdictional Wetlands. Cooperative Technical Publication.* U.S. Army Corps of Engineers, U.S. Environmental Protection Agency, U.S. Fish and Wildlife Service, and USDA Soil Conservation Service, Washington, D.C.

FORTNEY, R.H., 1975, *The Vegetation of Canaan Valley, West Virginia: A Taxonomical and Ecological Study*, Dissertation: Graduate School of West Virginia University.

FORTNEY, R.H., and D.STURM, 1998, *A Chronology of Post Logging Plant Succession Between 1945 and 1997 in Canaan Valley.* WV. Proceedings of the West Virginia Academy of Science, Vol. 70, No. 1, p24.

GERVIN, J., et al, 1996, *Determination of Forest Communities in a Temperate Mountainous Forest using Remotely Sensed and Ancillary Data of Varying Spatial Resolution*, Presented and Published in the International Archives of Photogrammetry and Remote Sensing, Commission vii, Vienna, Austria. Vol. xxxi, B7,

GOODCHILD, M.F., B.O.PARKS, and L.T.STEYART, 1993, *The State of GIS for Environmental Problem Solving, in Environmental Modeling with GIS.* Eds., Oxford University Press, Oxford, Chapter 2.

GORHAM, E., 1967, *Some Chemical Aspects of Wetlands Ecology.* Technical Mem. Committee on Geotechnical Research, National Research Council of Canada, No.90, pp.20-38.

HOWLAND, W.G., 1981, *Multispectral Aerial Photography for Wetland Vegetation Mapping*, Photogram. Eng. Remote Sensing, 46(1) 87-89.

JAHNE, B., 1991, *Digital Image Processing; Concepts, Algorithms and Scientific Applications.* New York: Springer-Verlag.

JEHNSON, J.R., 1986, *Introductory Digital Image Processing: A Remote Sensing Perspective.* (Englewood Cliffs, NJ: Prentice-Hall), pp. 254-271.

JI, W., 1993. *Integrating a Resource Assessment Model into Arc/Info GIS: a Spatial Decision Support System Development.* proceedings of ACSM/ASPRS Annual

- Conference. Lewis, A.J., Ed., American Society of Photogrammetry and Remote Sensing, New Orleans, LA.
- JOHNSON, A.H., et al, 1992, *Synthesis and Conclusion from Epidemiological and Mechanistic Studies of Red Spruce Decline*, Zagar and Adams (eds.), Ecology and Decline of Red Spruce in the Eastern United States, Springer-Verlag New York, Inc., pp. 385-411.
- LUDLUM, J.C., and T.ARKLE, 1971, *Blackwater Falls State and Canaan Valley State Park Resources, Geology, and Recreation*, WV State Park Series Bull, No.6, 60p.
- LYON, J.G., and J.MCCARTHY, 1995, *Wetland and Environmental Applications of GIS*, Lewis Publishers, CRC Press, FL.
- MACCONNELL, W., et al, 1992. Recording Wetland Delineations on Property Records. The Massachusetts DEP Experience 1972-1992. Department of Forestry and Wildlife Management, University of Massachusetts, Amherst, MA.
- MILLS, H.L., et al, 1963, *The Quantitative Physiognomic Analysis of Vegetation of the Florida Everglades*, Final Report Submitted to the USACOE, Waterways Experiment Station, Vicksburg, Mississippi, DA-22-079-eng-322.
- MITSCH, W.J., and J.G.GOSSELINK, 1993, *Wetlands*, Van Nostrand Reinhold.
- PAINE, R.T., and S.A.LEVIN, 1981, *Intertidal Landscapes: Disturbance and Dynamics of Patches*, Ecological Monographs, 51.
- PARKER, H.D., 1988, *The Unique Qualities of a Geographical Information System: a commentary*, Photogramm. Eng. Remote Sensing, 54, 1547-1549.
- PHILIPSON, W.R., 1997, *Manual of Photographic Interpretation*, 2nd ED. American Society of Photogrammetry and Remote Sensing, Bethesda, MD.
- SABINS, F.F., 1997, *Remote Sensing: Principles of Interpretation*, W.H. Freeman and Company, New York, 3rd Ed., p280.
- TEILLET, P.M., K.STAENZ, and D.J.WILLIAMS, 1997, *Effects of Spectral, Spatial, and Radiometric Characteristics on Remote Sensing Vegetation Indices of Forested Regions*, Remote Sens. Environ., 61, pp. 139-149.
- TERRY, N.G., 1996, *How to Read the Universal Transverse Mercator (UTM) Grid* Advanstar Communications Eugene, OR., GPS World.

- THOMPSON, M.M., and G.H.ROSEFIELD, 1987, *How Accurate is that Map?* Survey and Map. 31:57-64.
- TINER, R.W., 1977, An Inventory of South Carolina's Coastal Marshes, Tech. Rep. 23., South Carolina Marine Resource Center, Charleston, SC.
- TINER, R.T., 1999, *Wetland Indicators: A Guide to Wetland Identification, Delineation, Classification, and Mapping*, CRC Press LLC., pp. 347-380.
- WHITTAKER, R.H., 1970, *Communities and Ecosystems*, Collier-Macmillan, NY.

Software Inventory

Software	Version	Vendor	Web Site	Type
ArcView®	3.01	ESRI	www.esri.com	GIS
ArcExplorer®	1.1a	ESRI	www.esri.com	GIS
ERMapper®	5.5	ERM	www.ermapper.com	GIS
IDRISI®	2.008	Clark Univ.	www.idrisi.clarku.edu	GIS
Imagine®	6	ERDAS	www.erdas.com	GIS
Surfer®	6	Golden Soft.	http://www.goldensoftware.com	Map
AutoCAD®	14	Autodesk	www.autodesk.com	Draw
Designer®	4	Micrographix	www.micrografx.com	Draw
Visio Tech.®	5	Visio Corp.	www.visio.com	Draw
Photoshop®	5.5	Adobe	www.adobe.com	Image
Acrobat®	4	Adobe	www.adobe.com	Docs
Word®	97	Microsoft	www.microsoft.com	Docs
Excel®	97	Microsoft	www.microsoft.com	Table
NT4®	SP4	Microsoft	www.microsoft.com	OS
MSTAR®	N/A	Magellan	www.magellan.com	Conv
TOSCA®	1.0	Clark Univ.	www.idrisi.clarku.edu	DIG
FullShot®	6	Fullshot	www.inbit.com	Image
JASC MCP®	3	JASC Soft.	www.jasc.com	Image
EDM	Prof. Dewey Sanderson, Geology Dept. Marshall University, WVa.Conv.			

Hardware Inventory

Field Equipment

Name of Equipment	Vendor	Web Site
Global Positioning System	Magellan® ProMARK X-CP	www.magellan.com
Theodolite	Nikon® DM310 Total Station	www.nikonusa.com
Alidade / Plane table		www.yorksurvey.co.uk
Laser Range Finder	Leica®	www.leica-geosystems.com
Sonic Range Finder	SONIN®	www.sonin.com
Brunton Compass	Brunton®	www.brunton.com
Munsell Soils Color Chart	Munsell®	www.munsell.com
Soil Probe	Geoprobe®	www.geoprobe.com

Laboratory Equipment

Name of Equipment	Vendor	Web Site
Latitude Cpi	Dell®	www.dell.com
High Res. Digitizer	Calcomp®	www.gtcocalcomp.com
Flatbed High Res. Scanner	Nikon®	www.nikon.com

Appendix A – Description of the UTM Coordinate System

TERRY, N.G., 1996, How to Read the Universal Transverse Mercator (UTM) Grid
Advanstar Communications Eugene, OR., GPS World.

The Universal Transverse Mercator (UTM) grid is most appropriate for scales of 1:250,000 and larger. On large-scale maps such as U.S. Geological Survey (USGS) 1:24,000, 7.5 minute quadrangles, the simple numbers of the UTM grid make plotting precise locations easier than with the complex degrees, minutes, and seconds of latitude and longitude. For example, you might readily use the UTM grid while hiking to report the location of an emergency by cellular phone to 9-1-1 or to record the location of a favorite campsite or trailhead. The UTM grid has tremendous value for emergency service organizations.

The UTM grid is of particular interest to anyone using a GPS receiver because most models offer UTM as a coordinate system option. UTM coordinates simply measure in meters east and north from two perpendicular reference baselines. All USGS 1:250,000 and 1:100,000 topographic maps carry a full UTM grid. On those maps, grid lines are 10,000 meters (10 kilometers) apart. On 1:24,000 maps, grid lines are spaced 1,000 meters apart. Coordinates are written along the sides of a map designating specific grid lines or tic marks. The two larger numbers are known as principle digits. To plot coordinate values, read right, then up. Abbreviated coordinates can be used for locally defined areas (not larger than 100 kilometers x 100 kilometers). Abbreviated coordinates are always given as an even number of digits (as in Figure 1, 0491) so you know where to separate easting and northing coordinates. This allows you to abbreviate to the degree of precision you require, as will be shown later. A full UTM coordinate value defines a worldwide unique position ("map address").

Reading UTM Coordinates. Think of UTM grid coordinates as the drill hole's (geospatial) address. First check the bottom left corner of your map for the map's datum and for its grid. The default datum for most GPS receivers is the World Geodetic System of 1984 (WGS 84). A mismatch between datums on your map and GPS receiver can cause errors of several hundred meters. On the USGS 7.5 minute, 1980 edition Sierra Madera NE, Texas map sheet, the note reads like this: 1,000-meter Universal Transverse Mercator grid, zone 13 1927 North American Datum While most USGS topographic maps use the 1927 North American Datum (NAD 27), maps are being slowly revised to NAD 83. When building a waypoint or writing a grid coordinate, the first part is the grid zone. In this case, we see in the note it is Zone 13.

To find a complete UTM coordinate, read right to the grid intersection before your place of interest. In this case, it's line 704, also known by its principle digits as line 04. Then count grid lines up to the intersection (for example, 3391 or 91). The abbreviated coordinate 0491 (think 04/91) gives the location to within 1,000 meters. Measuring right in meters from line 04, we find the drill hole is another 250 meters. The complete easting component is 704250E. Measuring up in meters from grid line 91, the drill hole is another 520 meters. The complete northing component is 3391520N. The complete grid coordinate for the drill hole is Zone 13 704250E 3391520N or abbreviated as 04259152 (think: 0425/9152).

This coordinate defines a location of the drill hole to within 10 meters, or about the size of a modest home. The abbreviated coordinates can be seen embedded in the full coordinates:

04259152 = 0425 9152
Zone 13 704250E 3391520N

In the field, an expedient grid reader can be made by tearing off a corner of the map and marking both edges out from the corner in 100-meter increments. Use the map's bar scale as a guide. Plastic grid readers are available from USGS and commercial vendors. With these you can easily measure coordinates to 10 meters, or near the precision of the USGS 7.5-minute map. One of the great features of UTM coordinates is the ability to provide a more precise location by simply adding a pair of digits to abbreviated coordinates.

Appendix B – An Example of the Gridding Algorithm Report.

Data Filter Report

Source Data File Name: C:\My_Documents\Y2\Surfer\xyzcor1.dat
X Column: A
Y Column: B
Z Column: C

Data Counts

Number of Active Data: 212
Number of Original Data: 212
Number of Excluded Data: 0
Number of Deleted Duplicates: 0
Number of Retained Duplicates: 0
Number of Artificial Data: 0

Filter Rules

Duplicate Points to Keep: First
X Duplicate Tolerance: 0
Y Duplicate Tolerance: 0

Exclusion Filter String: Not In Use

Data Statistics Report

Data Counts

Number of Active Data: 212

Number of Original Data: 212
Number of Excluded Data: 0
Number of Deleted Duplicates: 0
Number of Retained Duplicates: 0
Number of Artificial Data: 0

X Variable Statistics

X Range: 75.92
X Midrange: 636395

X Minimum: 636357
X 25%-tile: 636387
X Median: 636410
X 75%-tile: 636427
X Maximum: 636433

X Average: 636406
 X Standard Deviation: 21.9955
 X Variance: 483.803

Y Variable Statistics

Y Range: 81.26
 Y Midrange: 4.33407E+006
 Y Minimum: 4.33403E+006
 Y 25%-tile: 4.33406E+006
 Y Median: 4.33408E+006
 Y 75%-tile: 4.33409E+006
 Y Maximum: 4.33411E+006
 Y Average: 4.33408E+006
 Y Standard Deviation: 20.4757
 Y Variance: 419.254

Z Variable Statistics

Z Range: 2.74
 Z Midrange: 99.37
 Z Minimum: 98
 Z 25%-tile: 98
 Z Median: 99.37
 Z 75%-tile: 99.7
 Z Maximum: 100.74
 Z Average: 99.1583
 Z Standard Deviation: 0.760719
 Z Variance: 0.578693
 Z Coef. of Variation: 0.00767176
 Z Coef. of Skewness: -0.420201

Inter-Variable Correlation

	X	Y	Z
X:	1	-0.0101096	-0.821242
Y:		1	0.0868447
Z:			1

Inter-Variable Covariance

	X	Y	Z
--	---	---	---

X:	483.803	-4.55322	-13.7414
Y:		419.254	1.35275
Z:			0.578693

Gridding Report

Search Rules

Use All Data: true

Gridding Rules

Gridding Method: Kriging
Kriging Type: Point

Semi-Variogram Model

Component Type: Linear
Variogram Slope: 1
Anisotropy Angle: 0
Anisotropy Ratio: 1

Polynomial Drift Order: 0
Kriging standard deviation grid: no

Grid Summary

Grid File Name: C:\My_Documents\Y2\Surfer\xyzcor1.grd

Minimum X: 636357
Maximum X: 636433

Minimum Y: 4.33403E+006
Maximum Y: 4.33411E+006

Minimum Z: 97.855
Maximum Z: 100.779

Number of Rows: 100
Number of Columns: 93

Number of Filled Nodes: 9300
Number of Blanked Nodes: 0
Total Number of Nodes: 9300

Appendix C – Glossary of All Image Processing

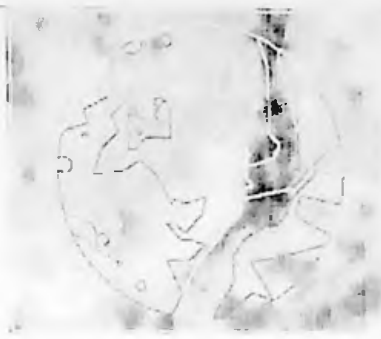
 <p>Blurred image of a person's face.</p>	 <p>Blurred image of a person's face.</p>	 <p>Blurred image of a person's face.</p>
 <p>Blurred image of a person's face.</p>	 <p>Blurred image of a person's face.</p>	 <p>Blurred image of a person's face.</p>
 <p>Blurred image of a person's face.</p>	 <p>Blurred image of a person's face.</p>	 <p>Blurred image of a person's face.</p>

Yellow Creek Site 1 1995 Imagery



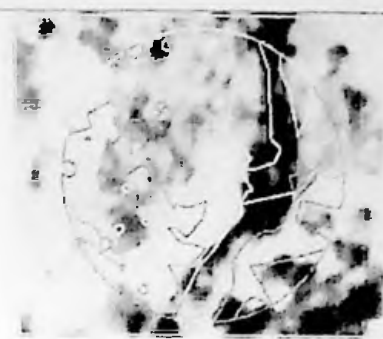
3 bands with vegetation overlay, linear enhancement.

Plate 1



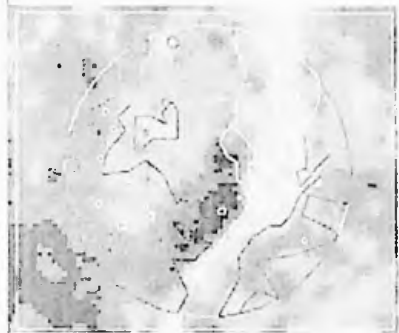
3 bands with veg overlay, histogram equalization enhancement in green band

Plate 2



3 bands with vegetation overlay, with histogram equalization enhancement in all three bands

Plate 3



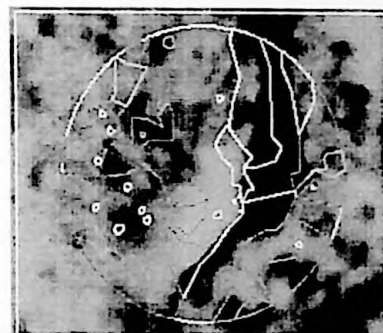
Composite, veg overlay, with Level slice transform enhancement isoclass 15 classes and default

Plate 4



3 bands, PC1 ALL Log transform enhancement limits set to actual

Plate 5



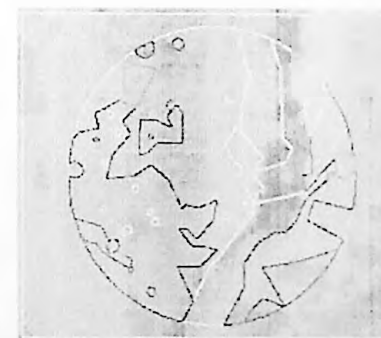
NIR & Green bands, PC1, vegetation overlay, with histogram equalization enhancement

Plate 6



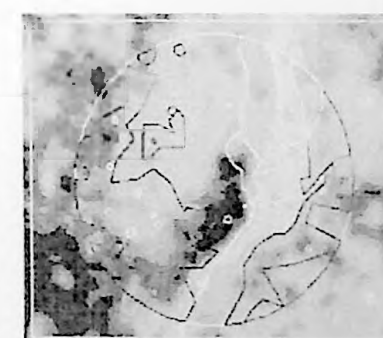
3 bands, PC1,2,3 linear transform enhancement limits set to actual

Plate 7



IRGPC1, IRPC2, and GPC3 with level slice transform enhancement limits set to actual

Plate 8



PCA composite, veg overlay, with Level slice transform enhancement isoclass 15 classes and default

Plate 9

Site 1 1997 Imagery



3 bands with vegetation overlay, linear enhancement.

Plate 10



3 bands with veg overlay, histogram equalization enhancement in green band

Plate 11



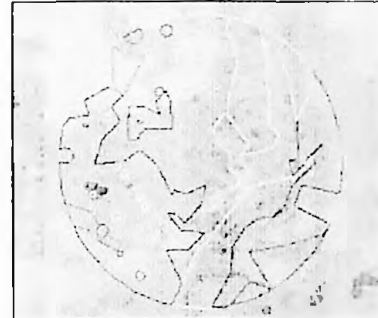
3 bands with vegetation overlay, level slice enhancement in all bands.

Limits set to actual Plate 12



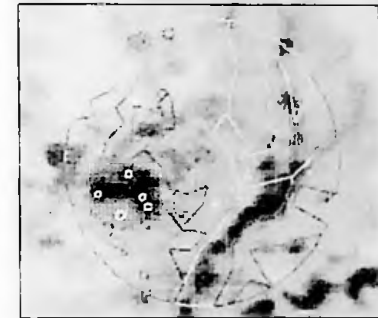
Composite, veg overlay, with Level slice transform enhancement isoclass 15 classes and default

Plate 13



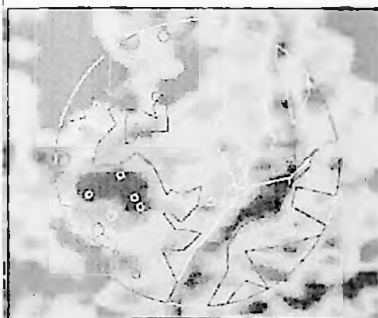
3 bands, PC1 ALL Log transform enhancement limits set to actual

Plate 14



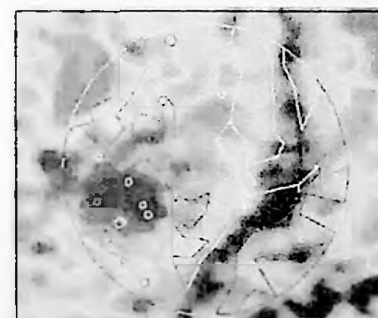
3 bands, PC1,2,3 linear transform enhancement limits set to actual

Plate 15



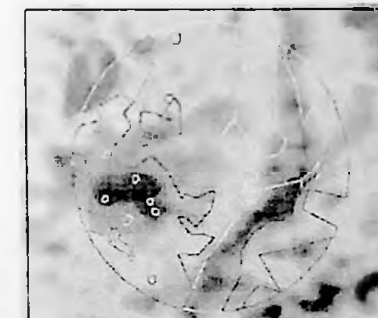
PC1,2,3, composite, veg overlay, level slice transform.

Plate 16



PCA composite, veg overlay, with Level slice transform enhancement isoclass 15 classes and default

Plate 17



PCA composite, veg overlay, with Level slice transform enhancement isoclass 30 classes and default

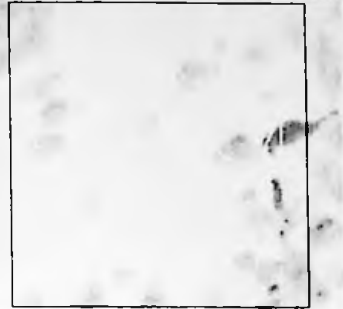
Plate 18

Yellow Creek Site 2 1995 Imagery



3 bands with vegetation overlay, linear enhancement.

Plate 19



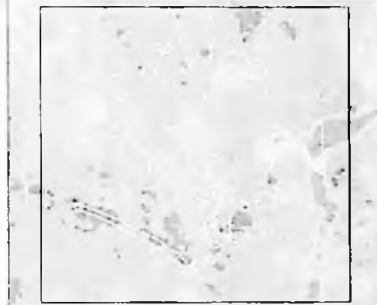
3 bands with vegetation overlay, with histogram equalization enhancement in all three bands

Plate 20



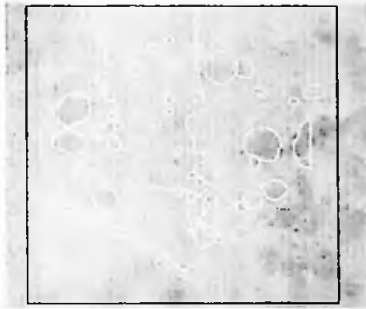
Composite, veg overlay, with Level slice transform enhancement

Plate 21



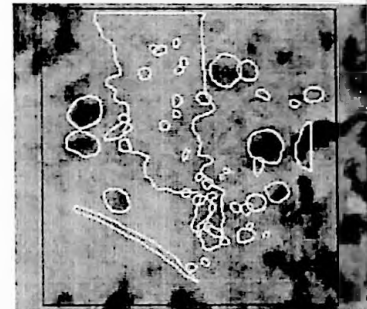
Composite, veg overlay, with Level slice transform enhancement, isoclass 15 classes and default

Plate 22



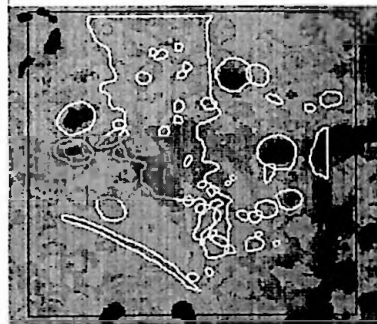
3 bands, PC1 ALL Log transform enhancement NIR Gaussian in R and G bands

Plate 23



3 bands, PC1,2,3 linear transform enhancement, limits set to actual

Plate 24



3 bands, linear transform enhancement, 15 classes

Plate 25



Composite, log transform enhancement, 10 classes

Plate 26



Composite, veg overlay, Level slice transform enhancement, NDVI (IR - R) / (IR + R)

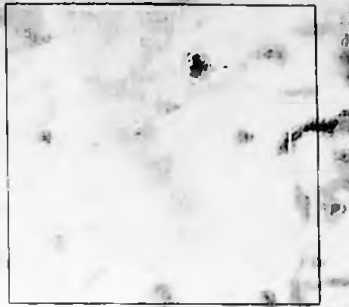
Plate 27

Yellow Creek Site 2 1997 Imagery



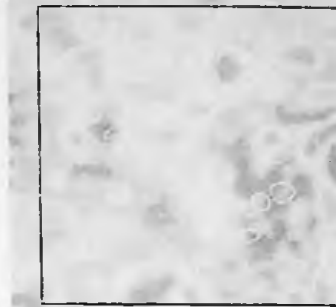
3 bands with vegetation overlay, linear enhancement.

Plate 28



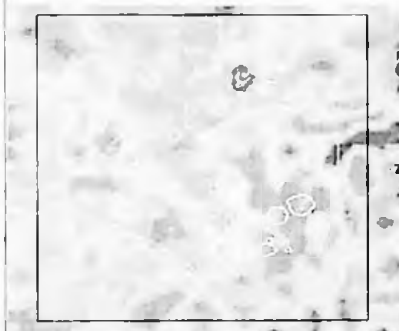
3 bands with veg overlay, histogram equalization enhancement in green band

Plate 29



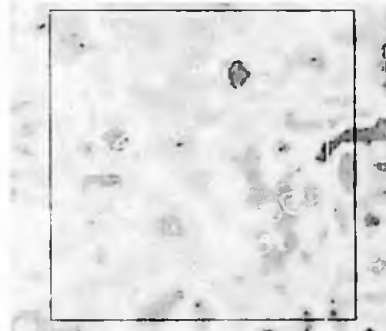
Composite, veg overlay Histogram only

Plate 30



Composite, veg overlay, with Level slice transform enhancement isoclass 15 classes and default

Plate 31



Composite, veg overlay, with Level slice transform enhancement isoclass 10 classes

Plate 32



NIR, R & Green bands, vegetation overlay, with 95% Clip equalization Isoclass 20 Classes

Plate 33



NIR, R & Green bands, vegetation overlay, with 95% Clip equalization Isoclass 10 Classes

Plate 34



3 Bands, veg overlay, Histogram equalize enhancement NDVI $(IR - R) / (IR + R)$

Plate 35



3 Bands, veg overlay, 95% Clip enhancement NDVI $(IR - R) / (IR + R)$

Plate 36

Yellow Creek Site 3 1995 Imagery



3 bands with vegetation overlay, Histogram enhancement in the Infra Red,

Plate 28



3 bands with veg overlay, Level slice transform enhancement in green band

Plate 29



Composite, veg overlay 95% clip only

Plate 30



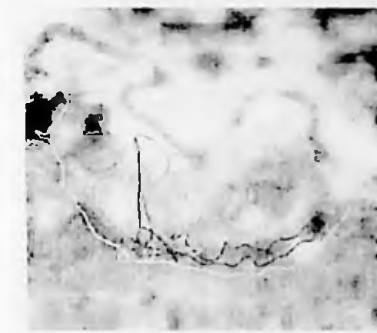
Composite, veg overlay, with Level slice transform enhancement isoclass 20 classes and default

Plate 31



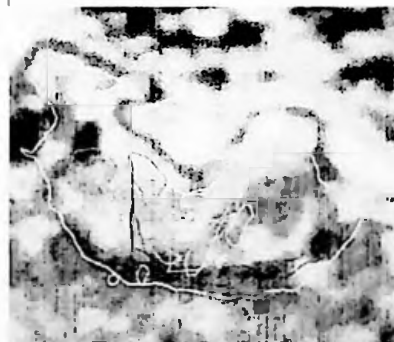
Composite, veg overlay, with Level slice transform enhancement isoclass 10 classes

Plate 32



3 bands, PC1 ALL Log transform enhancement NIR Gaussian in R and G bands

Plate 33



3 bands, PC1,2,3 linear transform enhancement limits set to actual

Plate 34



Composite, veg overlay, with Level slice transform enhancement

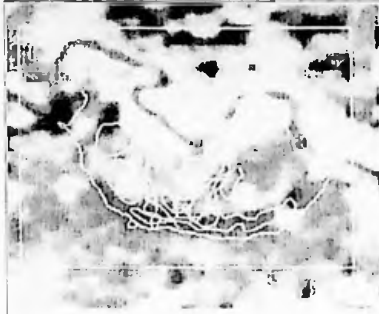
Plate 35



3 Bands, veg overlay, 95% Clip enhancement, Green, NDVI (IR - R) / (IR + R)

Plate 36

Yellow Creek Site 3 1997 Imagery



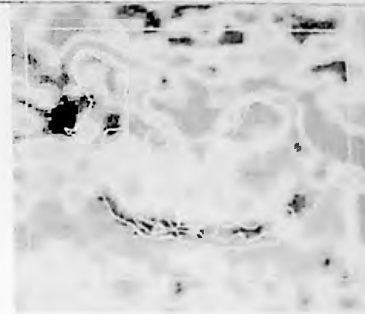
3 bands with vegetation overlay, Histogram enhancement in the Infra Red,

Plate 28



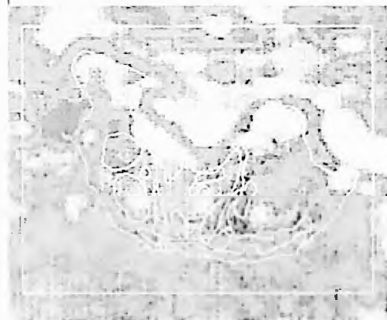
3 bands with veg overlay, histogram equalization enhancement in green band

Plate 29



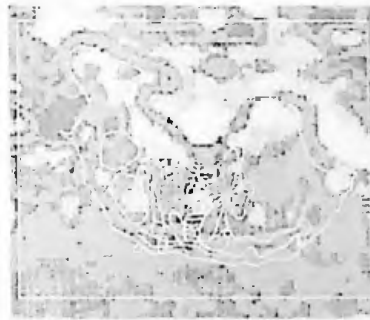
Composite, veg overlay 95% clip only

Plate 30



Composite, veg overlay, with Level slice transform enhancement isoclass 20 classes and default

Plate 31



Composite, veg overlay, with Level slice transform enhancement isoclass 10 classes

Plate 32



NIR & Green, PC1 Gaussian transform enhancement NIR Gaussian in R and G bands

Plate 33